

**Nonlinear finite element modelling of a simply supported beam
at ambient temperature and under fire**



Bachelor's thesis

HAMK University of Applied Sciences
Construction Engineering

Spring semester 2020

Amrit Chaulagain

Degree Programme in Construction Engineering
Hämeenlinna University Centre

Author	Amrit Chaulagain	Year 2020
Subject	Nonlinear finite element modelling of a simply supported beam at ambient temperature and under fire	
Supervisor(s)	Zhongcheng Ma	

ABSTRACT

The primary purpose of this Bachelor`s thesis was to develop a finite element model of simply supported IPE beam with nonlinear behaviour material definition, which can numerically simulate the structural response of IPE beam and replicate the simulation results with the physical lab test under mid-span loading by using FEA techniques in LS-DYNA. Mesh sensitivity analysis, structure only the analysis of IPE in a fire, implicit and explicit static analysis was also performed in LS-DYNA. Seven finite element models of simply supported IPE beam were created, and simulation was run in LS-DYNA.

The thesis presents the finite element modelling of a simply supported beam to examine the deformations, mesh sensitivity analysis, load versus displacement curve with explicit and implicit code, deformation in the fire of the steel IPE beam under mid-span loading. In addition, a detailed description of the numerical simulations and the theoretical background are presented in this thesis. The theoretical part of the thesis includes the general description of the finite element method; numerical method; input possible in LS-DYNA; the manual calculation of time-step; the detailed temperature calculation of unprotected steel IPE beam in a fire; LS-DYNA, and its history.

Findings revealed that LS-DYNA was able to replicate the simulation results with the physical lab test under mid-span loading, although there was a huge difference in load versus displacement curve between the LS-DYNA simulation and experimental results. Lateral torsional buckling failure was noticed on the structure with and without fire in both cases, during numerical simulation in LS-DYNA. The maximum effect of loading was observed in the mid-span of a beam by the local deformation in the upper flange of the structure.

Keywords LS-Dyna, LS-PrePost, FE modelling, Nonlinear analysis, Explicit code, Implicit code, structural analysis in a fire, mesh sensitivity analysis, temperature calculation.

Pages 95 pages including appendices 25 pages

CONTENTS

1	INTRODUCTION	1
1.1	Background.....	1
1.2	Aim and objectives	2
1.3	Methodology.....	2
2	THEORETICAL BACKGROUND	3
2.1	FINITE ELEMENT METHOD	3
2.1.1	Basic Concept	3
2.1.2	Brief history of FEM	4
2.1.3	General steps involved in Finite Element Analysis.....	5
2.1.4	Possible errors by Finite element Method	7
2.2	Types of Analysis in FEA	8
2.2.1	Linear Analysis	8
2.2.2	Nonlinear analysis	9
2.2.3	Finite Element Methods in Static Analysis	11
2.2.4	Dynamic Analysis in Finite Element Analysis.....	11
2.3	Structural Fire Analysis.....	12
2.3.1	Heat reaction in steel material.....	14
2.4	Material properties	18
2.4.1	Tensile tests	18
2.4.2	Behaviour of the material at larger strains	19
2.4.3	True stress and strain	19
3	LS-DYNA.....	21
3.1	LS-DYNA BACKGROUND	21
3.2	LS-PrePost.....	22
3.3	Capabilities of LS-DYNA.....	22
3.4	Implicit analysis in LS-DYNA	23
3.5	Explicit analysis in LS-DYNA.....	24
3.6	Time step Controls	25
4	EXPERIMENTAL TESTING RESULTS	28
5	MANUAL CALCULATION DATA	31
5.1	Element size calculation.....	31
5.2	Effective plastic stress-strain calculation	32
5.3	Temperature calculation of steel beam under ISO fire	34
6	3D FINITE ELEMENT MODEL DESCRIPTION	38
6.1	3D Modelling of the geometry in LS-PRE-POST	38
6.1.1	General dimensions and process of modelling in LS-PrePost	38
6.1.2	Meshing	43
6.1.3	Creation of Three different Part ID	44
6.2	Boundary Conditions.....	46

6.3	Material	47
6.4	Choice of the element type in LS-DYNA.....	48
7	MESH SENSITIVITY ANALYSIS.....	49
7.1	Mesh sensitivity analysis using implicit code.....	49
7.2	Mesh Sensitivity analysis using explicit code	53
8	STRUCTURAL RESPONSE ANALYSIS TO THERMAL LOAD IN LS-DYNA.....	54
8.1	Analysis time in LS-DYNA.....	57
9	ANALYSIS RESULTS AND COMPARISON WITH TEST	58
9.1	Implicit and Explicit simulation results	58
9.2	Comparing the lab test and numerical simulation results.....	62
9.3	The structural analysis of IPE Beam in fire.....	64
10	CONCLUSION AND FUTURE STEPS.....	66
	REFERENCES.....	68

Appendices

Appendix 1	Von mises stress simulation
Appendix 2	Temperature Calculation from Excel
Appendix 3	General Control cards input in LS-DYNA for implicit static analysis
Appendix 4	General Control keywords input in LS-DYNA Implicit code for structure in Fire.
Appendix 5	Material properties calculation sheet for Mat_255 according to Eurocode.
Appendix 6	Thermal expansion versus temperature curve plotted from LS-PrePost

Symbols and Abbreviations

CAD	Computer-Aided Design
CFL	Courant-Friedrichs-Lewy
DEM	Discrete Element Method
DOF	Degree of Freedom
FEM	Finite Element Method
MPP	Massively Parallel Processing
SMP	Shared Memory Parallel
FEA	Finite Element Analysis

Latin Letters

A	Area of the element
c	Speed of sound
E	Elastic modulus
f	Time step safety factor
L	Shell dimension
Δt	Time step, time interval.
K	Total heat transfer coefficient
A_m	Perimeter surface area per unit length exposed to fire
Q_f	Temperature of hot gases.
Q_s	Temperature of steel during the time interval.
Q_{cr}	Critical temperature
α_c	Heat transfer coefficients for convection
α_r	Heat transfer coefficients for radiation
ε_r	Resultant emissivity of the flames
A_m/V	Section factor for unprotected steel members
C_i	Protection coefficient of member's face I
E_a	Modulus of elasticity of steel for nominal temperature design
V	Volume of a member per unit length
f_y	Yield strength at 20°C
$f_{y,\theta}$	Effective yield strength of steel at elevated temperature
$f_{p,\theta}$	Proportional limit for steel at elevated temperature
$f_{u,\theta}$	Ultimate strength at elevated temperature
$h_{net,d}$	Design value of the net heat flux per unit area
k_{sh}	Correction factor for the shadow effect

Greek letters

γ	Shear strain
ρ	Density
Φ	Configuration factor
ε	Strain
σ	Stress
α	Convective heat transfer coefficient
ε_f	Emissivity of the fire
$\varepsilon_{z,m}$	Total emissivity of the flame
θ	Temperature
θ_a	Steel temperature

List of Figures

Figure 1. General stages in Finite Element Analysis (Akin, 2005, p.4)	7
Figure 2. Force vs Displacement curve in linear and nonlinear analysis. (communities.bently.com, n.d)	9
Figure 3. Nonlinear behaviour of structure with different categories. (Younis, 2009). ..	10
Figure 4. ISO Standard fire curve (University of Ljubljana, 2019)	12
Figure 5. Evolution of the gas temperature for different fire load densities (University of Ljubljana, 2019)	13
Figure 6. Evolution of gas temperature as a function of the ventilation. (University of Ljubljana, 2019)	13
Figure 7. Influence of insulation on the heating rate. (University of Ljubljana, 2019) ..	14
Figure 8. Specific heat of steel as a function of the temperature. (University of Ljubljana, 2019).....	15
Figure 9. Thermal conductivity of steel. (University of Ljubljana, 2019)	16
Figure 10. Heat flow for (a) element in continuum and (b) length of the steel section. (University of Ljubljana, 2019).....	17
Figure 11. The behaviour of metal at small strains. (Wikipedia.com, n.d)	18
Figure 12. Illustration of necking and final rupture of a ductile test in large strains. (Engineeringnotes.com, n.d)	19
Figure 13. True stress-strain and engineering stress-strain curves. (Engineeringnotes.com, n.d)	21
Figure 14. Transforming to explicit analysis in LS-DYNA.	25
Figure 15. Simply supported beam under point loading.....	28
Figure 16. Beam testing in Lab.	29
Figure 17. Properties of steel, stress versus strain diagram	30
Figure 18. Load versus Displacement Graph from lab test results.	31
Figure 19. Element size calculation in Excel sheet.	31
Figure 20. Effective plastic strain calculation sheet from Excel.	32
Figure 21. Graphical representation of Effective stress, strain curve after calculation. ..	32
Figure 22. Effective plastic stress-strain curve in LS-PrePost after inputting values.	33
Figure 23. Definition of section factor from EN 1994-1-2.....	35
Figure 24. Box value of the section factor $[AmV]_{\text{box}}$	36
Figure 25. Influence of shape on the shadow effect.....	36
Figure 26. Graphical representation of gas and steel temperature till 2000 seconds... ..	38
Figure 27. Cross-section of IPE 100 beam.	39
Figure 28. 3D point input in LS-PrePost.....	40
Figure 29. 3D Sketch input of point in LS-PrePost.....	41
Figure 30. 3D sketch input of line segment in LS-PrePost.....	42
Figure 31. 3D model of IPE Beam in LS-PrePost.	43
Figure 32. The meshing of IPE Beam in LS-PrePost.	44
Figure 33. Process of separating the Part ID in LS-PrePost.	45
Figure 34. Creating an entity in LS-PrePost for the definition of Boundary condition (BC).	46
Figure 35. Connecting the set data with BC in LS-PrePost.	47
Figure 36. Keyword input for Steel IPE Beam in LS-PrePost.....	48
Figure 37. Element formulation type 16 keyword in shell section.	49

Figure 38. Load versus displacement curve of a simply supported beam with different mesh size.	50
Figure 39. Meshing with the different element size of IPE beam in LS-PrePost of (a) 2mm (b) 4mm (c) 6mm (d) 8mm.....	51
Figure 40. Displacement resultant of a simply supported beam (a) 2mm mesh (b) 4mm mesh size (c) 6mm mesh size and (d) 8mm mesh size.....	52
Figure 41. Load versus displacement curve of a simply supported beam with different mesh size.	53
Figure 42. Material input for MAT_255 in LS-PrePost.	55
Figure 43. Calculation of Young`s modulus according to the EN.	55
Figure 44. Graphical representation of Temperature versus Young`s modulus in LS-PrePost.....	56
Figure 45. Graphical representation of thermal expansion due to fire on steel.	56
Figure 46. Graphical representation of Temperature versus plastic stress-strain curve.	57
Figure 47. Force versus Time curve of steel IPE beam with a mesh size of 6mm.....	59
Figure 48. Load versus displacement curve of the simply supported beam.....	59
Figure 49. Displacement result from the explicit analysis.	60
Figure 50. Displacement result from the implicit analysis.	61
Figure 51. Lab test (a) and (b) LS-Dyna simulation.....	62
Figure 52. Plastic deformation of the beam.....	62
Figure 53. Simulation results of simply supported steel beam.....	63
Figure 54. Load versus displacement curve of a simply supported beam from a lab test and LS-DYNA.....	63
Figure 55. Mid-span displacement by shell element model.	65
Figure 56. Lateral torsional buckling in mid-span loading of a simply supported beam under fire.....	65

List of Tables

Table 1: Application of FEM (Akin, 2005, p.5).....	4
Table 2. Summarized history of FEM (Rao, 2014, p.4).....	5
Table 3. Capabilities of LS-PrePost (Livermore Software Technology Corporation, n.d)22	
Table 4. Capabilities of LS-DYNA (Livermore Software Technology Corporation, 2006).....	23
Table 5. Calculation of characteristic dimension for low order element. (Sormunen, 2016).....	27
Table 6. Material properties of the steel IPE Beam.	47
Table 7. Mesh sensitivity analysis results.....	54
Table 8. Analysis cases and simulation time in LS-DYNA Manager.....	58

1 INTRODUCTION

1.1 Background

Finite element method (FEM) is a mathematical computer-based numerical technique for calculating the strength and behaviour of engineering structures. The development of finite element analysis (FEA) software tools make it easy to analyse dynamic loads, static loads, structural fire and blast loads et cetera. Structures subjected to extreme loads, including fire loads, blast loads are challenging to study experimentally, and the evaluation of the damages caused by loads is hard to conduct, expensive and dangerous.

Using FEA software in predicting damages and replicating the physical lab test caused by different loads (static, dynamic, blast, fire) in the structures is widely used in modern engineering analysis. It is because of the variety of material models, the ease of accessing them and changing parameters, the ability to simulate problems that are difficult to conduct in laboratories, the costless efforts compared to laboratories, and the safety of using FEA software. There are many FEA software tools available for nonlinear static analysis, but for this thesis, LS-DYNA software is used. (Younis, 2010, p.4)

Nonlinear analysis is an analysis which uses nonlinear material and geometrical behaviour for performance evaluation of structural systems at the life safety and collapse prevention levels. In the modern product design engineering, it is important to understand the sources of nonlinearities and their effect on designs during their lifetime for a better performance and durability of the product. With the help of nonlinear fem simulation solutions, we can simulate product behaviour accurately, reducing the possible failures, warranty costs and saving on material costs. (Krawinkler, 2007)

Computational tools are often necessary for the safe design of structures under fire conditions due to the complex structure's response. In recent years, the use of the finite element code in LS-DYNA has increased in research and industry for structural fire analysis. The nature of isolated structural elements under standard fire conditions through furnace testing has been extensively studied. (Rackauskaite et al., 2017)

The purpose of this thesis is to develop a finite element modelling of steel IPE beam for nonlinear static analysis at both ambient and elevated temperatures. To achieve this, the FEM software LS-DYNA was used for nonlinear static analysis of structures in three dimensions using implicit and explicit solvers.

1.2 Aim and objectives

The aim of this thesis is to develop a nonlinear FE model, numerically simulate the structural response of simply supported IPE steel beam, compare the simulation results with the physical lab test under point load by using FEA techniques in LS-DYNA.

The following objectives are set to achieve the aim of the study:

1. To develop an FEA model to simulate steel IPE beam under point load in LS-DYNA to replicate lab test.
2. To perform a mesh sensitivity analysis from four different element sizes of 2mm, 4mm, 6mm and 8mm meshing using implicit code and 6mm, 8mm, 12mm and 14mm meshing using explicit code.
3. To develop an FEA model to simulate the structural response of IPE beam in a fire, heated from four sides in an unprotected IPE beam.
4. Manual calculation of the temperature of carbon steel in unprotected IPE beam using Eurocode.
5. To compare the load versus displacement curve from the lab test and the numerical simulation.
6. Running the finite element model with implicit and explicit solvers in LS-DYNA.

1.3 Methodology

To complete this study and meet the objectives set first publications and studies were conducted on nonlinear analysis, FEA, LS-DYNA, Fire design, static analysis, explicit analysis and implicit analysis in LS-DYNA. Also, LS-DYNA software and material model definition for steel were explored in detail including videos about the LS-DYNA and successfully running them in LS-DYNA Manager.

Calculation of material definition for steel based on Eurocode were completed in excel sheet. Modelling was carried out for the numerical simulation in LS-DYNA. The several approaches involved in solving physical problems by using LS-DYNA are as follows:

- Creating a finite element model in LS-PrePost.
- Choosing material model and properties.
- Assigning material and property.
- Assigning loads and boundary condition.
- Specifying the control parameters. Selecting implicit or explicit solver.
- Creating input files and saving them.
- Running the input files in LS-DYNA manager to get a results output file
- Post-processing the d3plot file in LS-PrePost.

By using the above approaches eleven finite element model was created (four implicit static analysis, five quasi-static explicit analysis and two structure fire analysis) and run successfully in LS-DYNA.

2 THEORETICAL BACKGROUND

LS-DYNA is an advanced multipurpose finite element code for analysing the large deformation with a static and dynamic response of structures. This chapter presents the basic theoretical background for the finite element simulation in LS-DYNA.

2.1 FINITE ELEMENT METHOD

2.1.1 Basic Concept

The finite element method is a numerical method for solving the problems of engineering and mathematical physics. In modern engineering analysis, it is rare to find a project that does not require some types of finite element analysis (FEA). The basic idea in the Finite Element Method (FEM) is to obtain the solution of a complicated problem by analysing the real-life structures into finite pieces. FEM is a numerical or computational technique for solving different complex engineering problems.

FEM can be applied to solving different static and dynamic engineering problems, from stress analysis of simple beam structure or a large, complicated machine to dynamic responses under different mechanical, structural, or thermal loading. In manufacturing, FEA is used in simulation and optimization of manufacturing processes like casting, machining, plastic molding, forging, metal forming, heat treatment and welding etc. Structural, dynamic, thermal, magnetic potential and fluid flow problems can easily be handled accurately by using Finite Element Analysis. (Radhakrishnan., 2008, p.189)

In the finite element method, the boundary and interior of the region are subdivided by lines or surfaces into a finite number of discrete sized subregions or finite elements. Several nodal points are established with the mesh. The size of an element is usually associated with a reference length. Table 1 shows the application of the finite element method. (Akin, 2005, p.6)

Table 1. Application of FEM (Akin, 2005, p.5)

Area of Study	Application examples
Solid or Structure mechanics	Structure failure analysis, crash simulation, nuclear reactor, wind turbine blade design, beam and truss design, limit load analysis.
Acoustic Conduction	Aerodynamic analysis of cars and aeroplane, seepage analysis, air conditioning modelling of a building.
Heat Conduction	Cooling and casting modelling, combustion engine, electronic cooling modelling.
Electromagnetics	Electromagnetic interference suppression analysis, sensor and actuator field calculations, antenna design performance predictions.

2.1.2 Brief history of FEM

The Finite Element Method was developed originally for the analysis of aircraft structures. Courant first developed the foundation of the FEM in the 1940s (Rao, 2014, p.3). The stiffness matrix for truss, beam and other elements were developed during 1956. Clough created the name 'finite element' presents the application of simple finite elements for the analysis of aircraft structure and is considered as one of the key commitments in the advancement of a finite element method. The digital computer provided a rapid means of performing the many calculations involving the finite element analysis, which made the method practically possible. Several significant developments have emerged in FEM software with the introduction of integrations sensitivity, FEM codes and development of CAD programs to model complex geometry in recent years. Table 2 below summarizes history of finite element modelling from the year 1943 till 2014. (Rao, 2014, p.3)

Table 2. Summarized history of FEM (Rao, 2014, p.4)

Year	Major Achievements
1943	Variation method which was the foundation of FEM
1956	Stiffness method for beam and truss
1960	A finite element was created
1967	The first book of FEM by Zienkiewicz and Chung was published
1970	FEM applied to non-linear problems and large deformation
1970	Digitalization of FEM in computers
1980	Used of GUI and microcomputer
1990	Large structural systems analysis, nonlinear and dynamic problems
2000	Multiphysics and complex engineering problems
2014	Advanced FEA tools

2.1.3 General steps involved in Finite Element Analysis

In the finite element method, the actual body of matter, such as a solid, liquid, or gas, is represented as an assemblage of subdivisions called finite elements. These elements are interconnected at specified joints called nodes or nodal points. The nodes usually lie on the element boundaries where adjacent elements are connected. The general procedure of FEM, which is shown in Figure 1 below, can be summarized as an orderly step by step process with reference to static structural problems as follows:

1. Select the element type and discretize (Rao, 2004, p.16)

The first step in the finite element method is to divide the structure into subdivisions or elements. Therefore, the structure is to be modelled with suitable finite elements. The number, type, size, and arrangement of the elements are to be decided.

2. Selection of proper interpolation to connect different nodes (Rao, 2004, p.16)

Since the displacement solution of a complex structure under any predefined load conditions cannot be anticipated precisely, we expect some reasonable solution within an element to approximate the unknown solution. The expected solution must be straightforward from a computational point of view; however, the solution or the interpolation model is taken in the form of a polynomial.

3. Development of the element stiffness matrices and load vectors (Rao, 2004, p.16)

From the assumed displacement model, the stiffness matrix $[k^{(e)}]$ and the load vector $p^{(e)}$ of an element, (e) is to be derived by using either equilibrium conditions or a suitable variational principle.

4. Assembly of the element matrices to an obtained global matrix for entire FEM modal (Rao, 2004, p.16)

Since the structure is composed of several finite elements, the individual element stiffness matrices, and load vectors are to be assembled in a suitable manner and the overall equilibrium equations should be formulated as $[k]\Phi=P$.

Where $[k]$ is the assembled stiffness matrix, Φ is the vector of nodal displacements, and P is the vector of nodal forces for the complete structure.

5. Solution for the unknown nodal displacements (Rao, 2004, p.16)

The overall equilibrium equations must be modified to account for the boundary conditions of the problem. After incorporation of the boundary conditions, the equilibrium equations can be expressed as $[k]\Phi=P$.

6. Computation of element strains and stresses

From the known nodal displacement Φ , if required, the element strains and stresses can be computed by using the necessary equations of solid or structural mechanics (Rao, 2004, p.16).

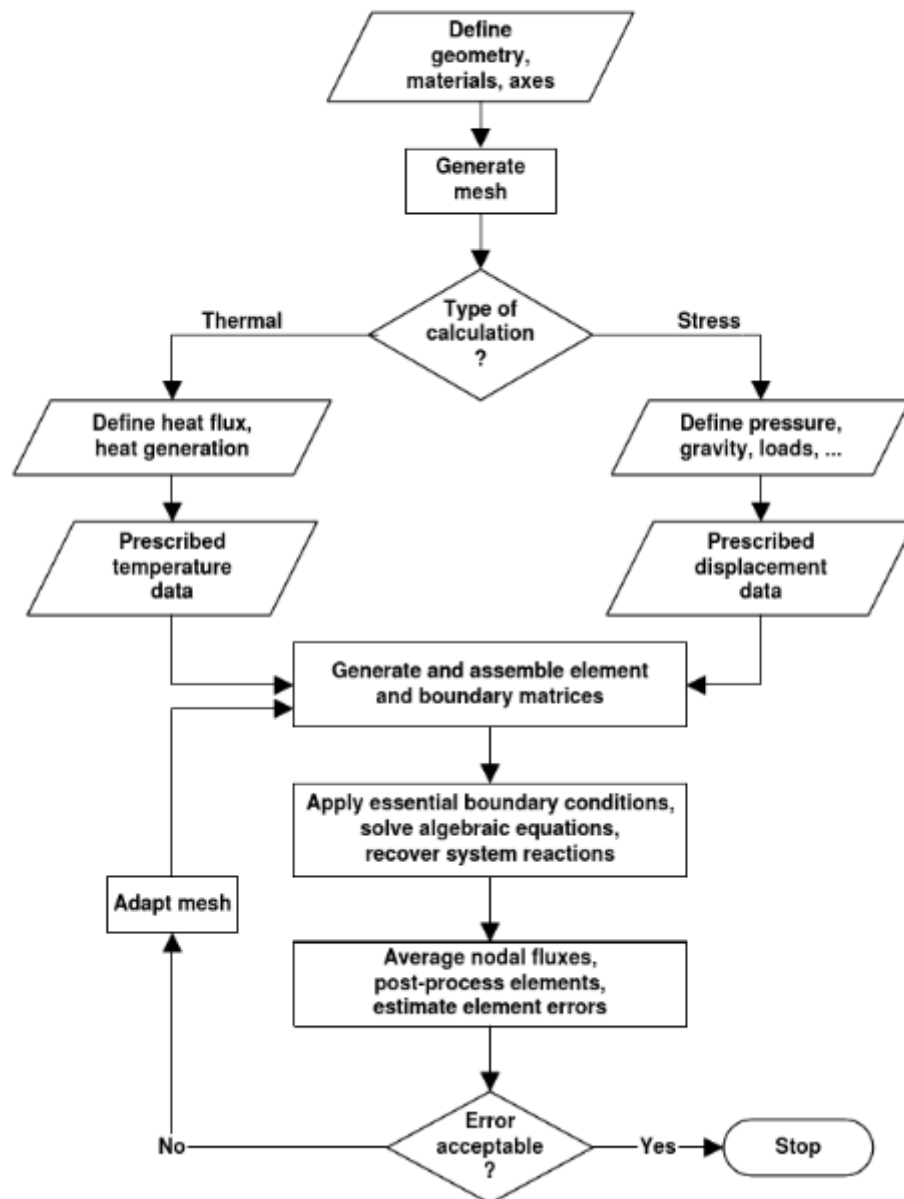


Figure 1. General stages in Finite Element Analysis (Akin, 2005, p.4)

2.1.4 Possible errors by Finite element Method

FEM is a numerical method or computational technique which discretises the structure into finite pieces. The result of these types of technique contains the following types of errors. (Akin, 2005, p.12)

Modelling errors due to simplification

The finite element description is a boundary value problem (BVP), which means there is a differential equation with several constraints. Errors of this type can include the wrong geometric description, the wrong definition of the material, wrong boundary conditions, the wrong type of analysis and wrong definition of a load.

Discretization errors

These types of error are due to the discretization of the structure into finite pieces. The geometry and displacement distribution of a real structure is continuously changing. When using a finite number of elements to model the structure, the discretized structure cannot be fully matched with a real model which causes errors. These errors can be reduced using smaller element sizes checking the software is operating with the input value and good interpolation functions.

Numerical errors

These errors are due to round off errors from the computer floating-point calculation and errors generated by numerical integration. These errors cannot be eliminated but can be reduced so that they do not influence the results. Rounding error in FEA can be caused by adding, subtracting minimal and large numbers.

2.2 Types of Analysis in FEA

2.2.1 Linear Analysis

Linear Analysis is the properties of the structure in which stiffness remained constant during the entire analysis. A linear analysis is an analysis where a linear relation holds between applied forces and displacements. In a linear, the stiffness matrix is constant and solving process is relatively short compared to nonlinear analysis. Figure 2 denotes force versus displacement curve in linear and nonlinear analysis.

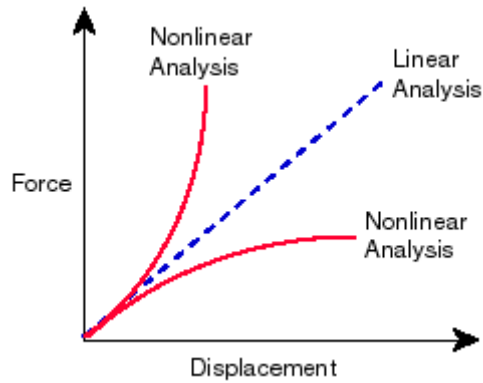


Figure 2. Force vs Displacement curve in linear and nonlinear analysis. (communities.bentley.com, n.d)

A linear FEA analysis is performed when:

- The structure is expected to behave linearly (for small deformation /strain).
- The stress is proportional to the strain.
- The structure will return to its original state when the load is removed.
- Superposition principle applies

2.2.2 Nonlinear analysis

Nonlinear analysis is the analysis in which properties vary due to large displacements in the structure (geometric nonlinearity), large scale yielding in the material (material nonlinearity) or changes in boundary conditions.

Nonlinear analysis is an analysis where a nonlinear connection holds between applied forces and displacements. Nonlinear effects can start from geometrical nonlinearities (i.e. Big deformations), material nonlinearities (i.e elasto-plastic material), and contact. These impacts bring about a firmness framework which is not steady during the heap application. This is against the linear static analysis, where the stiffness matrix remained constant. As a result, a different solving strategy is required for the nonlinear analysis. Modern analysis software makes it possible to solve complex nonlinear problems. (Femto.eu, n.d)
Figure 3 denotes the stress-strain curve of steel material with nonlinear behaviour of structures with different categories.

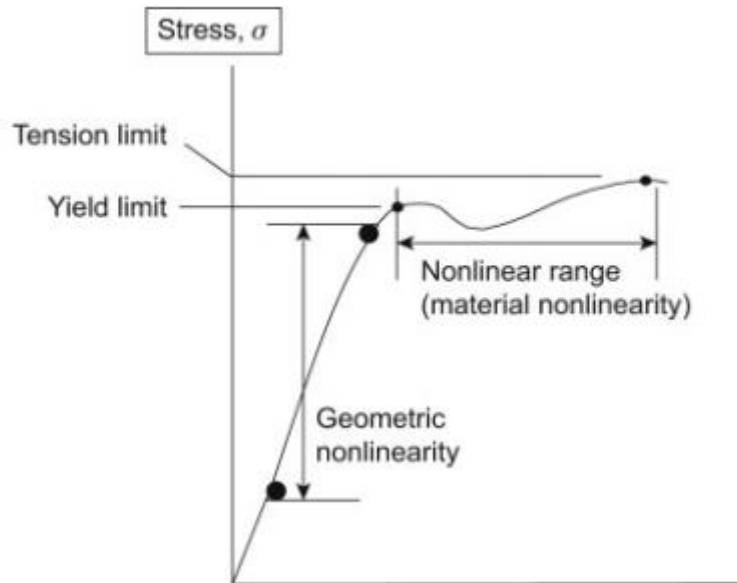


Figure 3. Nonlinear behaviour of structure with different categories. (Younis, 2009)

Types of Nonlinear Analysis:

Geometric Nonlinearity

Geometrical nonlinearity is about a change in geometry where it significantly affects load-deformation treatment no matter how small or big deformation happens. Geometrical nonlinearity can be defined for extremely large deformations where the relation between displacement and strain is nonlinear.

Material nonlinearity

Material nonlinearity involves the nonlinear behaviour of a material based on a current deformation, deformation history, rate of deformation, temperature, pressure, etc. Examples of nonlinear material models are large strain Visco elastoplasticity and hyperelasticity (rubber and plastic materials).

Constraint and contact Nonlinearity

Constraint nonlinearity in a system can occur if kinematic constraints are present in the model. The kinematic degrees-of-freedom of a model can be constrained by imposing restrictions on its movement.

2.2.3 Finite Element Methods in Static Analysis

FEM has been most broadly utilized in both linear and nonlinear static analysis. The different kinds of static problems are solved using FEM different field, which includes elastic, elastoplastic, viscoplastic analysis of beam, frame, truss, plate, shells and solid structure. Usually, the static analysis includes an analysis of stress, strain, and displacement under static loading for one-dimensional, two-dimensional or three-dimensional problems. Basic static analysis is the static loading analysis which can cause non-permanent or permanent deformation generally used for determining stresses and strains caused by a force that does not create notable inertia or damping effects. (Jenkins, 2019)

A linear static analysis is an analysis where a linear relation holds between applied forces and displacements. In practice, this is between applied forces and displacements. In practice, this is applicable to structural problems where stresses remain in the linear elastic range of the used material. In linear static analysis, the model stiffness matrix is constant, and the solving process is relatively short compared to a nonlinear analysis on the same model. Therefore, for the first estimate, the linear static analysis is often used before performing a fully nonlinear analysis. (Rusu, 2017)

2.2.4 Dynamic Analysis in Finite Element Analysis

Dynamic FEA is a powerful simulation technique which can be applied in complex engineering systems. Dynamic analysis is used to evaluate the impact of transient loads or to design out potential noise and vibration problems. Vibration analysis testing is expensive in real life in which dynamic analysis at the design stage can avoid or reduce the requirement and the cost of testing.

Modal analysis is used to identify natural frequencies. Modal analysis is a powerful tool in FEM software which allows an engineer to design the product to avoid excitation to coincide with natural frequencies which minimize excessive vibration. Animations can be produced with valuable information into how the structure behaves under dynamic loading. Modal analysis is a standard tool in design to avoid the vibration in the structure design. Dynamic loading on a machine will introduce vibrations. Transient dynamic analysis is used to determine the dynamic result of a structure under the action of time-dependent loads. The flexible, dynamic analysis is the most versatile dynamic analysis which is used to determine the time-varying displacements, strains, stresses, and forces in a structure as it responds to transient loads. (trivista.co.uk, n.d.)

2.3 Structural Fire Analysis

Finite Element Analysis (FEA) is a powerful and well-recognized tool used in the analysis of heat transfer, thermal stresses, thermal displacement, temperature distribution problems. The two types of heat transfer are convection and radiation, which is approximated by boundary conditions in FEA. Modelling all three mechanisms of heat transfer without arbitrary assumption requires the combined use of FEA and Computational Fluid Dynamic (CFD). (sae.org, n.d)

Fire is a complex process which has many forms, involves in different chemical reactions and causes structural damage. During design criteria for structure, structural fire safety requires expectation for the structural and heating models.

A temperature vs time curve usually represents fire. Fire safety in buildings is concerned with achieving two fundamental objectives to reduce the loss of life in, or in the neighbourhood of, building fires and to reduce the property or financial loss. (University of Ljubljana, 2019)

Figure 4 is a temperature vs time curve, which gives the average temperature reached during a fire in a small size compartment or the furnaces used for fire resistance tests. International standards are based on the standard fire defined by the ISO 834 curve (Figure 4)

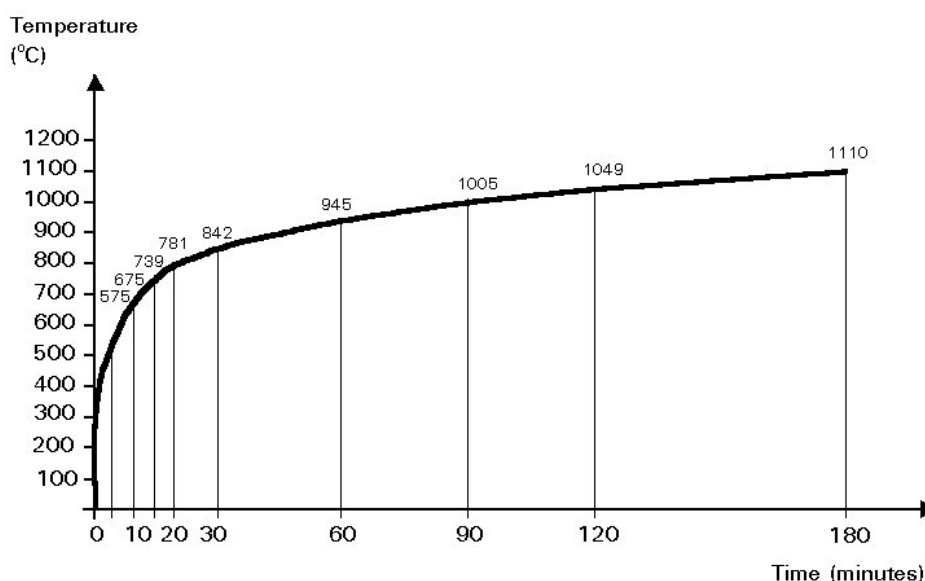


Figure 4. ISO Standard fire curve (University of Ljubljana, 2019)

Below Figure 5 and 6 illustrate the influence of fire load density and ventilation of compartment gas temperature.

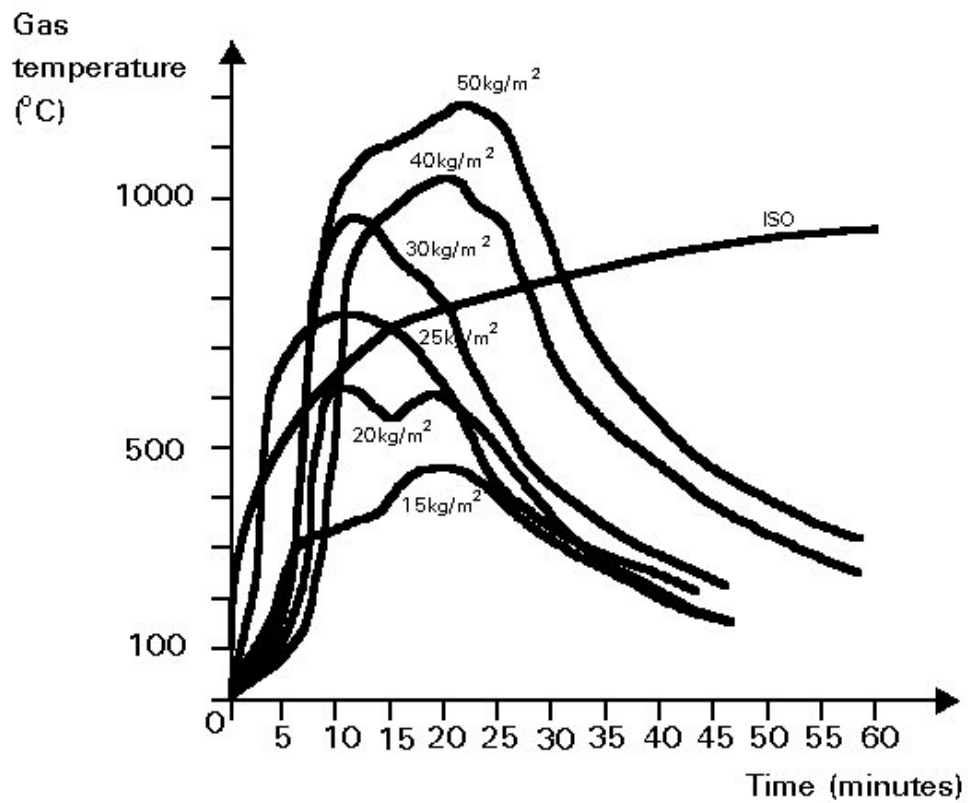


Figure 5. Evolution of the gas temperature for different fire load densities (University of Ljubljana, 2019)

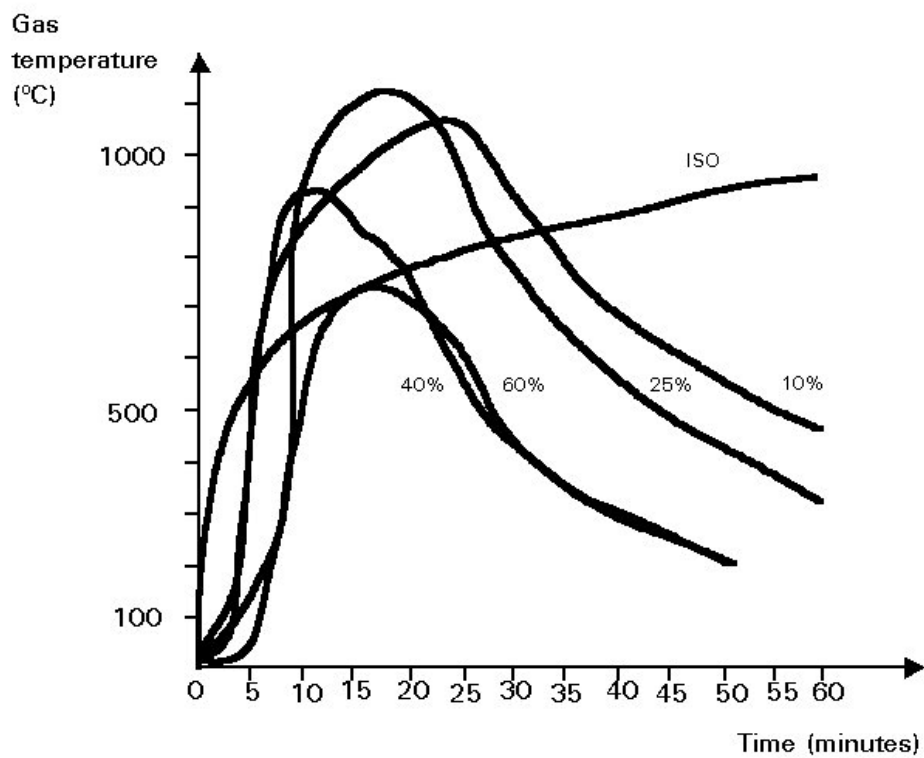


Figure 6. Evolution of gas temperature as a function of the ventilation. (University of Ljubljana, 2019)

The temperature of steel increases similarly but with some delay compared to the gas temperature in the fire. When a structural member is exposed to fire the response is governed by the rate heated due to mechanical properties of materials decrease as temperature rises and the structural resistance of a member reduces with temperature rise. (University of Ljubljana, 2019)

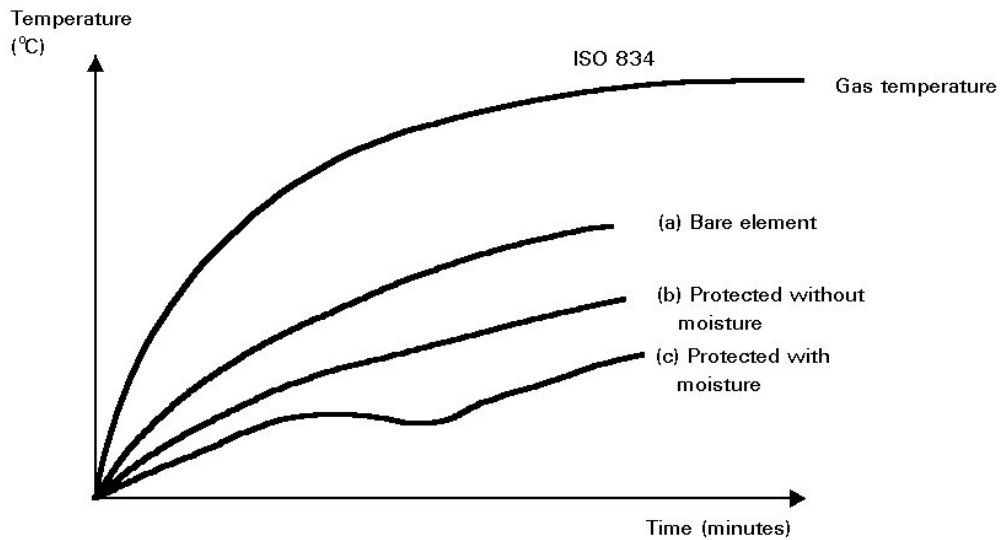


Figure 7. Influence of insulation on the heating rate. (University of Ljubljana, 2019)

In Figure 7, the temperature rise in the three cases is compared to the same element. Curve (a) denotes the delay for the bare element, while curve (b) and (c) apply to the cases of some protective coating, without and with moisture content. (University of Ljubljana, 2019)

2.3.1 Heat reaction in steel material

Steel is isotropic material in which no heat is generated within the body of steel elements. The rise of temperature in steel structure depends on the heat transfer between the fire environment and the element. According to the second law of thermodynamics, energy in the form of heat is transferred between any two elements, which are at different temperatures. Conduction, radiation and convection are the modes by which thermal energy flows from regions of high temperature to low temperature. The approach to study the increase of temperature in structural elements exposed to fire is based on the integration of the Fourier heat transfer equation for non-steady heat conduction inside the element. (University of Ljubljana, 2019)

$$\frac{k_s}{\rho_s c_s} \Delta^2 \theta = \frac{d\theta}{dt} \quad (1)$$

Fourier heat transfer equation Equation (1)
where for steel material,

The specific mass of steel(ρ_s) = 7850 kg/m³

The thermal conductivity (K_s) depends on the temperature.

The specific heat c_s depends on the temperature.

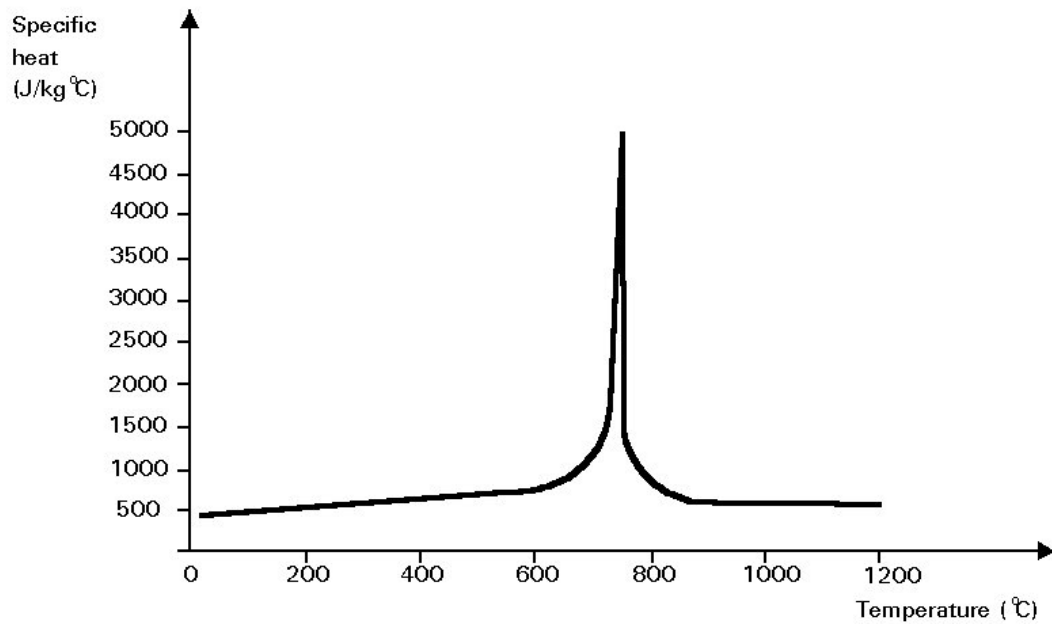


Figure 8. Specific heat of steel as a function of the temperature. (University of Ljubljana, 2019)

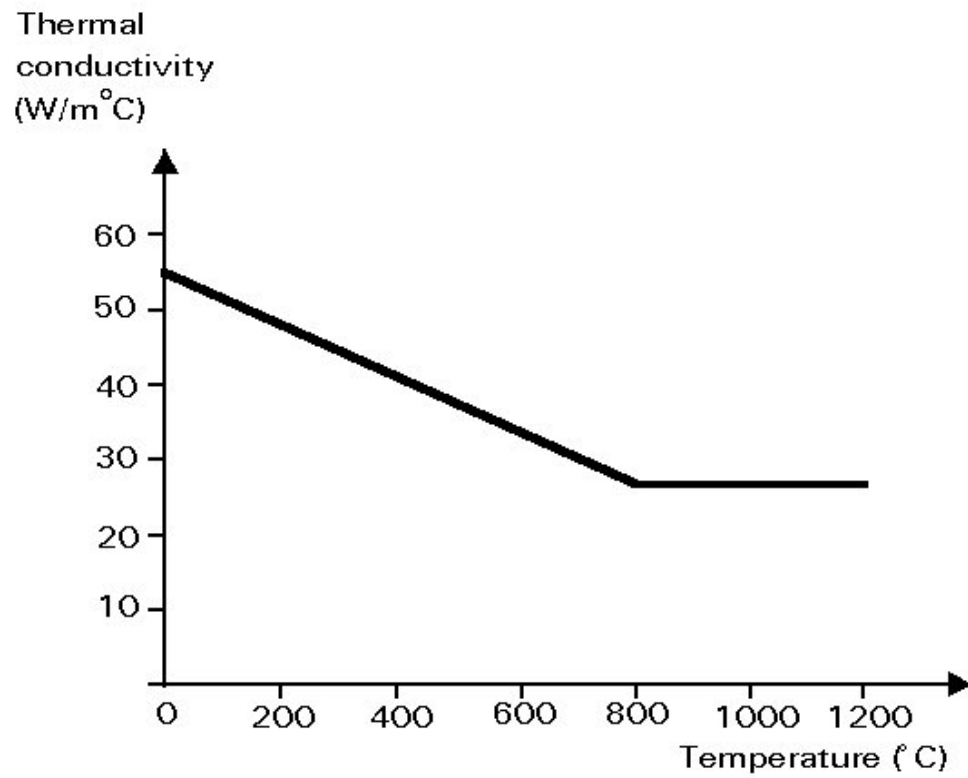
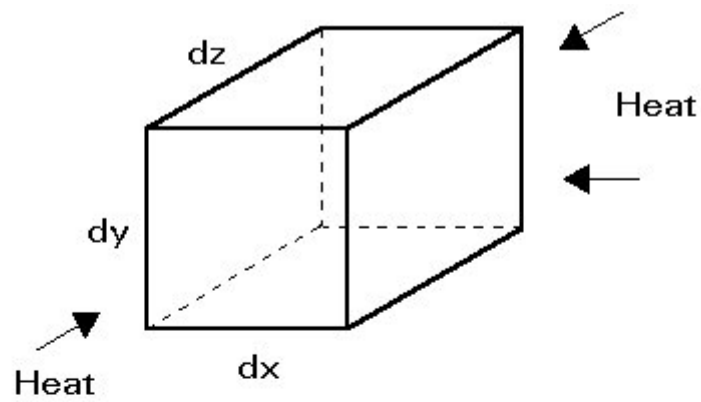
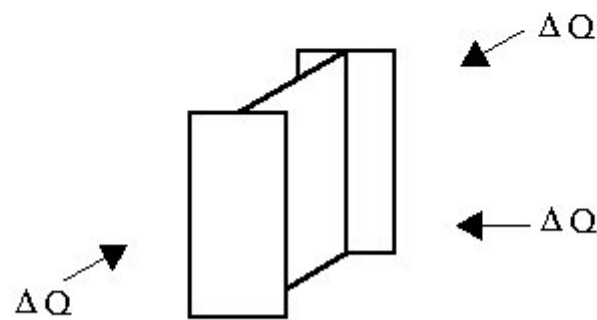


Figure 9. Thermal conductivity of steel. (University of Ljubljana, 2019)

Figure 8 denotes the specific heat of steel in temperature and Figure 9 illustrates the thermal conductivity of steel in fire.



(a)



(b)

Figure 10. Heat flow for (a) element in continuum and (b) length of the steel section. (University of Ljubljana, 2019)

The quantity of heat transferred per unit length in the time interval Δt is,

$$\Delta Q = K \cdot A_m \cdot (\theta_f - \theta_s) \cdot \Delta t \quad (2)$$

where,

K is a total heat transfer coefficient

A_m is the perimeter surface area per unit length exposed on fire

θ_f is the temperature of hot gases

θ_s is the temperature of steel during the time interval Δt

If this quantity of energy is entirely absorbed by the section, i.e no loss of heat is considered, the internal energy of the unit length of a steel element increases by the same quantity.

$$\Delta Q = c_s \cdot \rho_s \cdot A \cdot \Delta \theta_s \quad (1)$$

where,

A is the cross-sectional area of the member(m²)

The temperature rise of the steel is given by combining mass density ρ_s and specific heat c_s ,

2.4 Material properties

2.4.1 Tensile tests

The aim of the tensile test is to assess material properties for the metal. The properties obtained are utilized for the plan of parts. For the tensile test first, the specimen is placed in the testing machine and then a force is applied. The force is increased gradually, and a strain gauge measures the change of length in the specimens. The results of a single test can be applied to all sizes and cross-sections of specimens if the force is converted to stress and the distance between gauge marks to strain. (Askieland et al. 2010, p. 160.)

$$\sigma = \frac{F}{A} \quad (2)$$

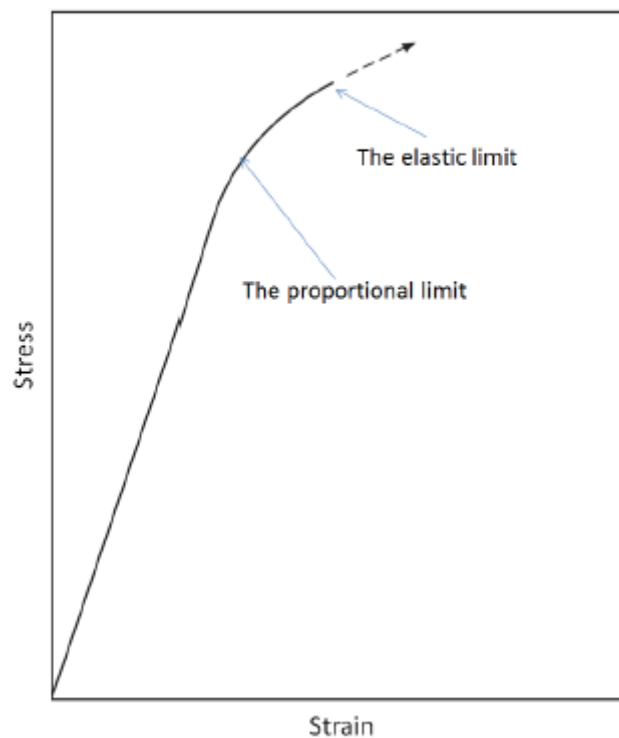


Figure 11. The behaviour of metal at small strains. (Wikipedia.com, n.d)

Figure 11 above presents a typical stress-strain curve at the small strains obtained from a tensile test. The maximum stress that can be applied without causing permanent deformations is called the elastic limit.

2.4.2 Behaviour of the material at larger strains

Figure 12 below shows the behaviour of test material at larger strains. After the initial region, the specimen becomes plastic. The maximum stress on the stress-strain curve is the point at which necking starts. In necking the cross-sectional area of the specimen starts to decrease, and with a reduced area, less force is needed to continue the deformation. As engineering stress is based on the initial cross-sectional area A , the curve starts to decrease. Due to necking, the stress becomes rather localized, and the final rupture takes place. (Baeker 2006, p. 40)

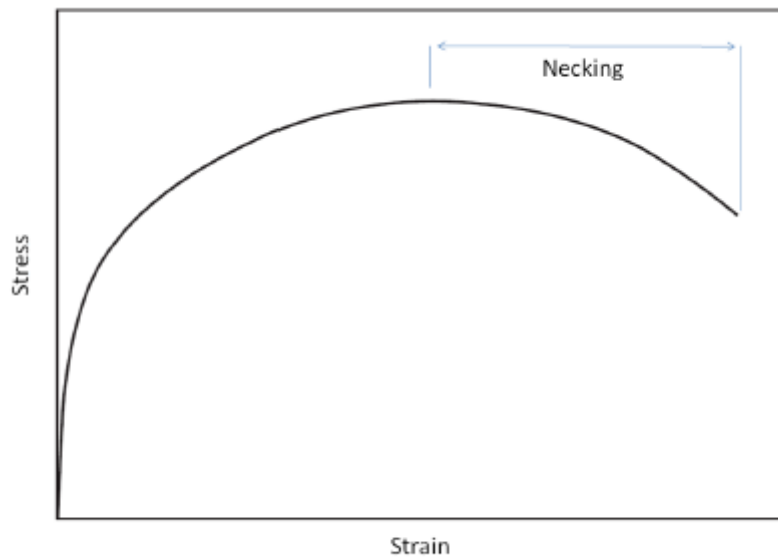


Figure 12. Illustration of necking and final rupture of a ductile test in large strains. (Engineeringnotes.com, n.d)

2.4.3 True stress and strain

Engineering strain (ϵ) is a small strain result, which is computed using original geometry. The engineering strain result is a linear measure since it depends on the initial geometry. Engineering strain is defined as the change in length divided by the original length.

$$\varepsilon = \frac{\Delta l}{l} \quad (5)$$

Where,

ε is an engineering strain [Pa]

Δl is changed in length [m]

l is original length

Engineering stress (σ), is the conjugate stress measure to engineering strain (ε). It is also defined as the force per unit area. Which is given by,

$$\sigma = \frac{F}{A} \quad (3)$$

Where

σ is engineering stress [Pa]

F is force [N]

A is the cross-sectional area [m²]

True stress is defined by using the deformed cross-section instead of the initial one.

$$\sigma_t = \sigma(1 + \varepsilon) \quad (4)$$

A true strain is a logarithmic strain which provides a correct measure of the strain.

$$\varepsilon_t = \ln(1 + \varepsilon) \quad (5)$$

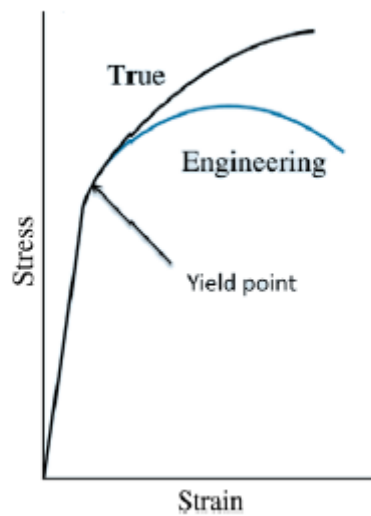


Figure 13. True stress-strain and engineering stress-strain curves. (Engineeringnotes.com, n.d)

The true stress-strain curve (Figure 13) is compared with the engineering stress-strain curve in the above figure. The curve is the same until the yield point after that true stress continues to rise although the required load fall. (Beer et al, 2012, p.62)

3 LS-DYNA

3.1 LS-DYNA BACKGROUND

LS-DYNA is an advanced Finite Element Package software which specializes in highly nonlinear transient analysis using an explicit integration scheme. LS-DYNA was known as DYNA3D earlier in 1974. John Hallquist developed his code on a language called FORTRAN. FORTRAN was a programming language which was related to mathematics. In 1984 LSTC was born as a software company where they developed or expanded the code as LS-DYNA. (d3view.com, n.d.)

LS-DYNA is an advanced general-purpose finite element program capable of solving and simulating complex real-world problems created by the Livermore Software Technology Corporation (LSTC). While the package continues to contain more and more possibilities for the calculation of many complex, real-world problems, its origins and core-competency lie in highly nonlinear transient dynamic finite element analysis (FEA) using explicit time integration. LS-DYNA is used by a wide range of industries such as automobile, aviation, structural designing, military, manufacturing, construction and bioengineering industries.

LS-DYNA potential applications are numerous and can be tailored to numerous fields. In a given simulation, any of LS-DYNA's numerous features can be combined to model a broad scope of physical occasions. An example of a simulation, which involves a one of a kind features, is the NASA JPL Mars Pathfinder landing simulation which simulates the space test's utilization of airbags to help in its landing. LS-DYNA is one of the most flexible finite element analysis software packages available.

LS-DYNA run requires a command shell, executable, an input file and enough free disk space to run the calculation because LS-DYNA consists of a single executable document and is entirely command-line driven. All input files are in a simple ASCII format and along these lines can be prepared using any content editor. Input documents can also be prepared with the instant help of a graphical processor. (lstc.com, n.d.)

3.2 LS-PrePost

LS-PrePost is an advanced pre-processing and post-processing software by Livermore Software Technology Corporation that can be downloaded free. For this thesis, LS-PrePost was used for post-processing and pre-processing software. Table 3 shows the list of features of LS-PrePost. (lstc.com, n.d)

Table 3. Capabilities of LS-PrePost (Livermore Software Technology Corporation, n.d)

Pre-processing capabilities	Post-processing capabilities
Modelling the specimen	D3PLOT Animation
Meshing	Eigen Mode Animation
Importing different format files	BINOUT Processing
Editing the imported files	DYNAIN Generation
Model-checking	ASCII Plotting
Metal forming	Time history plotting
Timestep checking	Fringe Plotting

3.3 Capabilities of LS-DYNA

Analysis capabilities in modern CAE software are extended to spread composite solid, laminated composite shell, sandwich shell, fatigue, and fracture. Typical loading situations are concentrated loads, surface forces, body forces, non-zero nodal displacement, nodal temperature gradients etc. Table 4 gives the capabilities of finite element software packages and illustrates the capabilities of LS-DYNA. (Radhakrishnan, 2008, p. 215)

Table 4. Capabilities of LS-DYNA (Livermore Software Technology Corporation, 2006)

Capabilities	Application
Static analysis	Stresses and displacements calculation of structure under static loading.
Dynamic analysis	Transient and steady-state response of a structure calculation under dynamic loading.
Modal analysis	Computation of natural frequencies associated mode shapes of the structure, response spectrum analysis, random vibration and forced vibration problems.
Stability analysis	Determination of buckling loads on the structure
Heat transfer	Computation of temperature distribution and heat flow within a structure under steady-state and transient conditions
Field problems	Analysis of field intensity and flux, the density of a magnetic field, analysis of field problems in acoustics and fluid mechanics.
Coupling effects	Solution techniques for interfacing multiple field effects such as displacement, forces, temperature, heat flows, electrical voltage and current, magnetic field intensity and flux, and fluid pressure and velocity.
Non-linear	Computations considering the temperature dependence of material properties, plasticity, non-linear elasticity, creep, swelling, large deflections, and work hardening.
Material properties	Analysis of isotropic, orthotropic, sandwich plates, and composites.

3.4 Implicit analysis in LS-DYNA

An implicit code is a numerical code which uses iterative solving method to solve the static problem. Static analysis is done using an implicit solver in LS-DYNA. In the nonlinear implicit analysis, the solution of each step requires a series of trial solutions to establish equilibrium within an individual tolerance. Implicit analysis requires a numerical solver to invert the stiffness matrix once or even several times throughout a load/time step in which matrix inversion is an expensive operation, especially for large models. (dynasupport.com, n.d.)

Benefits of implicit analysis

- Can be used to apply pre-loads (gravity, bolt pre-load) to a structure before an explicit analysis.
- Good for static and quasi-static problems.
- Time step size is in practice limited by accuracy consideration, automatic time step control is available.

Implicit keyword setup in LS-PREPOST to activate implicit analysis in LS-DYNA are as follows:

```
*CONTROL_IMPLICIT_GENERAL
*CONTROL_IMPLICIT_SOLVER
*CONTROL_IMPLICIT_SOLUTION
*CONTROL_IMPLICIT_AUTO
*CONTROL_IMPLICIT_DYNAMICS
*CONTROL_IMPLICIT_EIGENVALUE
```

Objectives of LS-DYNA Implicit

- To provide a complete implicit solver, fully comparable to any implicit code when it comes to functionality, robustness and performance.
- Implicit functionality, both linear and nonlinear, is implemented in LS-DYNA
- Efficiently parallelized code in both MPP and SMP

3.5 Explicit analysis in LS-DYNA

Explicit code is the direct solving method used to solve the dynamic problem. In the explicit analysis, no iteration is required as the nodal accelerations are solved directly. Explicit analysis handles nonlinearities with relative ease as compared to implicit analysis. (dynasupport.com, n.d.)

The explicit analysis runs into its limit for long-duration processes in which implicit analysis is more preferable than explicit analysis in LS-DYNA.

In general, implicit input card can easily be transformed into explicit input card. After running the implicit analysis, *CONTROL_IMPLICIT_GENERAL card is edited with IMFLAG= 0. Figure 14 shows transforming the implicit code to explicit code in LS-Dyna keyword.

Keyword Input Form ✕

Use *Parameter Comment
 (Subsys: 1 ellipse.k)

*CONTROL_IMPLICIT_GENERAL (1)

1	IMFLAG	DT0	IMFORM	NSBS	IGS	CNSTN	FORM	ZERO_V
	q	0.0100000	2	0	2	0	0	0

COMMENT:

```
$ imflag dt0 iefs nstepsb igso
```

IMFLAG:=Implicit/Explicit switching flag
 EQ,0: explicit analysis (default)
 EQ,1: implicit analysis
 EQ,2: explicit followed by one implicit step (springback analysis)
 EQ,4: implicit with automatic implicit-explicit switching
 EQ,5: implicit with automatic switching and mandatory implicit finish

Figure 14. Transforming to explicit analysis in LS-DYNA.

Quasi-static analysis solves the static problem in which kinetic energy should equal to zero using explicit code.

3.6 Time step Controls

Time integration is the relation between physical properties (time) with the numerical method. Time step is only specific to explicit code in LS-DYNA. During the solution, a new time step size is determined by taking the minimum value overall elements. (dynasupport.com, n.d)

$$\Delta t^{n+1} = \alpha * \min (\Delta t_1, \Delta t_2, \Delta t_3, \dots, \Delta t_n) \quad (6)$$

where n is the number of elements. For stability, the scale factor α is typically set to a value of 0.90 or smaller. (lstc.com, 2006)

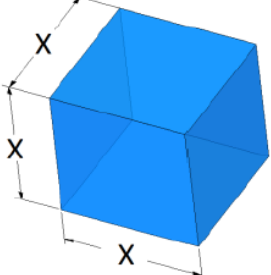
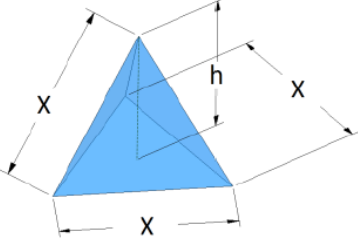
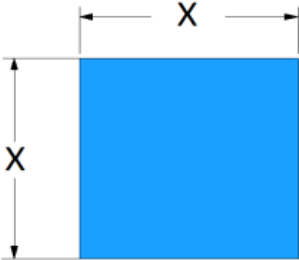
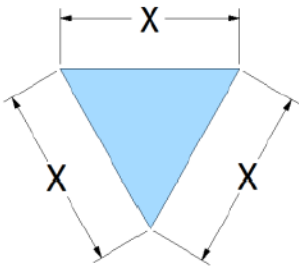
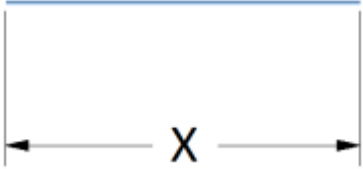
“Shock wave propagation speed in any material cannot exceed acoustic wave speed in that material” according to Courant-Friedrichs-Lewy (CFL). (Sormunen, 2016, p.9)

The maximum time step Δt that can be used in the analysis is limited by CFL condition as

$$\Delta t \leq f \left[\frac{h}{c} \right] \quad (10)$$

where c is the speed of sound in the material, f is the time step safety factor (0.9 is the default) and h is the characteristic element dimension. (simscale.com, n.d) The CFL condition restricts the wave from travelling more than the dimension h in a one-time step. Characteristic dimensions for different element types are calculated by the differential equation as shown in Table 5. (Sormunen, 2016)

Table 5. Calculation of characteristic dimension for low order element. (Sormunen, 2016)

Element Type	Geometry	Characteristic dimension(h)
Hexahedral solid		<p>The volume of the element divided by the area of the largest face</p> <p>$h=x$</p>
Tetrahedral solid		<p>Minimum distance from a node to an opposing surface.</p> <p>$h = \sqrt{\frac{2}{3}}x$</p>
Quad shell		<p>The square root of the area of the element.</p> <p>$h=x$</p>
Triangular shell		<p>Two times the area of the element divided by the length of the longest side.</p> <p>$h=x$</p>
Beam		<p>Length of the element</p> <p>$h=x$</p>

Time step Control for Beam and Truss Elements (Dynamore, 2019)

$$\Delta t = \frac{l}{c}, \quad (7)$$

where l is the length of the element and c is the sound of speed

$$c = \sqrt{\varepsilon/\rho}, \quad (8)$$

where ε is the Modulus of elasticity and ρ is the density.

4 EXPERIMENTAL TESTING RESULTS

In the lab test, IPE 100 Steel Beam of length 1700mm with steel grade S 355 was used. One end of the beam was placed in a hinge support and the other end of span was placed in a roller support. The force was applied exactly at the centre of the beam and the maximum deflection of the beam is noted as shown in Figure 15 and 16 below.

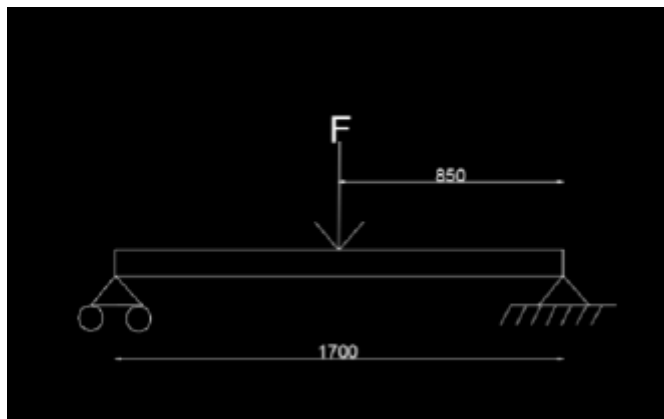


Figure 15. Simply supported beam under point loading.



Figure 16. Beam testing in Lab.

Figure 18 below shows the load versus displacement curve during the lab test. The ultimate load on the beam was 34.19 kN and its corresponding displacement was 19.12mm. Figure 17 below shows the stress versus strain curve of the steel.

Manual Analysis

From the statics table, the elastic deflection of the beam in the simply supported beam is given by

$$f = \frac{F \cdot L^3}{48 \cdot E \cdot I} \quad (9)$$

Where,

f=deflection
F=point load

L=distance between support

E=Elastic modulus

I=Second Moment Area

In this case, From the test result Figure 18

F=34.19 Kn

L=1700mm

E=210Gpa

I=1710000mm⁴

Therefore, From Equation (13), the elastic deformation corresponding to maximum load is given by f,

$$\begin{aligned}
 f &= F \cdot L^3 / 48 \cdot E \cdot I \\
 &= 34.19 \cdot 1700^3 / 48 \cdot 210 \cdot 171000 \\
 &= 9.74 \text{ mm}
 \end{aligned}$$

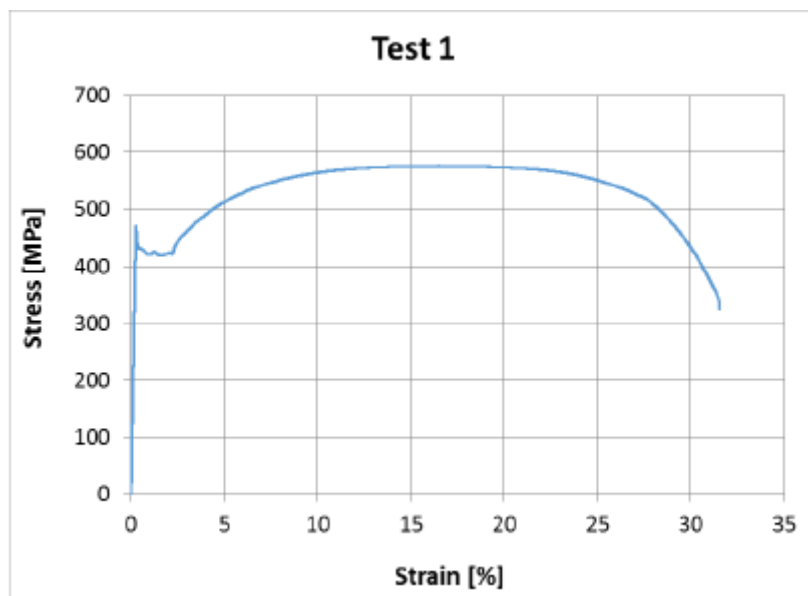


Figure 17. Properties of steel, stress versus strain diagram

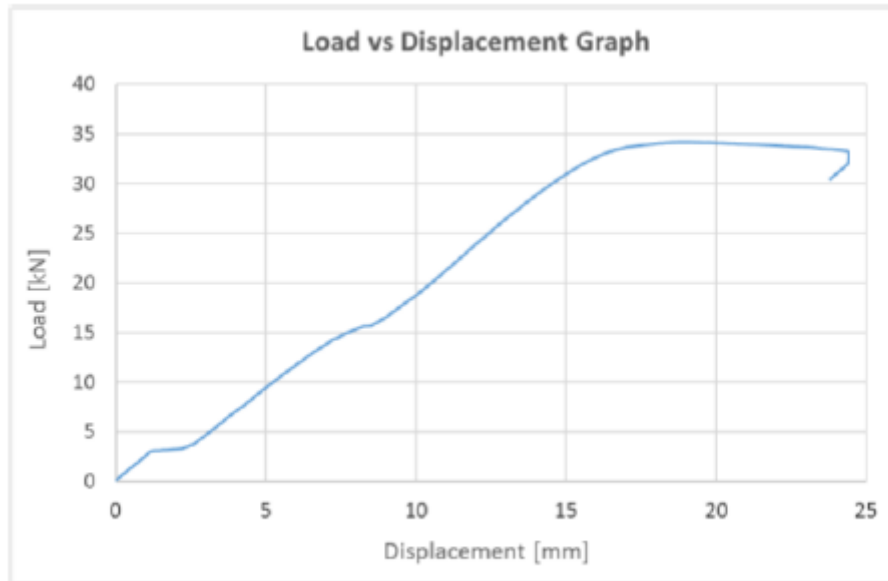


Figure 18. Load versus Displacement Graph from lab test results.

5 MANUAL CALCULATION DATA

5.1 Element size calculation

In numerical modelling, element size is defined by mesh refinement. During this research analysis time step (Δt) was defined as 0.3 microseconds for the calculation of the fine mesh size. The formula used in the calculation of the element size taken from excel sheet is described below in Figure 19.

In an explicit analysis, the time step is affected by element size and material wave speed. Time step is proportional to the element size/ speed of a wave.

The smaller the time step, the more steps it takes to complete the analysis and more time steps means longer run time at LS-DYNA. (dynasupport.com, n.d)

$$\text{Speed of sound } (c) = \sqrt{\epsilon/\rho}$$

$$\text{Characteristic length } (L_c) = \Delta t \times c$$

$$\text{Edge Length } (L_e) = \sqrt{2} \times L_c$$

User defined	Micro Sec	Sec																
Time Step(Delta T)	0,3	0,0000003																
Formula																		
Sound Speed(c)	SQRT(E/Rho)																	
Characteristic Length	Lc=(Delta T)*C																	
Edge Length, Le	Le=SQRT(2)*Lc																	
Value																		
SQRT (2)	1,414213562																	
Material	(Delta T) sec	Modulus of elasticity(E	Density(kg/m3)	Speed of Sound(m/s)	Chaeristic Length, Lc (m)	Edge Length le(m)	Edge Length Le(mm)	Chareistic length (mm)	DT 2ms	Speed (c)mm/sec								
Steel	0,0000003	2,10E+11	7850	5172,194153	0,001551658	0,002194376	2,194376136	1,551658246	4,24E-07	5172194,153								

Figure 19. Element size calculation in Excel sheet.

5.2 Effective plastic stress-strain calculation

The methodology of engineering to true strain and true stress is described below shortly. Figure 20 shows effective plastic stress-strain calculation in Excel sheet. (dynasupport.com, n.d)

True strain = $\ln(1 + \text{engineering strain})$ where \ln is the natural log

True stress = (engineering stress) \times exp (true strain)
 = (engineering stress) \times (1+ engineering strain)

where exp (true strain) is 2.71 raised to the power of (true strain).

Calculating the effective plastic strain from using the experimental data from true stress vs true strain curve.

effective plastic strain (input value) = total true strain – true stress/E

Engineering Strain	Engineering Stress	True Strain	True Stress	Effective PI strain	Effective plastic stress
0,00209	402,253	0,002088	403,0937	0,000168325	403,0937088
0,00584	429,699	0,005823	432,2084	0,003764878	432,2084422
0,02728	453,507	0,026915	465,8787	0,024696063	465,878671
0,03652	482,183	0,035869	499,7923	0,033488985	499,7923232
0,06574	537,572	0,063669	572,912	0,060941241	572,9119833
0,08375	554,965	0,080427	601,4433	0,077563233	601,4433188
0,12266	572,385	0,115701	642,5937	0,112640899	642,5937441
0,14213	575,564	0,132895	657,3689	0,129764612	657,3689113

Figure 20. Effective plastic strain calculation sheet from Excel.

Figure 21 shows the graphical representation of the engineering stress and strain, effective plastic strain and true strain versus stress curve.

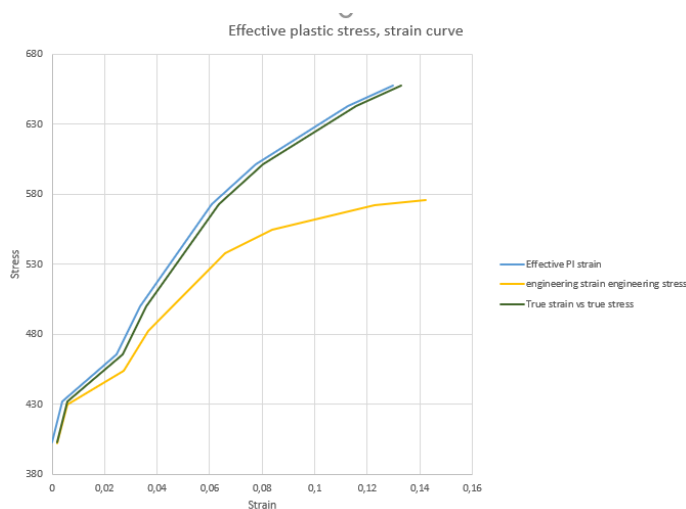


Figure 21. Graphical representation of Effective stress, strain curve after calculation.

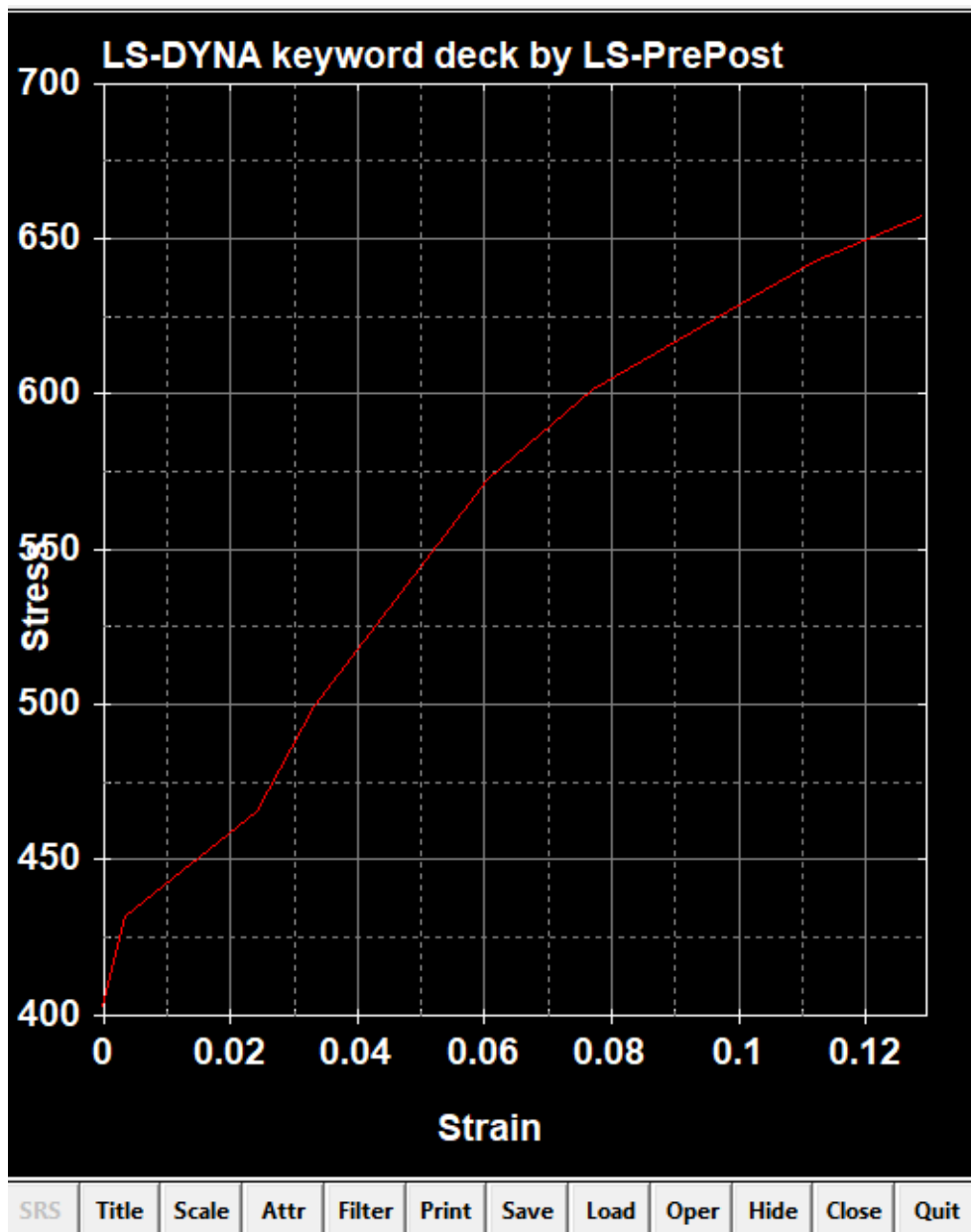


Figure 22. Effective plastic stress-strain curve in LS-PrePost after inputting values.

The data illustrated in Figure 22 above was taken for the material linear plasticity (Mat-24) in LS-PrePost.

5.3 Temperature calculation of steel beam under ISO fire

The temperature distribution and time history in the cross-section were conducted in the Excel for unprotected steel members under fire. The temperature of the carbon steel was calculated in every 5 seconds till 2000 seconds under fire. Later these value time in second and temperature of the carbon steel were used to run structural analysis in LS-DYNA. Below is the process of Excel calculation of the steel beam under fire.

Properties of carbon steel taken from Eurocode.
According to EN 1994-1-2,

The density of carbon steel (ρ) = $7850 \frac{\text{kg}}{\text{m}^3}$

Coefficient of heat transfer (α_c) = $25 \frac{\text{W}}{\text{m}^2 \cdot \text{K}}$

The surface emissivity of the member (ϵ_m) = 0.7

The emissivity of the fire (ϵ_f) = 1

Configuration factor (Φ) = 1

Specific heat capacity of the carbon steel (c_a) = $420 \frac{\text{J}}{\text{kg} \cdot \text{K}}$

Properties of IPE 100 steel beam exposed on fire,

Depth(h) = 100mm

Width(b) = 55mm

Web thickness(s) = 4.1mm

Flange thickness(t) = 5.7mm

Fillet(r) = 7mm

Section area (A) = 1030m²

According to the EN 1994-1-2,

Surface area of steel exposed on fire is given by (A_m) = $2 \cdot h + 4 \cdot b + 2 \cdot \pi \cdot r - 8 \cdot r - 2t$
= 397mm

Table 4.1: Definition of section factors for unprotected steel members

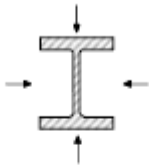
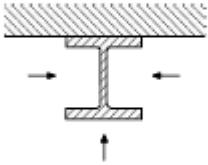
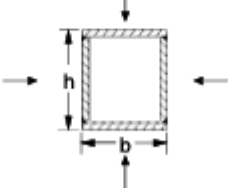
Sketch	Description	Section factor (A_m/V)
	4 sides exposed	$\frac{\text{steel perimeter exposed to fire}}{A}$
	3 sides exposed	$\frac{\text{steel perimeter exposed to fire}}{A}$
	4 sides exposed	$\frac{2(b+h)}{A}$
Note: A is the steel cross section area.		

Figure 23. Definition of section factor from EN 1994-1-2.

$$\text{Section factor } \left(\frac{A_m}{V}\right) = \frac{\text{Surface area} \cdot 1000}{\text{Area of IPE beam exposed to fire}} = 385.049 \frac{1}{m}$$

Where Figure 23 above illustrates the rate at which a steel member will increase in temperature is proportional to the surface, A, of steel, exposed to the fire and inversely proportional to the mass or volume (V) of the member. In the fire, a member with a low section factor will heat up more slowly than the one with a high section factor.

Sketch	Section factor $[A_m/V]_b$
	$\frac{2(b+h)}{\text{Steel cross-Section area}}$
	$\frac{2h+b}{\text{Steel cross-Section area}}$
	$\frac{\text{box perimeter}^*}{\text{Steel cross-Section area}}$

Figure 24. Box value of the section factor $[\frac{A_m}{V}]_{\text{box}}$

Above Figure 24 shows the formula for the calculation of section factor under different condition of heat in the section.

Surface factor $[\frac{A_m}{V_b}] = 2(b+h) = 310\text{mm}$, in our case for the section exposed with fire in four sides of the structure.

Where $[\frac{A_m}{V_b}]$ is the box value of the section factor.

Influence of shape on the shadow effect,



Figure 25. Influence of shape on the shadow effect.

Above Figure 25 shows the influence of shape on the shadow effect taken from the Eurocode. For cross-sections with a convex shape (e.g. rectangular or circular hollow sections) fully embedded in the fire, the shadow effect does not play a role and consequently the correction factor k_{sh} equals unity. For I-section under nominal fire actions, the correction factor for the shadow effect may be determined from.

$$\text{Correction factor } (k_{sh}) = 0.9 \frac{\frac{A_{m,box}}{v}}{\frac{A_m}{v}}$$

The time interval (Δt)=5s

$$\text{Time in minute } (T_m) = \frac{\Delta t}{60}$$

Nominal Temperature-Time Curves

Temperature-time curves are analytical functions of time that give the temperature. The term curve comes from the fact that these functions are continuous and can be used to draw a curve in a time-temperature plane.

Eurocode 1 proposes three different nominal temperature-time curves. The standard temperature-time curve is the one that has been historically used, and it is still used today, in standard fire tests to rate structural and separating elements. It is often referred to as the ISO curve because the expression was taken from the ISO 834 standard. This standard curve is given by

$$\theta_g = 20 + 345 \log_{10}(8t + 1) \quad (14)$$

where θ_g is the gas temperature in degree C and t is the time in minutes?

The surface temperature of the steel $\theta_m = 20$

$$\text{Heat convection } (h_{net.c}) = \alpha_c (\theta_g - \theta_m)$$

$$\theta_r = \theta_g$$

Heat radiation

$$h_{net.r} = \Phi \cdot \varepsilon_f \cdot \varepsilon_m \cdot 5.67 \cdot 10^{-8} \cdot \{(\theta_r + 273)^4 - (\theta_m + 273)^4\} \quad (15)$$

The same formula is applied to calculate the temperature of steel in every 5 seconds till 2000 second more calculation is presented in Excel file in Appendix 2. Figure 26 represents the temperature of steel and gas till 2000 seconds calculated in Excel which shows the temperature of steel is about 880° C in 2000 seconds.

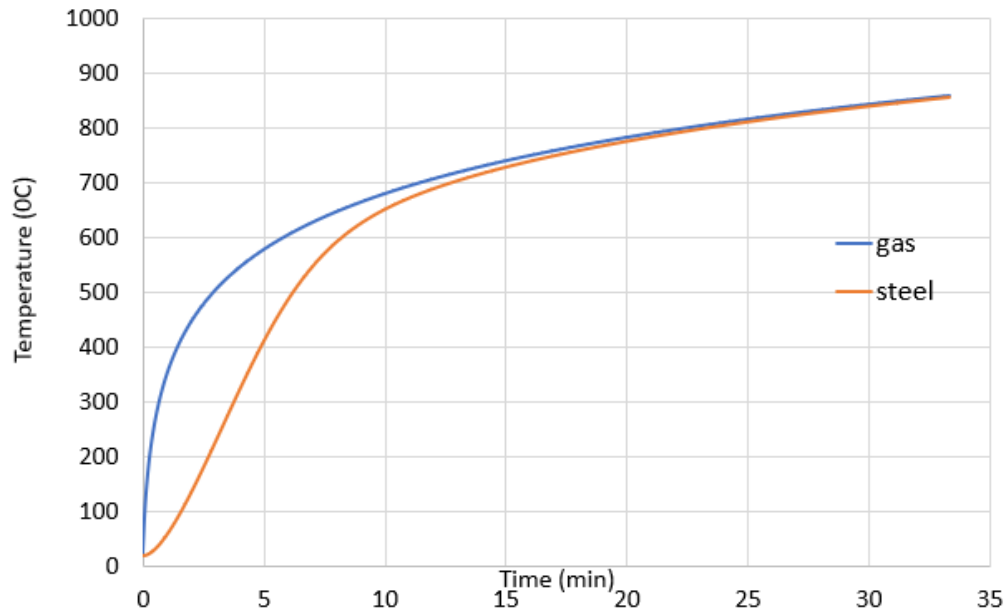


Figure 26. Graphical representation of gas and steel temperature till 2000 seconds.

6 3D FINITE ELEMENT MODEL DESCRIPTION

6.1 3D Modelling of the geometry in LS-PRE-POST

6.1.1 General dimensions and process of modelling in LS-PrePost

The Finite Element model is created using shell element with ELFORM 16 (fully integrated shell element modified for higher accuracy) in LS-PrePost. Figure 27 shows the dimensions of IPE Beam. The same specimen and same dimension were used in a lab test and FE model created on LS-PrePost with the length of 1700mm. Figure 27 shows the cross-section of a simply supported beam.

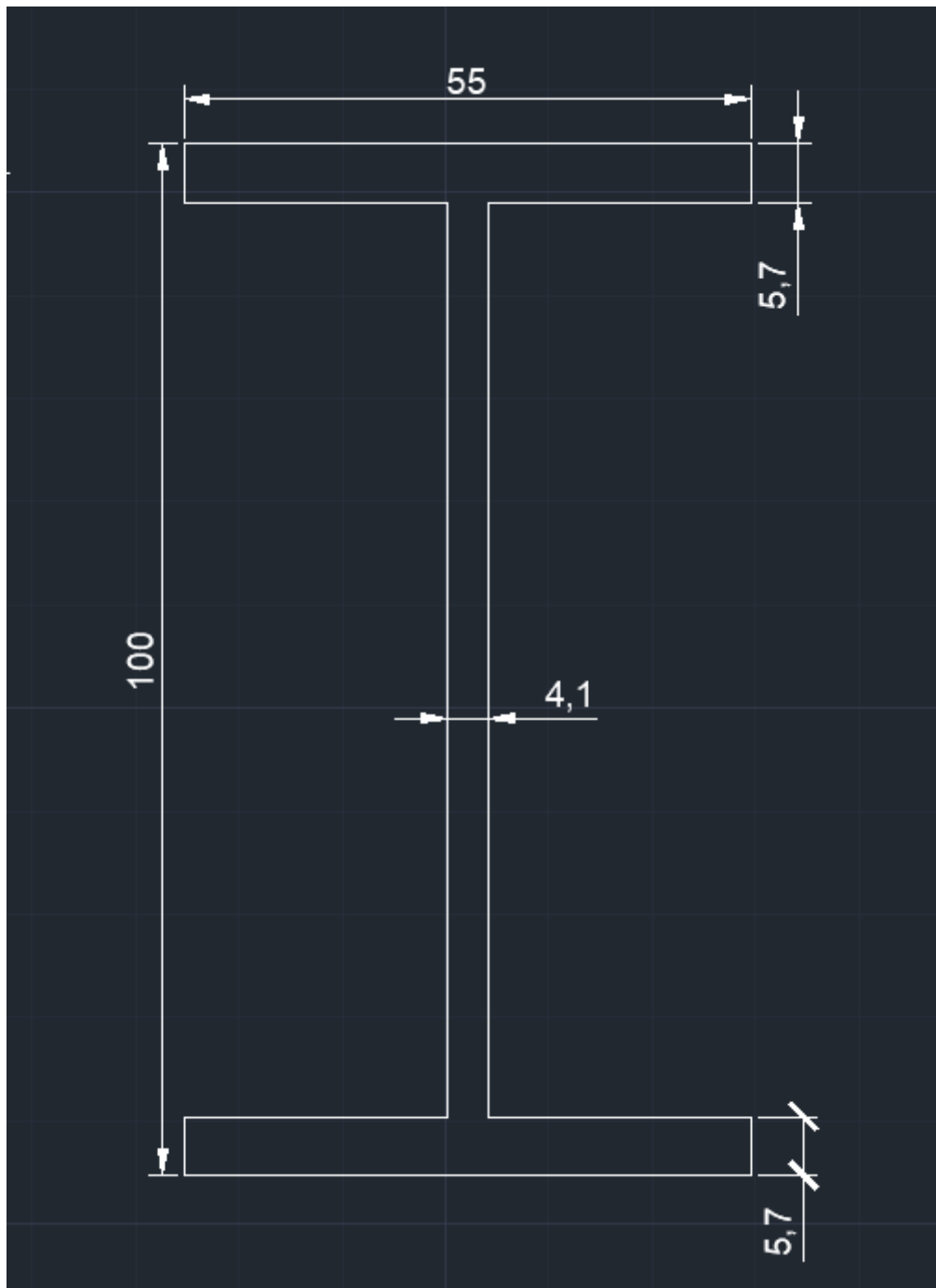


Figure 27. Cross-section of IPE 100 beam.

Figure 28 shows the definition of the dimensions of the IPE Beam in LS-PrePost(v4.6.8-29May2019). Seven points $(0,0,0)$, $(0, 47.15,0)$, $(27.5, 47.15, 0)$, $(-27.5, 47.15, 0)$, $(0,-47.15,0)$, $(27.5, -47.15,0)$ and $(-27.5, -47.15, 0)$ individually along (x,y,z) direction. Figure 29 shows the result after above inputs in LS-PrePost.

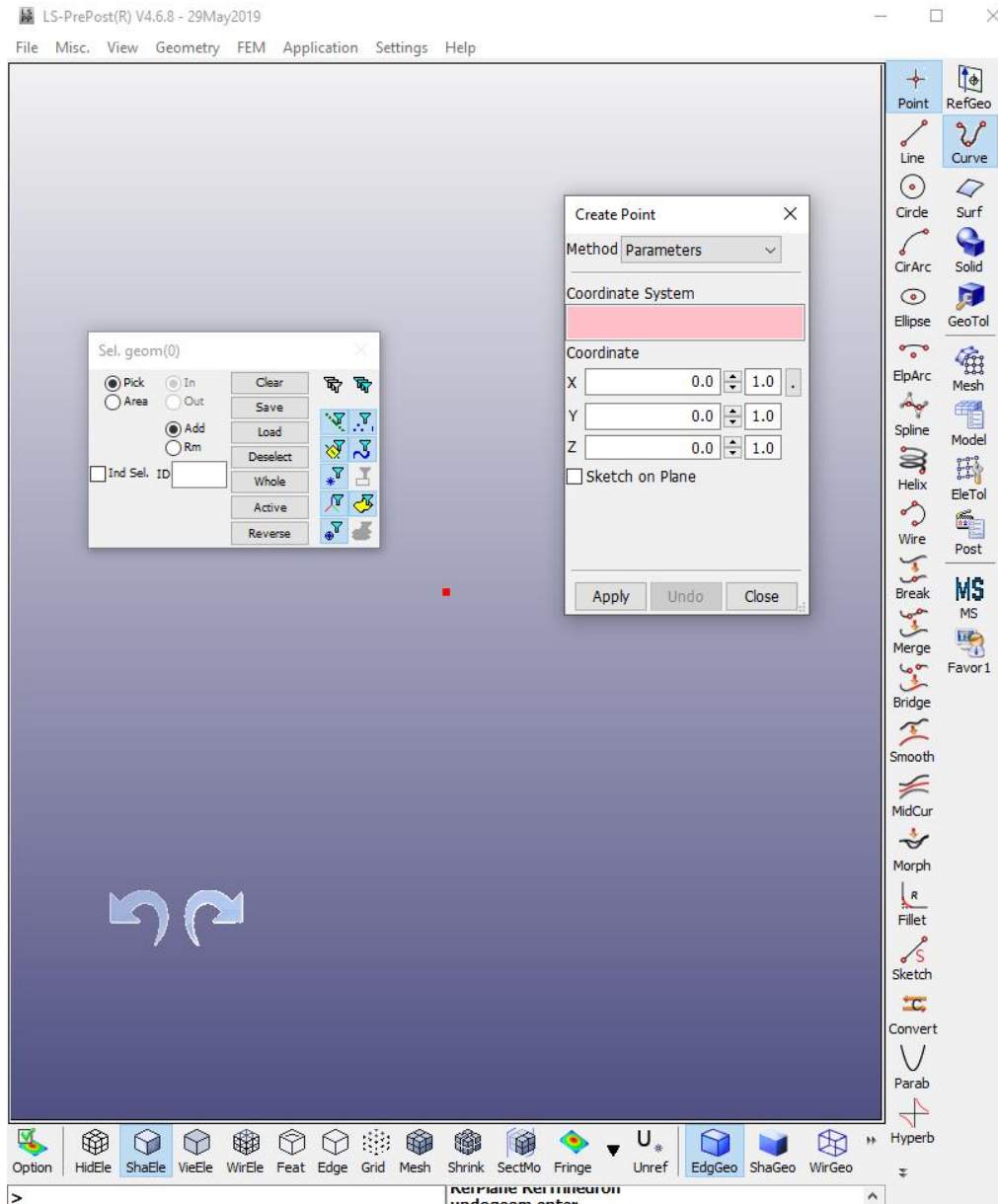


Figure 28. 3D point input in LS-PrePost.

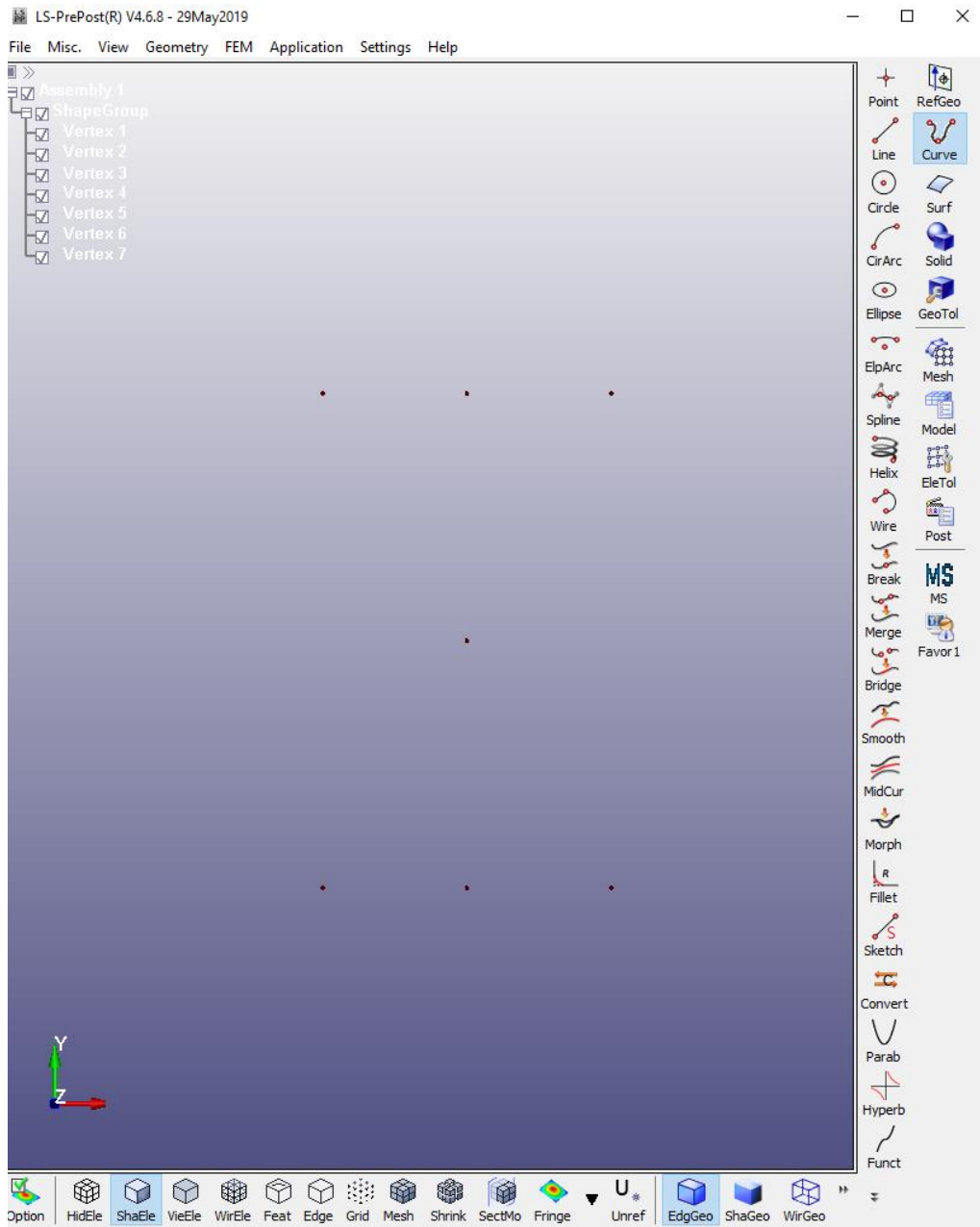


Figure 29. 3D Sketch input of point in LS-PrePost.

Figure 30 below shows the input parameter of the line segment of IPE Beam in LS-PrePost. Three lines were created one by one as shown in Figure 30.

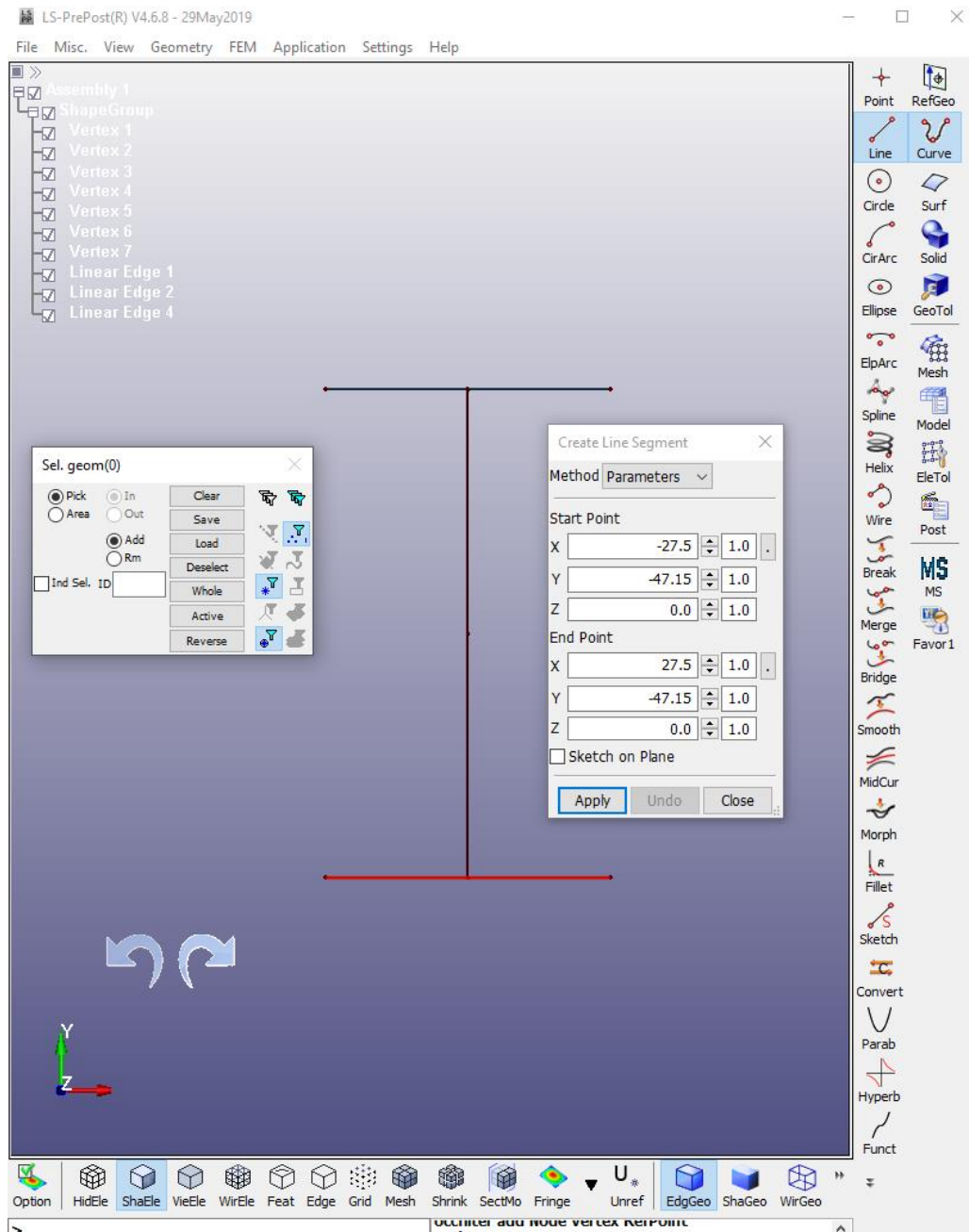


Figure 30. 3D sketch input of line segment in LS-PrePost.

Figure 31 below shows the 3D model of IPE Beam in LS-PrePost. After the input of the line segment, the length of 1700 mm is extruded through the surface and extrude command in LS-PrePost.

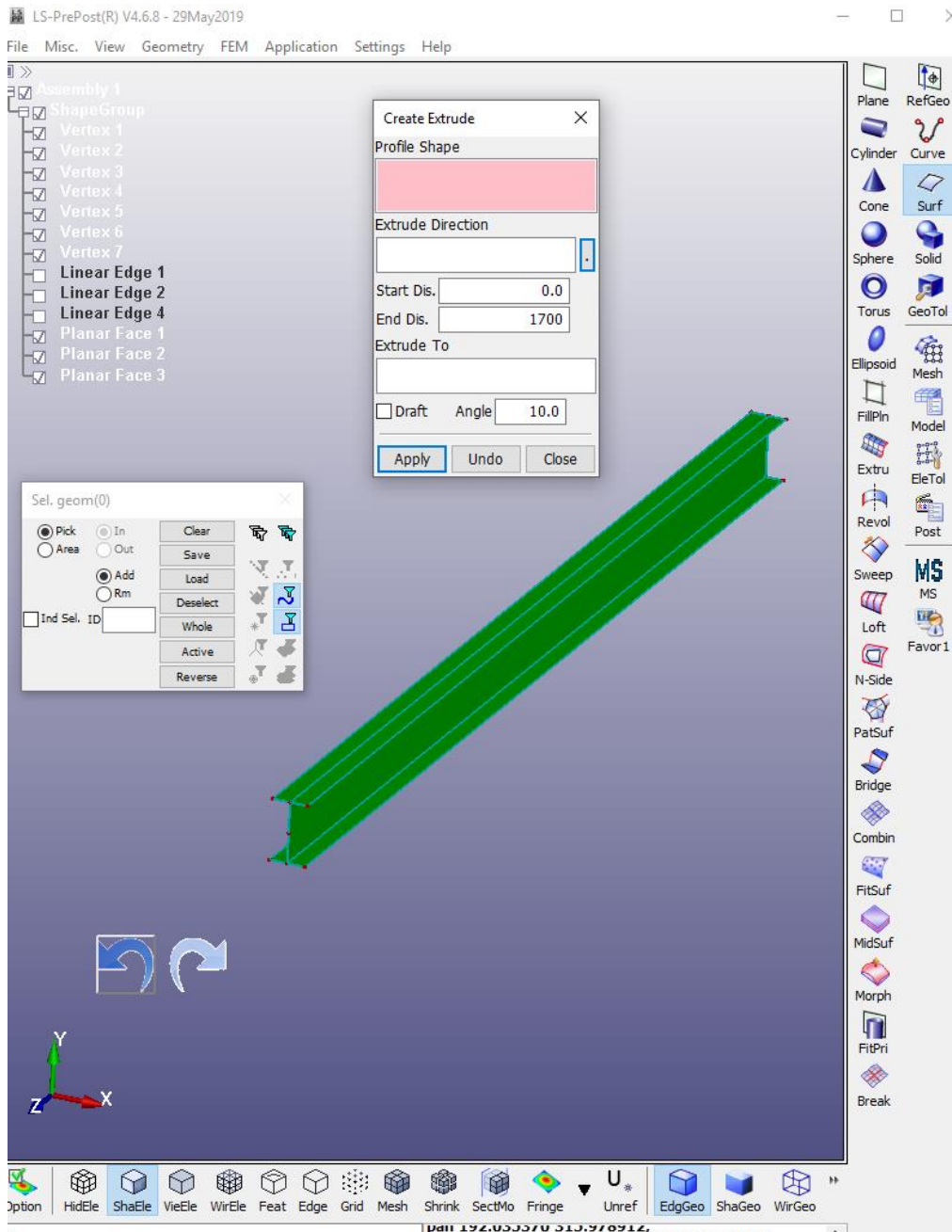


Figure 31. 3D model of IPE Beam in LS-PrePost.

6.1.2 Meshing

The IPE Beam has meshed with mixed type mesh with triangular and square types of mesh as shown in Figure 32. Mesh was created from Auto Mesher in LS-PrePost with the average value of 2.19mm mesh size.

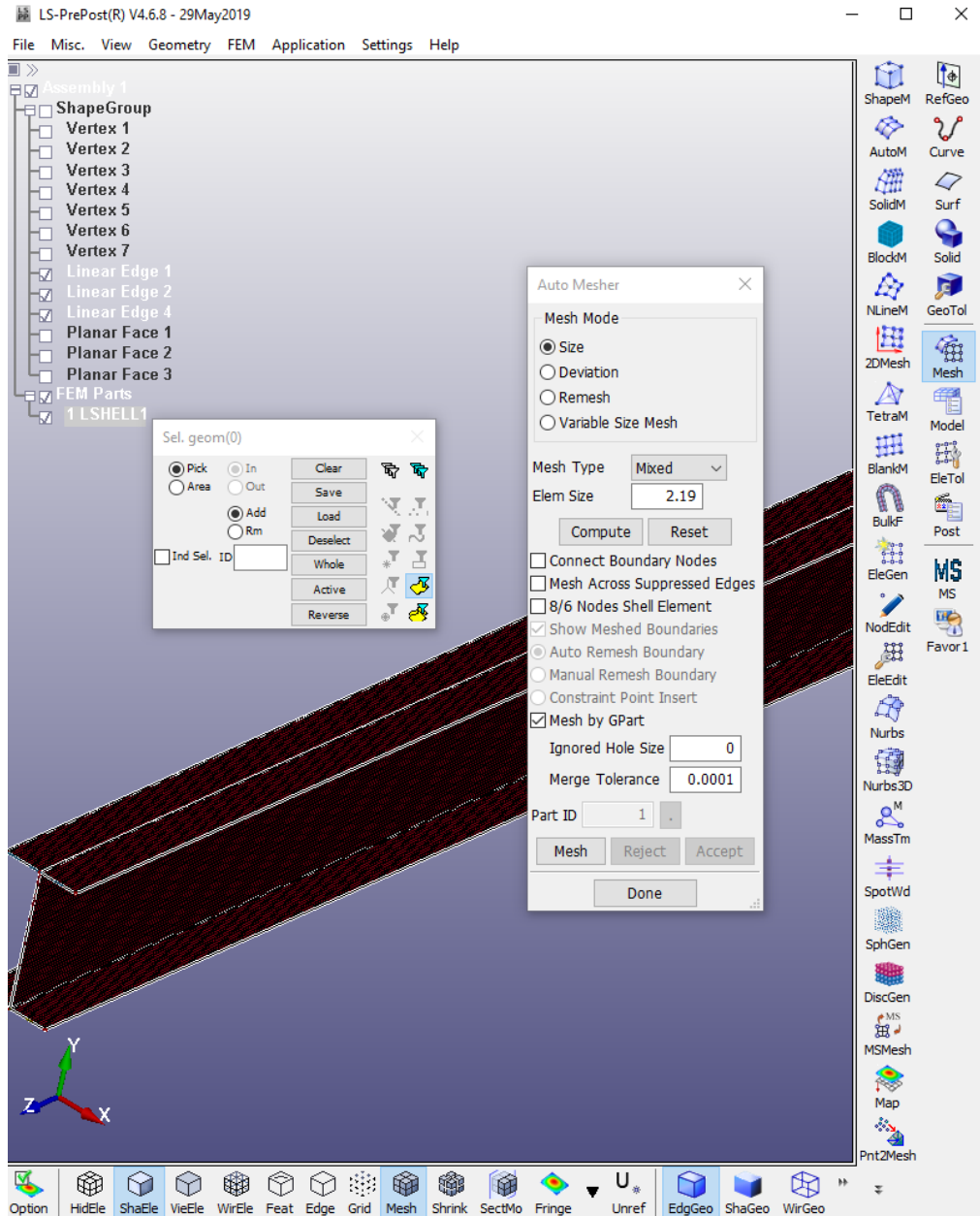


Figure 32. The meshing of IPE Beam in LS-PrePost.

6.1.3 Creation of Three different Part ID

This chapter shows how we can separate the Part ID in LS-PrePost from the single Part ID meshing. This is done using move or copy tool as in figure 33 below which separates the Part ID.

Whereby creating the mesh three-time can also be done during auto mesh which makes the process complicated and long.

As shown in Figure 33 using the move tool, the three-part id is created. Here unique name should be given each time.

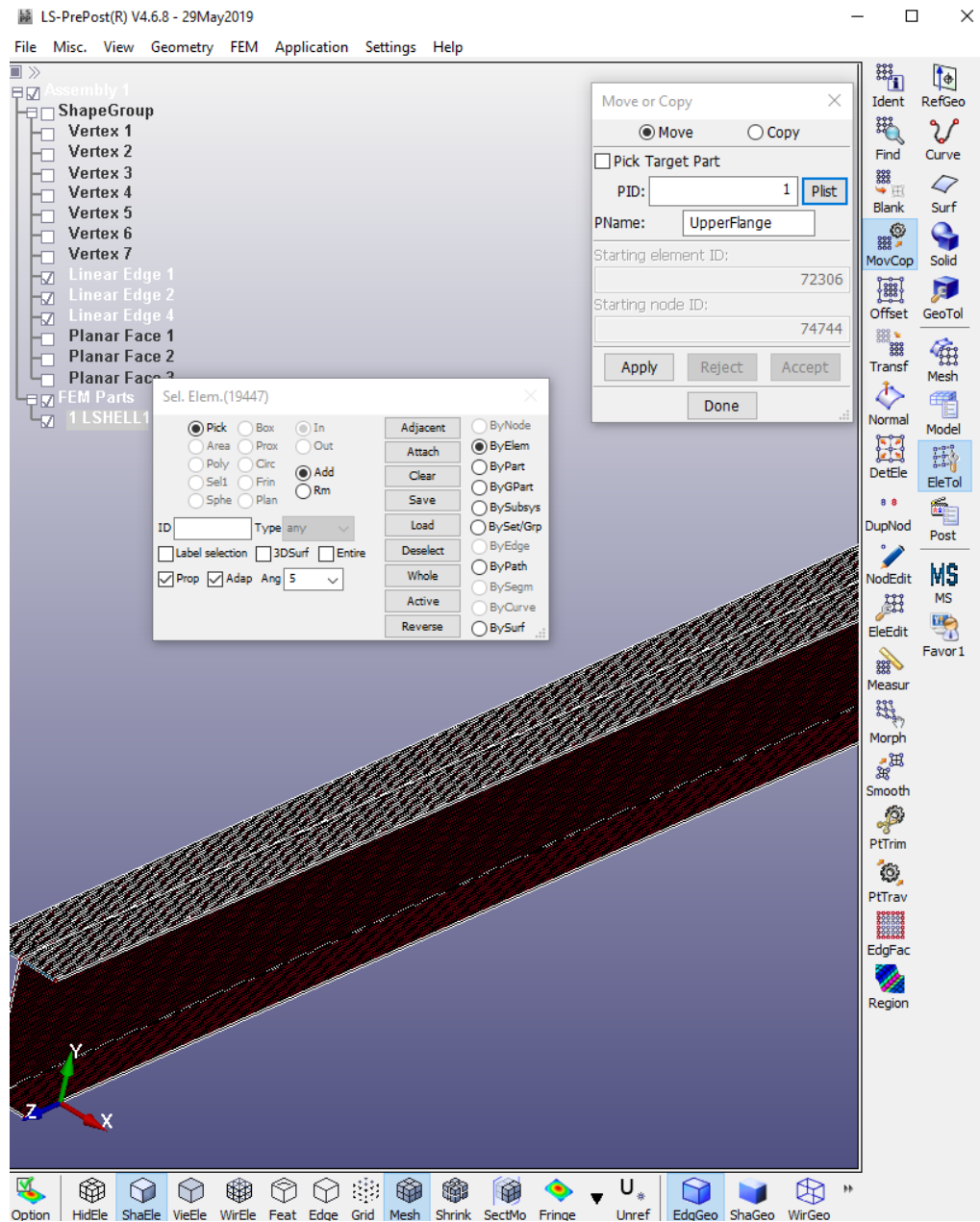


Figure 33. Process of separating the Part ID in LS-PrePost.

6.2 Boundary Conditions

Seven boundary conditions, shown in Figure 34, were applied in the model. From the create entity keyword different boundary conditions were created from set data set node in LS-PrePost. The different colour which represents the different node selected for the definition of the boundary conditions.

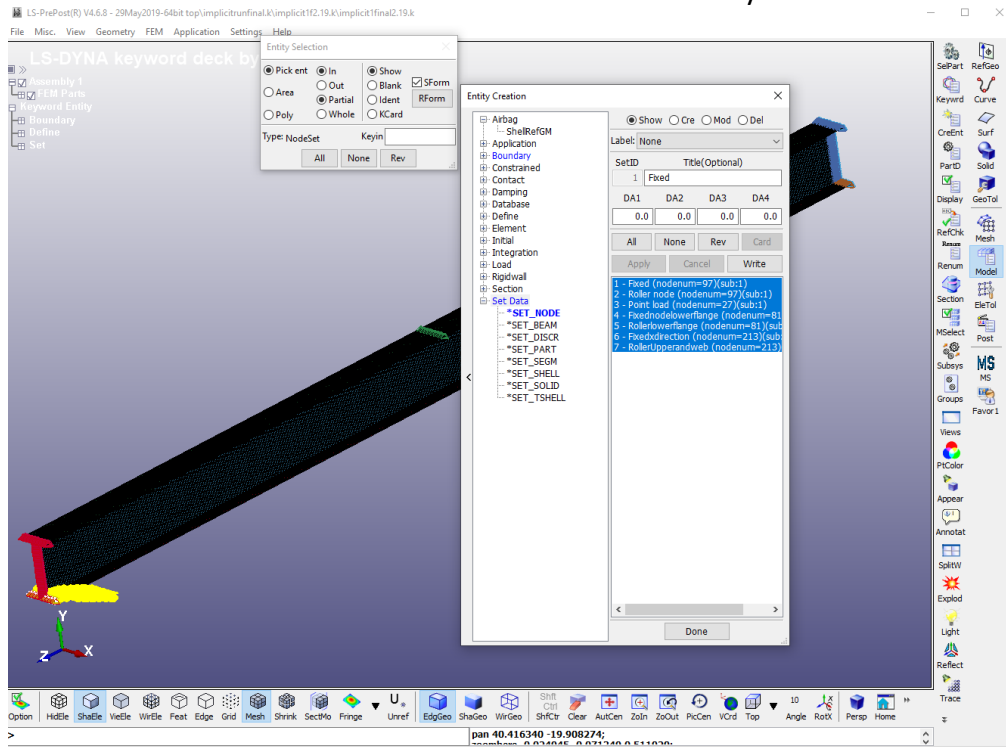


Figure 34. Creating an entity in LS-PrePost for the definition of Boundary condition (BC).

Figure 35 shows the definition of the Displacement loading in the IPE Beam from the keyword manager tool. Degree of Freedom for the displacement loading was along the z-direction.

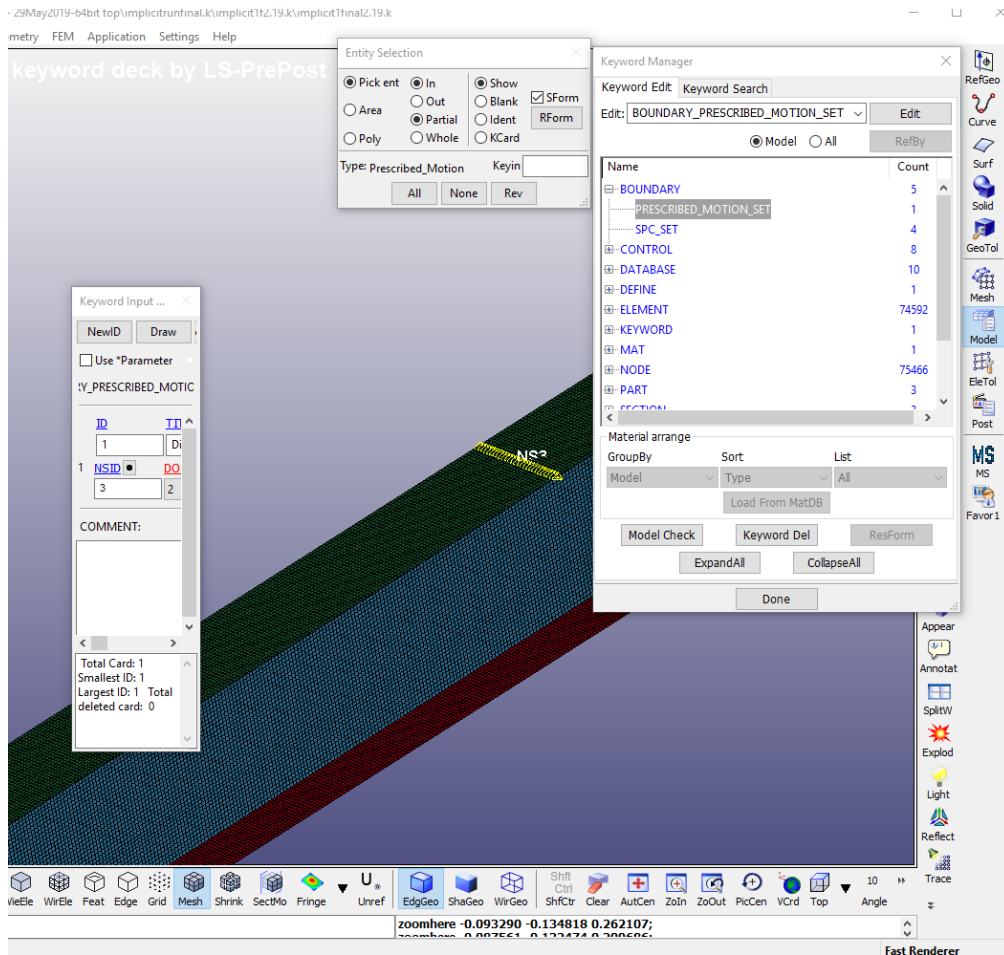


Figure 35. Connecting the set data with BC in LS-PrePost.

6.3 Material

Stainless steel IPE beam was modelled as an elastoplastic material during this research in LS-PrePost. Table 6 shows the material parameters used for steel.

Table 6. Material properties of the steel IPE Beam.

Property	Value
Modulus of Elasticity(E)	2.100e+05 Newton/ mm2
Mass density (ρ)	7.850e-09 ton/mm3
Poisson`s ratio (PR)	0.30
Yield stress (SIGY)	355 Mpa

*Mat- 024_PIECEWISE_LINEAR_PLASTICITY which is an elastoplastic material was used during the modelling of IPE Beam in LS-PrePost. Figure 36 below gives a detailed input in LS-PrePost. The effective plastic stress (EPS1) and strain (ES1) value were taken from the manual calculation from chapter 5.2.

Keyword Input Form

NewID MatDB RefBy Pick Add Accept Delete Default Done

Use *Parameter Comment (Subsys: 1 implicit1final2.19.k) Setting

*MAT_PIECEWISE_LINEAR_PLASTICITY_(TITLE) (024) (1)

TITLE
Steel

1	MID	RO	E	PR	SIGY	ETAN	FAIL	TDEL
	1	7.850e-09	2.100e+05	0.3000000	355.00000	0.0	1.000e+21	0.0
2	C	P	LCSS	LCSR	VP			
	0.0	0.0	0	0	0.0			
3	EPS1	EPS2	EPS3	EPS4	EPS5	EPS6	EPS7	EPS8
	0.0	0.0035844	0.0245015	0.0332803	0.0607020	0.0773121	0.1123726	0.1294901
4	ES1	ES2	ES3	ES4	ES5	ES6	ES7	ES8
	403.09369	432.20840	465.87869	499.79230	572.91199	601.44330	642.59381	657.36890

Plot Raise New Padd

Total Card: 1 Smallest ID: 1 Largest ID: 1 Total deleted card: 0

Figure 36. Keyword input for Steel IPE Beam in LS-PrePost.

6.4 Choice of the element type in LS-DYNA

During this research shell sections were created during modelling of IPE Beam. Shell elements are suitable for modelling structures that have one-dimension thickness small compared to the other side of the structure.

There are forty (40) available shell element formulation options that can be chosen for the model. Choosing the right element formulation depends on terms of robustness, accuracy and speed with full integration. From an accuracy standpoint, shell type 16 is preferred over under integrated formulations. Shell type 16 is chosen for modelling the section as shown in Figure 37. (LS-DYNA Theory Manual, 2006)

Keyword Input Form

Use *Parameter
 Comment
 (Subsys: 1 explicitfinal6.57.k)

*SECTION_SHELL_(TITLE) (3)

TITLE
Upperflange

1	SECID	ELFORM	SHRF	NIP	PROPT	QR/IRID	ICOMP	SETYP
1	16	1.0000000	7	1	0	0	1	

2	T1	T2	T3	T4	NLOC	MAREA	IDOF	EDGSET
5.6999998	5.6999998	5.6999998	5.6999998	0.0	0.0	0.0	0	

Repeated Data by Button and List

Data Pt.

Total Card: 3 Smallest ID: 1 Largest ID: 3 Total deleted card: 0

Figure 37. Element formulation type 16 keyword in shell section.

7 MESH SENSITIVITY ANALYSIS

In Finite element analysis, the size of the mesh is critical. The size of the mesh is closely related to the accuracy and number of mesh required for the meshing of the element. According to the theory of Finite Element Analysis, the finite model with small element size yields high accuracy as compared to the model with large element size. This chapter presents mesh sensitivity analysis with different element size using implicit code in 7.1 and explicit code in 7.2.

7.1 Mesh sensitivity analysis using implicit code

Convergence study on the different mesh size was studied in this finite element simulation model using implicit analysis in LS-Dyna. From the manual calculation of the element size, Figure 18 shows an edge length of 2.1943 mm for the fine mesh of the FE model. So, for the point load to be exactly on the middle node element size of 2mm was meshed. Four different mesh sizes were created in this research to accurately correlate with the test data. The mesh sizes ranged from 2 mm to 8mm as shown in Figure 38 below.

The results, plotted in Figure 38, shows that there is a huge change in the shape of the force history. For the mesh size of 2mm maximum force was 34.30 kN for 4mm maximum force of 30.50 kN, for 6mm maximum force of 36.30 kN and for 8mm maximum force of 34.20 Kn.

Four finite element model with the different mesh size of 2mm, 4mm, 6mm and 8 mm were modelled in LS-Prepost. In all four finite element model material properties, boundary conditions and load defined are similar. The models were run using implicit static analysis in LS-DYNA.

Figure 38 below illustrates the load vs displacement curve of the simply supported beam when the point load is applied in the mid-span of the beam. The maximum displacement for 2mm mesh size was 13mm while the load was 34.34 kN, for 4mm mesh size was 15 mm and load 30.54 kN, for 6mm mesh size model was 20 mm displacement and load 36.34 kN and for 8mm mesh size model 15.1 mm and load were 34.20 Kn. Figure 39 shows the finite element model of a simply supported beam with different mesh sizes.

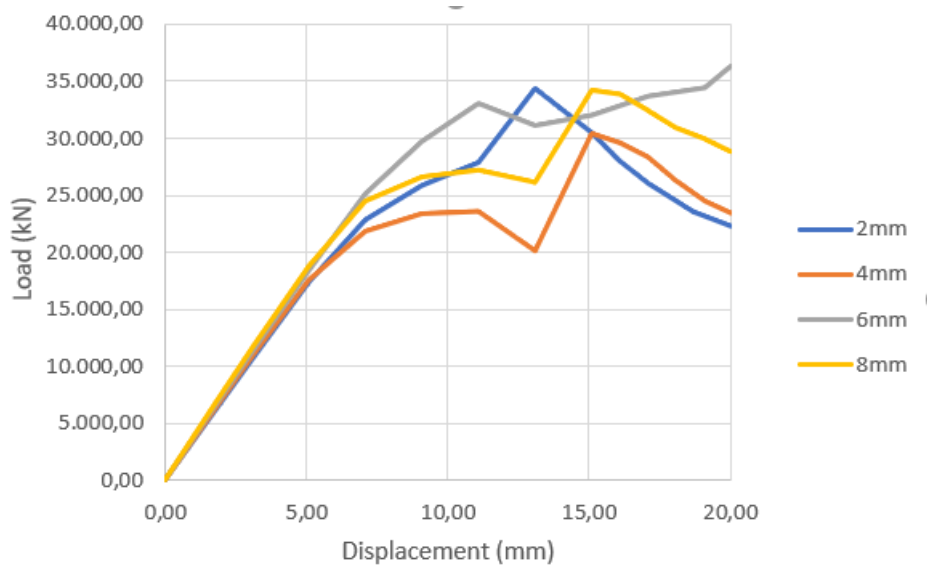
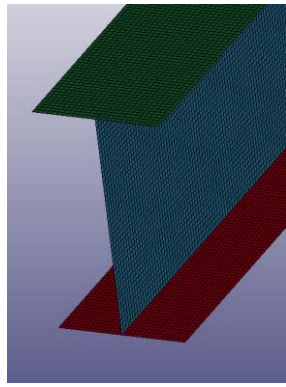
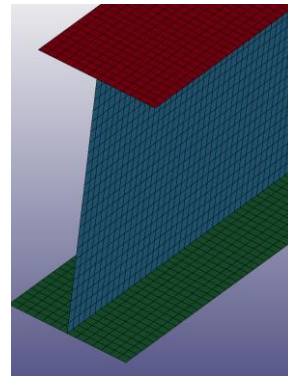


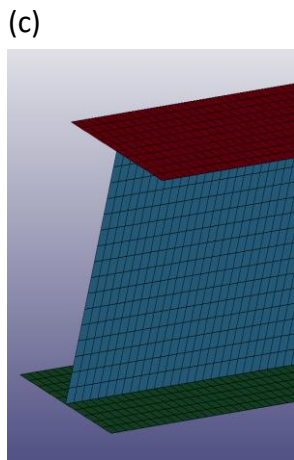
Figure 38. Load versus displacement curve of a simply supported beam with different mesh size.



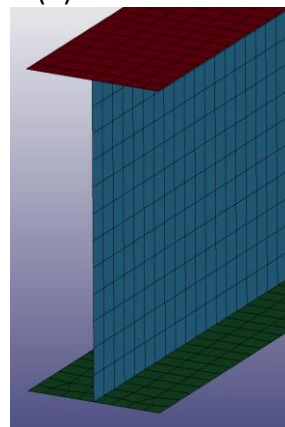
(a)



(b)



(c)



(d)

Figure 39. Meshing with the different element size of IPE beam in LS-PrePost of (a) 2mm (b) 4mm (c) 6mm (d) 8mm

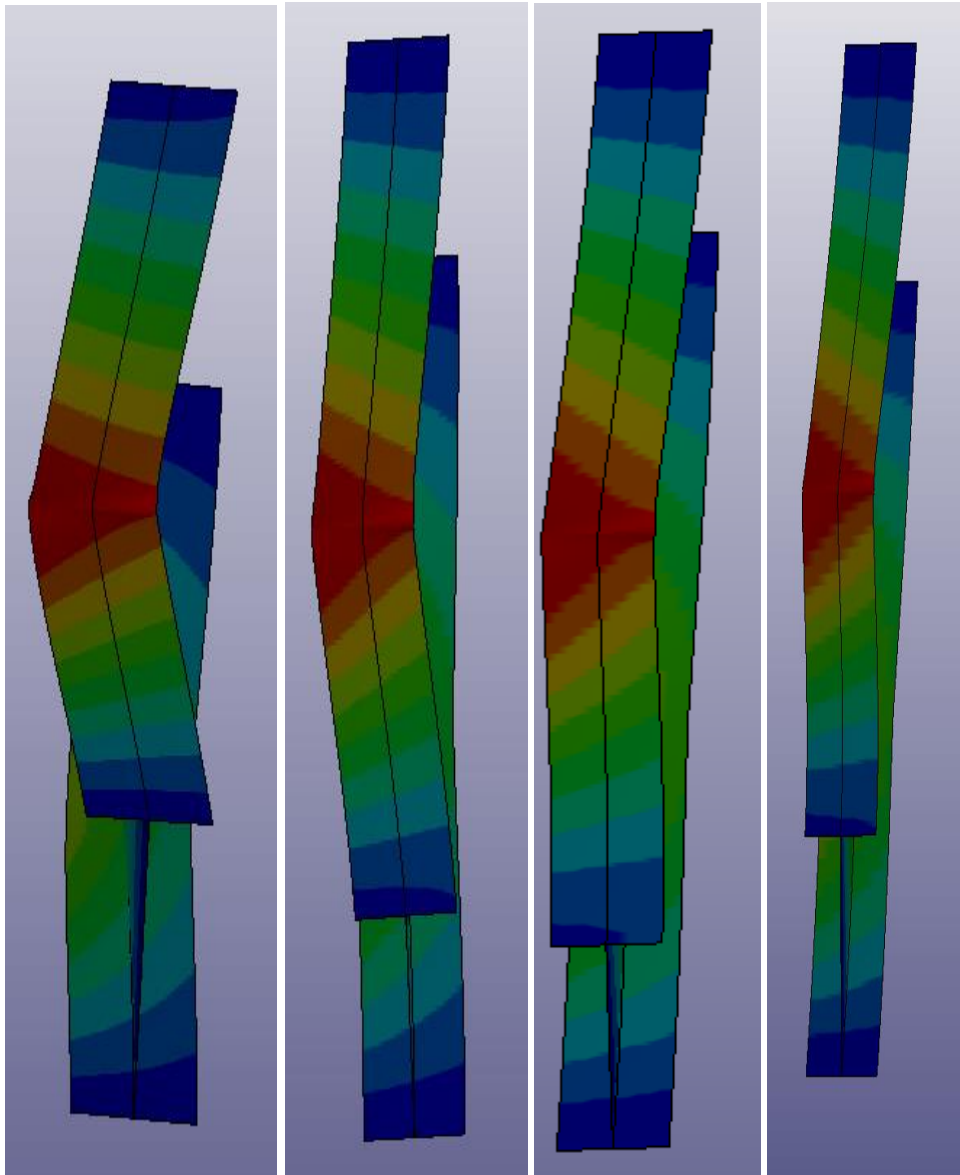


Figure 40. Displacement resultant of a simply supported beam (a) 2mm mesh (b) 4mm mesh size (c) 6mm mesh size and (d) 8mm mesh size.

Figure 40 above shows that the resultant displacement of a simply supported beam with different mesh size has similar later torsional buckling and the maximum impact is in the mid-span of the beam. The maximum resultant displacement was seen in fine mesh size of 2mm with 35.60mm, 31mm in 4mm mesh size, 27 mm in 6mm and 27mm in 8mm mesh size finite element model.

The results, plotted in Figure 38, show that there is a huge change in the shape of the force history as well as in the peak force as the mesh is refined. The solution time was also monitored along with the accuracy of the predicted force. The smallest mesh size of 2mm took 11 minutes and 41 seconds while the largest mesh size of 8mm took 44 seconds only while running with implicit analysis in LS-DYNA.

From the mesh sensitivity analysis results in Figure 38 analyzing the load-displacement curve of four different finite element model of the simply supported beam, it was observed that there was some error in a mesh sensitivity analysis. It was difficult to determine which element size was sufficient. Implicit static analysis was unsuccessful for the mesh sensitivity analysis in this research work.

7.2 Mesh Sensitivity analysis using explicit code

Again, to perform the mesh sensitivity analysis new finite element was modelled to run with the explicit code in LS-DYNA. The finite element model was modelled with different element size because while running the element size of 2 mm and 4mm it was taking more than 14 hours run time in LS-DYNA. In our University computers are automatically shut down after 14 hours So, a new finite element model was modelled with 12mm and 14mm element size.

Four finite element models with the different element size of 6mm, 8mm, 12mm, and 14mm were modelled in LS-PrePost. In all finite element material properties, boundary conditions and load defined are similar. The models were run using explicit static analysis in LS-DYNA.

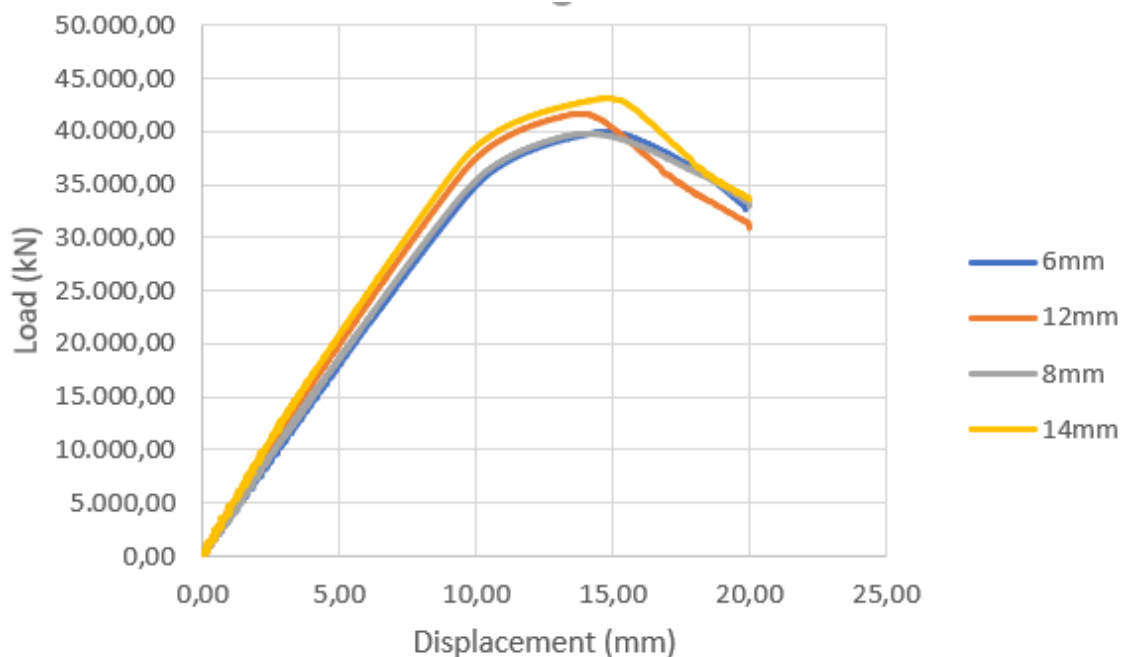


Figure 41. Load versus displacement curve of a simply supported beam with different mesh size.

Table 7. Mesh sensitivity analysis results.

Mesh size (mm)	Von mises (Mpa)	Number of nodes	Number of Elements	Simulation runtime
6mm	597	10545	10224	2hour 5 minutes
8mm	635	5373	5134	1hour 49 minutes
12mm	558.335	2447	2288	20 minutes 35 seconds
14mm	538.335	1853	1716	14 minutes 25 seconds

The results, plotted in Figure 41 above, show that there is little change in the shape of the load history as well as in the peak force as the mesh is refined. Table 7 shows the mesh sensitivity analysis results of the different element size. The solution was also monitored along with the accuracy of the predicted force. An explicit solver, LS-DYNA, was successful for the mesh sensitivity analysis in this research. By seeing the accuracy and the less solution time 8mm element size was sufficient.

8 STRUCTURAL RESPONSE ANALYSIS TO THERMAL LOAD IN LS-DYNA

The steel IPE beam was subjected to a thermal load in every node in the FEM model and point load in the middle of the steel IPE beam. The simulation was set up as “structural-only” analysis using static implicit time integration. For the definition of the thermal load, the keyword *LOAD_THERMAL_VARIABLE was used.

At first, FE model was created using shell elements with fully integrated shell element modified for higher accuracy. The element size of 10mm was chosen due to its shorter simulation time. Three integration points are defined through the thickness. Temperature-dependent piecewise linear plastic material model MAT255 was used in this model for shell element. The material properties and stress-strain relations are defined according to EN1993-1-2. The temperature distribution and time history in the cross-section are specified according to the

Excel calculation for the unprotected steel member open section exposed to the fire according to the EN 1991-1-2.

Keyword Input Form

NewID MatDB RefBy Pick Add Accept Delete Default Done

Use *Parameter Comment (Subsys: 1 implicitthermal14.k) Setting

*MAT_PIECEWISE_LINEAR_PLASTIC_THERMAL_(TITLE) (255) (1)

TITLE
Steel_Mat255

1	MID	RO	E	PR	C	P	FAIL	TDEL
1		7.850e-09	-2	-5	0.0	0.0	0.0	0.0

2	TABIDC	TABIDT	LALPHA
19	19	4	

3	ALPHA	TREF
0.0	20.000000	

COMMENT:

Total Card: 1 Smallest ID: 1 Largest ID: 1 Total deleted card: 0

Figure 42. Material input for MAT_255 in LS-PrePost.

Figure 42 above shows the material properties of steel were calculated according to the EN 1993-1-2.

Steel Temperature	Reduction factor(k_y, θ)	Slope of linear elastic(E_a, θ)
20	1	210000
100	1	210000
200	1	189000
300	1	168000
400	1	147000
500	0,78	126000
600	0,47	65100
700	0,23	27300
800	0,11	18900
900	0,06	14175
1000	0,04	9450
1100	0,02	4725
1200	0	0

Figure 43. Calculation of Young's modulus according to the EN.

Figure 43 above shows the calculation of the temperature vs Young's modulus curve where steel temperature and reduction factor were taken from EN 1993-1-2. The slope of the linear elastic (E_a, θ) were calculated using the formula

$$(E_a, \theta) = E_a * (k_y, \theta)$$

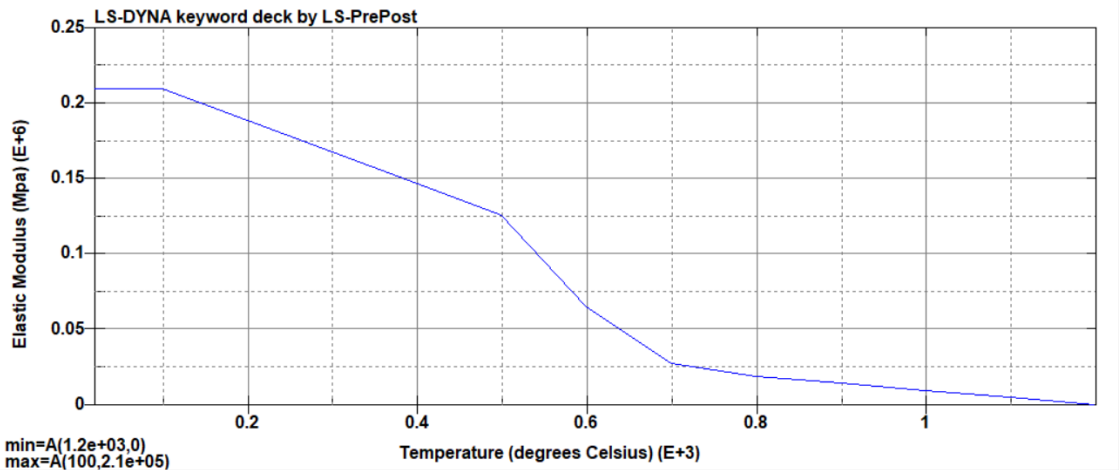


Figure 44. Graphical representation of Temperature versus Young's modulus in LS-PrePost.

Figure 44 above shows the Elastic Modulus vs Young's modulus curve during the material definition of structure analysis. Figure 45 below shows the coefficient of thermal expansion versus Temperature curve.

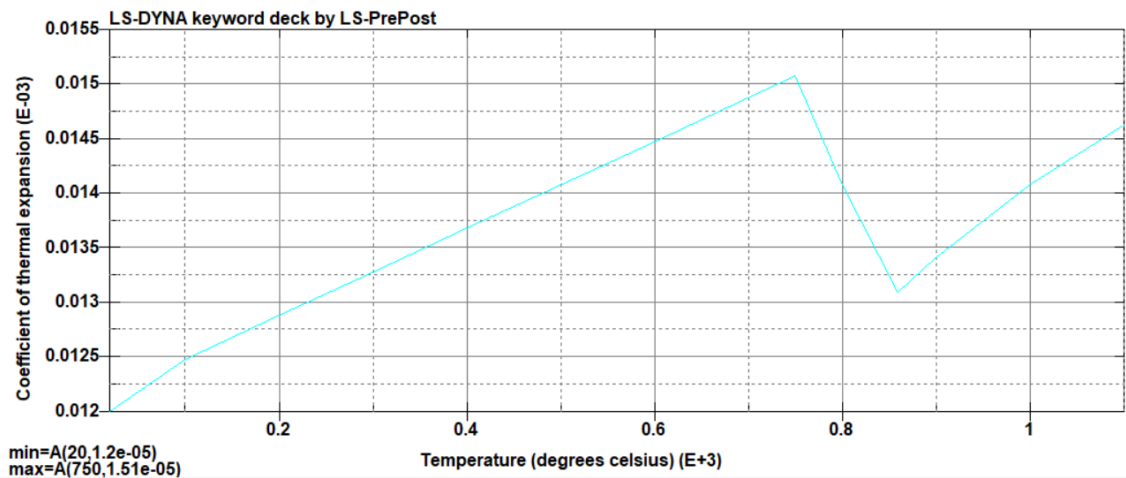


Figure 45. Graphical representation of thermal expansion due to fire on steel.

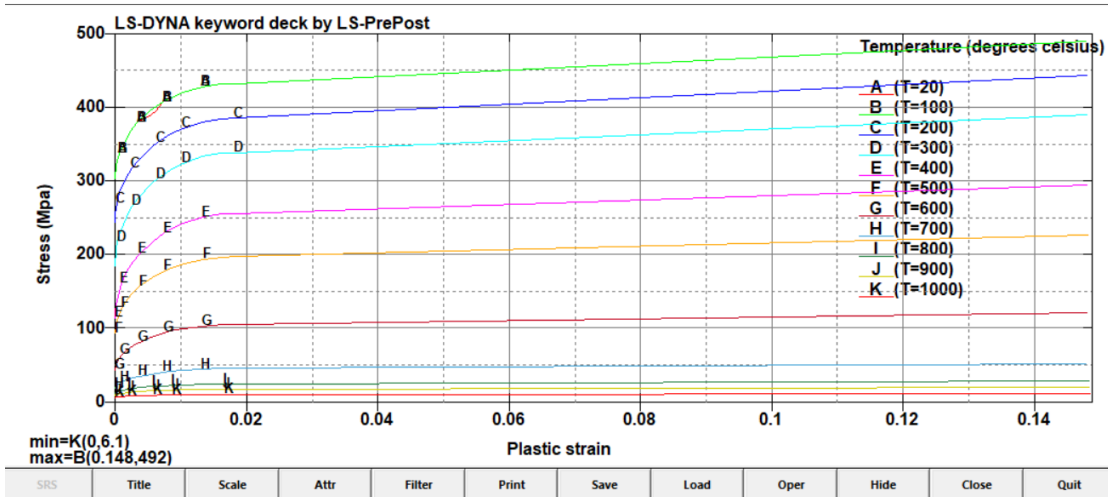


Figure 46. Graphical representation of Temperature versus plastic stress-strain curve.

Figure 46 shows the graphical representation of the plastic stress versus strain curve of steel S 355 20°C, 100°C, 200°C, 300°C, 400°C, 500°C, 600°C, 700°C, 800°C, 900°C and 1000°C temperature.

8.1 Analysis time in LS-DYNA

In an explicit analysis, the time step is affected by element size and material sound speed. The computing time to simulate the simply supported beam under displacement loading in the mid-span of the beam is shown in Table 8 below. All the analysis cases were run using shared memory parallel (SMP) double precision R9 version in LS-DYNA.

Table 8. Analysis cases and simulation time in LS-DYNA Manager.

Analysis cases during research	Total simulation time
2 mm mesh size implicit analysis	11 minutes 41 seconds.
4mm mesh size implicit analysis	3 minutes 13 seconds
6mm mesh size implicit analysis	58 seconds
8mm mesh size implicit analysis	43 seconds
6mm mesh size explicit analysis	2 hours 5 minutes and 15 seconds
10 mm mesh size implicit fire analysis with load 727 kN	1 hr 2 minutes and 21 seconds
10 mm mesh size implicit fire analysis with 1818 kN load.	47 minutes and 46 seconds

9 ANALYSIS RESULTS AND COMPARISON WITH TEST

In this chapter, the results of the finite element simulations using shell elements are presented and compared.

9.1 Implicit and Explicit simulation results

The FE model was run with the two cases static implicit analysis and explicit analysis in LS-DYNA with the same element size of 6mm. Point load was loaded in the middle of the steel IPE beam with the keyword *BOUNDARY_PRESCRIBED_MOTION_SET in LS-DYNA. The total CPU run time during explicit analysis was 2 hour and 5 minutes where only 58 seconds for the implicit analysis until normal termination.

Figure 47 shows the force vs time curve for the implicit and explicit analysis in LS-DYNA. The maximum peak load during the numerical simulation was 36.34 KN for implicit analysis and 40.04 KN for explicit analysis.

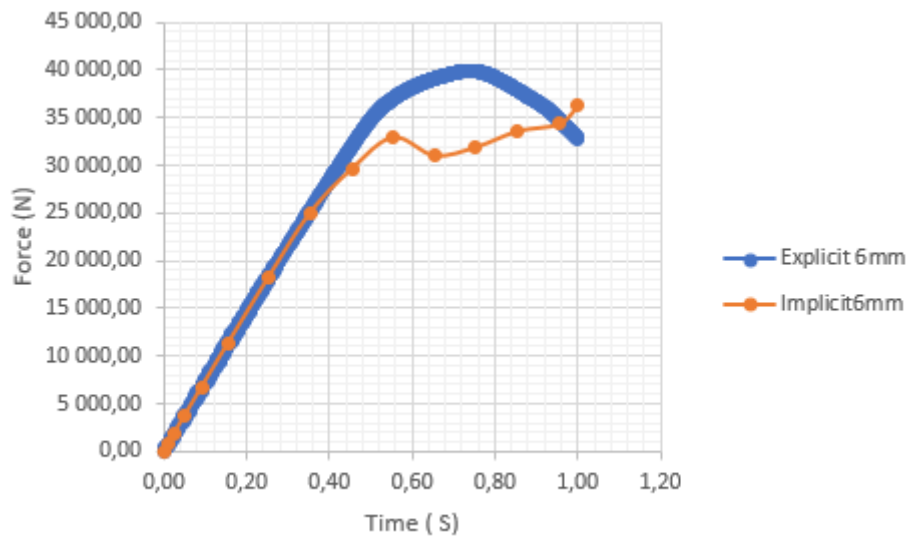


Figure 47. Force versus Time curve of steel IPE beam with a mesh size of 6mm.

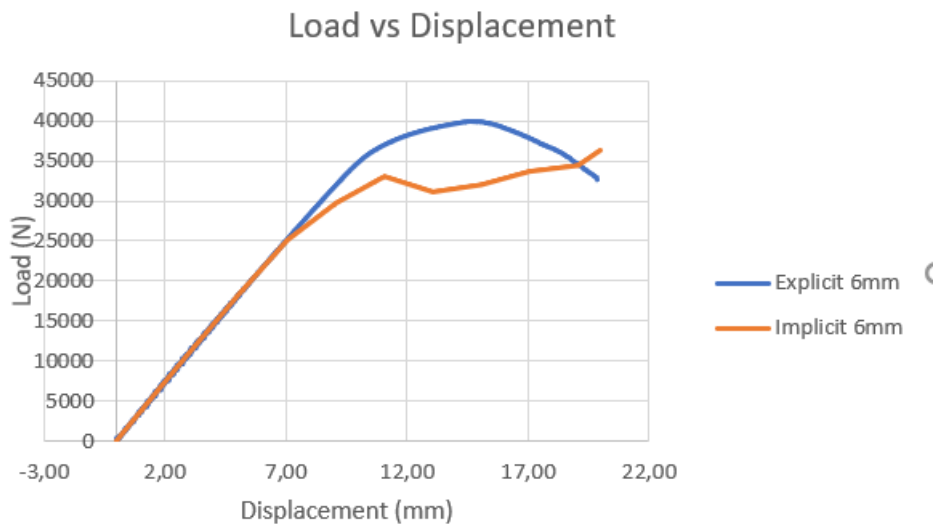


Figure 48. Load versus displacement curve of the simply supported beam.

Figure 48 shows the load vs displacement curve of simply supported beam modelled with the same material, size and mesh size but run with the two different types of solvers in LS-DYNA. The maximum load and vertical displacement in the implicit analysis was 20 mm displacement and load 36.34 kN wherein explicit analysis maximum displacement 15 mm and the load was 40.34 Kn. Figure 49 and Figure 50 shows the displacement result from the explicit code and implicit code respectively.

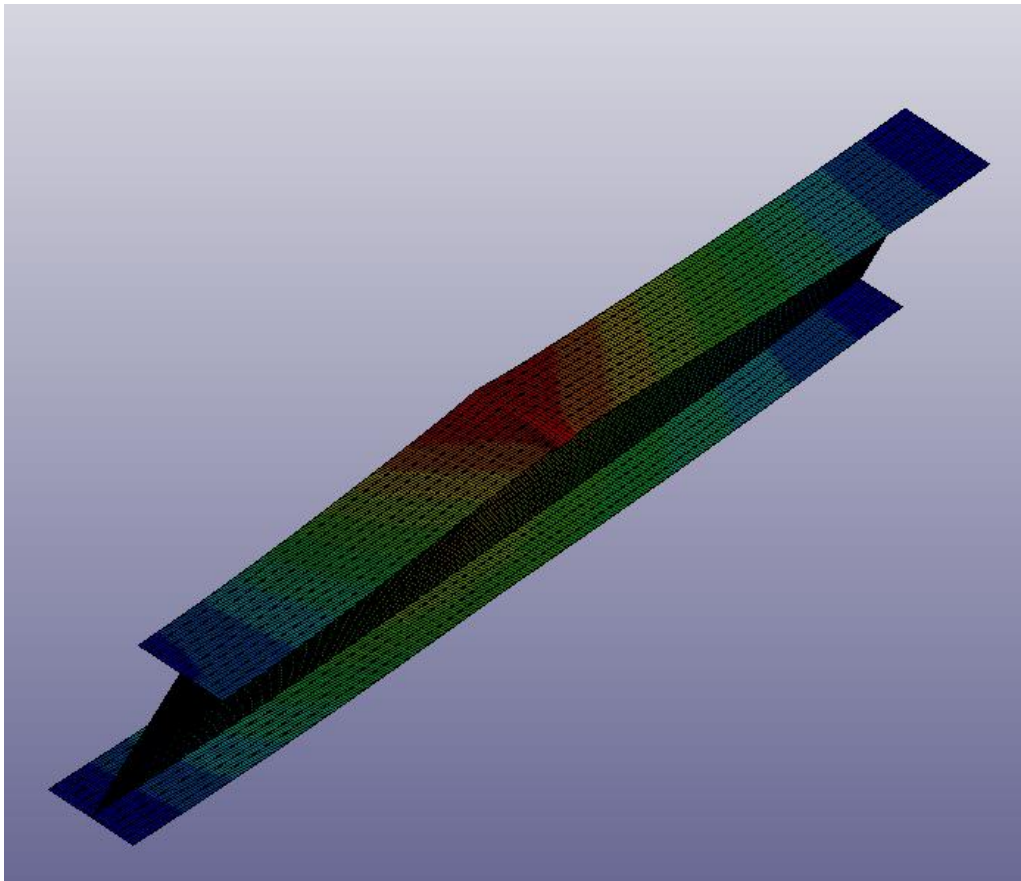


Figure 49. Displacement result from the explicit analysis.

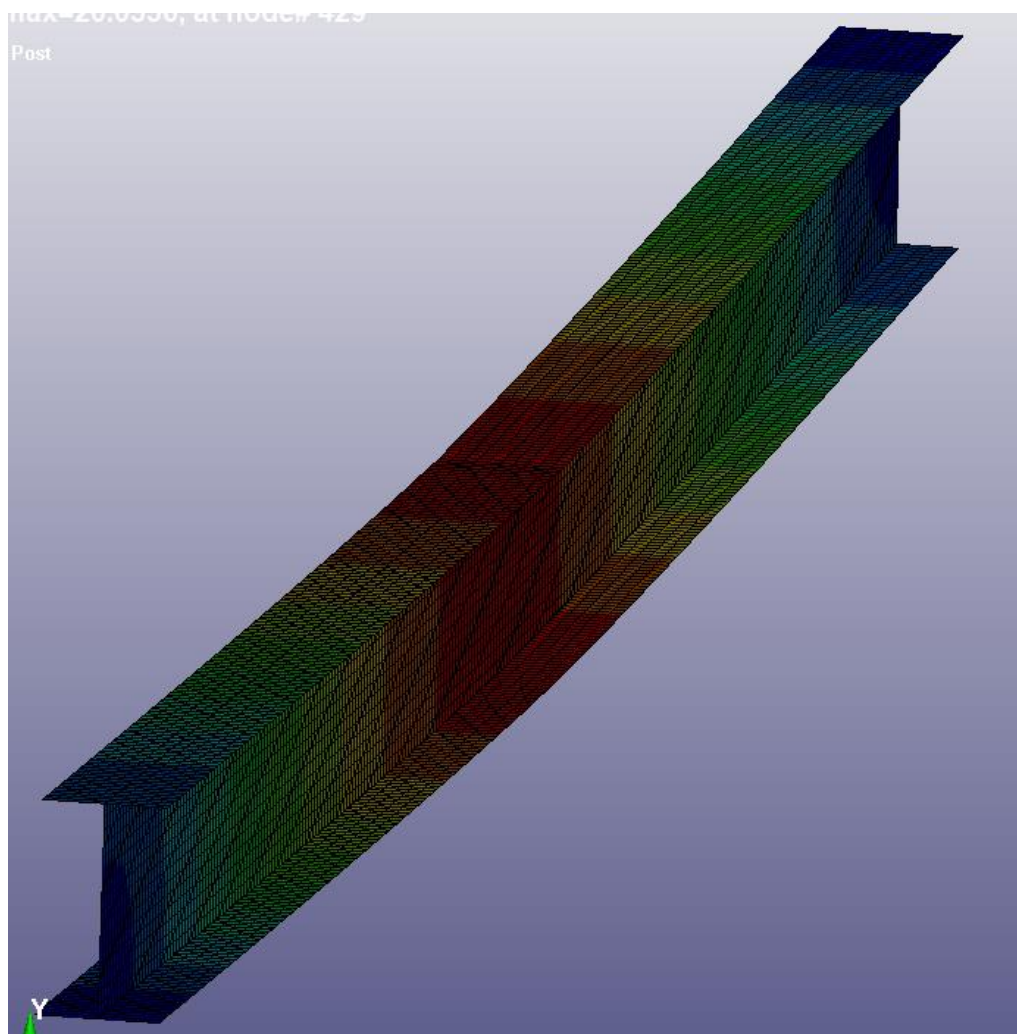


Figure 50. Displacement result from the implicit analysis.

9.2 Comparing the lab test and numerical simulation results.

Figure 51 shows the residual deformation of the steel beam under the mid-span point load. It was noticed from Figure 52 that later-torsional buckling behaviour is observed while the maximum of the lateral deformation is produced at mid-span of the simply supported beam.

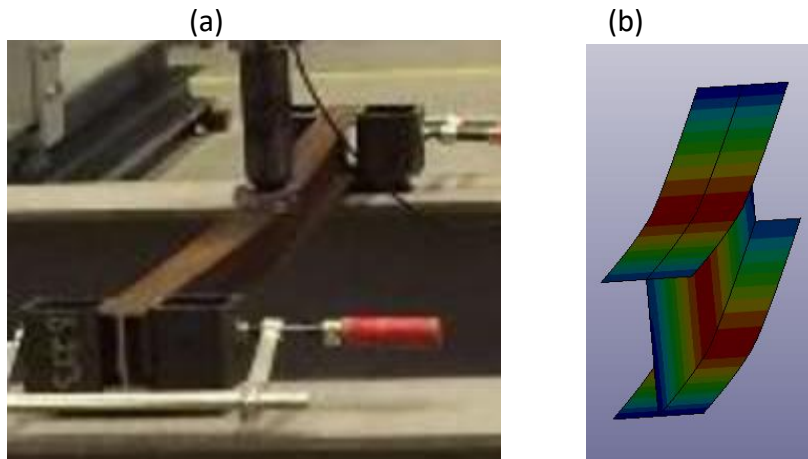


Figure 51. Lab test (a) and (b) LS-Dyna simulation.

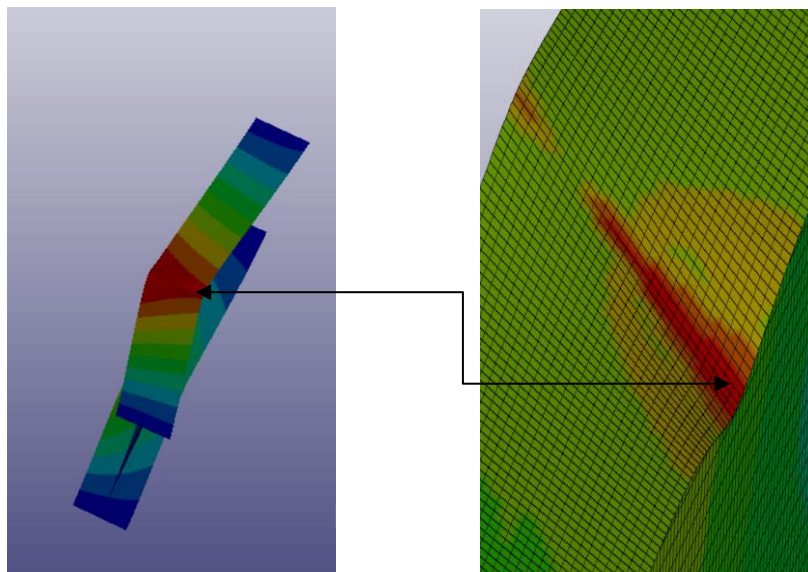


Figure 52. Plastic deformation of the beam.

Figure 53 below shows the simulation results of simply supported beam from beginning to normal termination.

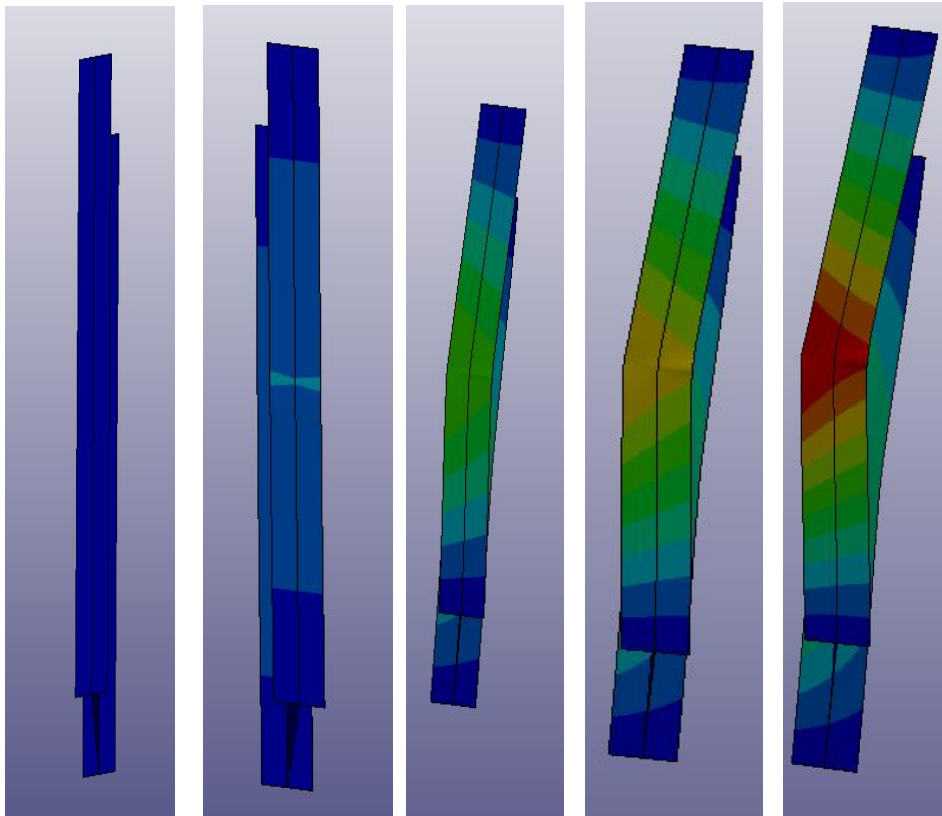


Figure 53. Simulation results of simply supported steel beam.

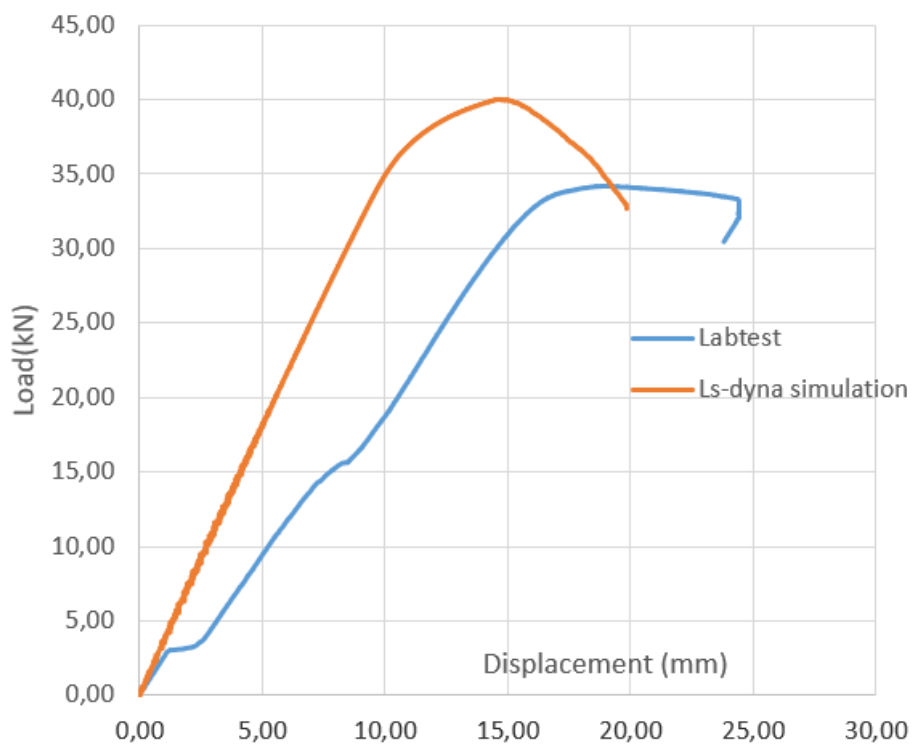


Figure 54. Load versus displacement curve of a simply supported beam from a lab test and LS-DYNA.

Above Figure 54 shows the comparison of load-displacement curves between the lab test and LS-DYNA simulation. It is seen that force and the maximum deformation comparing two tests look different. The possible reasons for different simulation and experimental results may be an error due to measurement, faulty equipment, an external force from an analyst during the experimental analysis.

9.3 The structural analysis of IPE Beam in fire

The FE model was created using shell elements with Fully integrated shell element for the accuracy and less simulation time. The element size created in finite element modelling was 10 mm and three integration points are defined through the thickness. This time different temperature-dependent piecewise linear plastic material MAT255 was used. The material properties and stress-strain relations are defined according to EN 1993-1-2.

Figure 55 below illustrates the deformation response of the simply supported beam in fire at mid-span using shell elements under two different kind of point load 5090 N and 12726 N. The deformation curve by FE analysis captures the major behaviour of the simply supported beam in a fire. The failure mode is a plastic bending failure and later-torsional buckling in the mid-span of loading within orange is 5090 N and blue 12726 N. The fire resistance time was 7.15 minutes when 5090 N load was applied on the simply supported beam and 3.30 minutes when 12726 N load was applied. The deformation response seems closer to 22mm on 12726 N load and 23 mm on 5090 N load. The fire resistance time decreased when the load was increased in a simply supported beam in a fire.

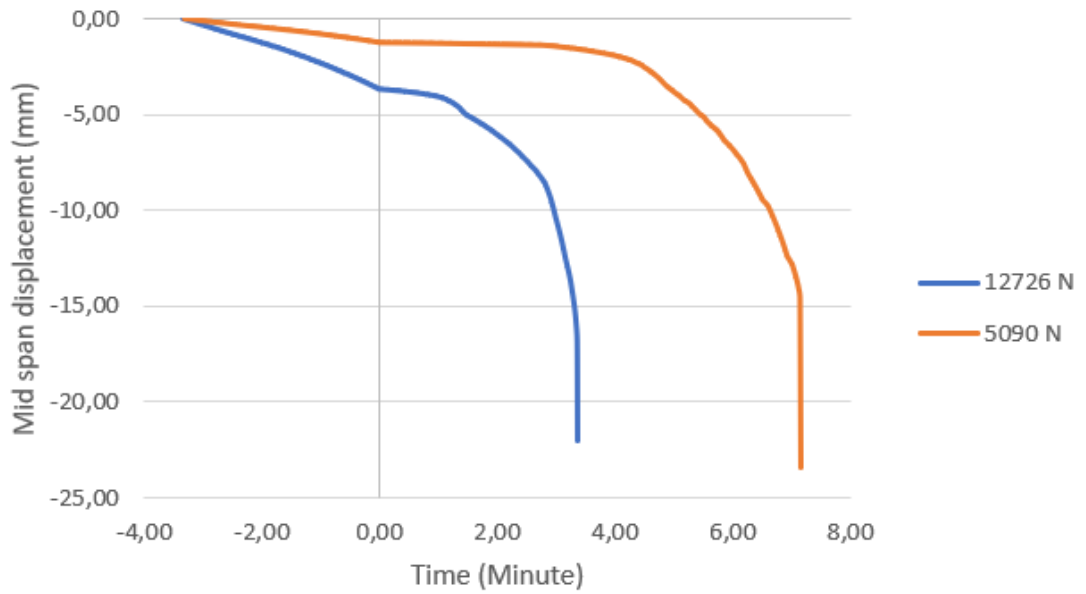


Figure 55. Mid-span displacement by shell element model.

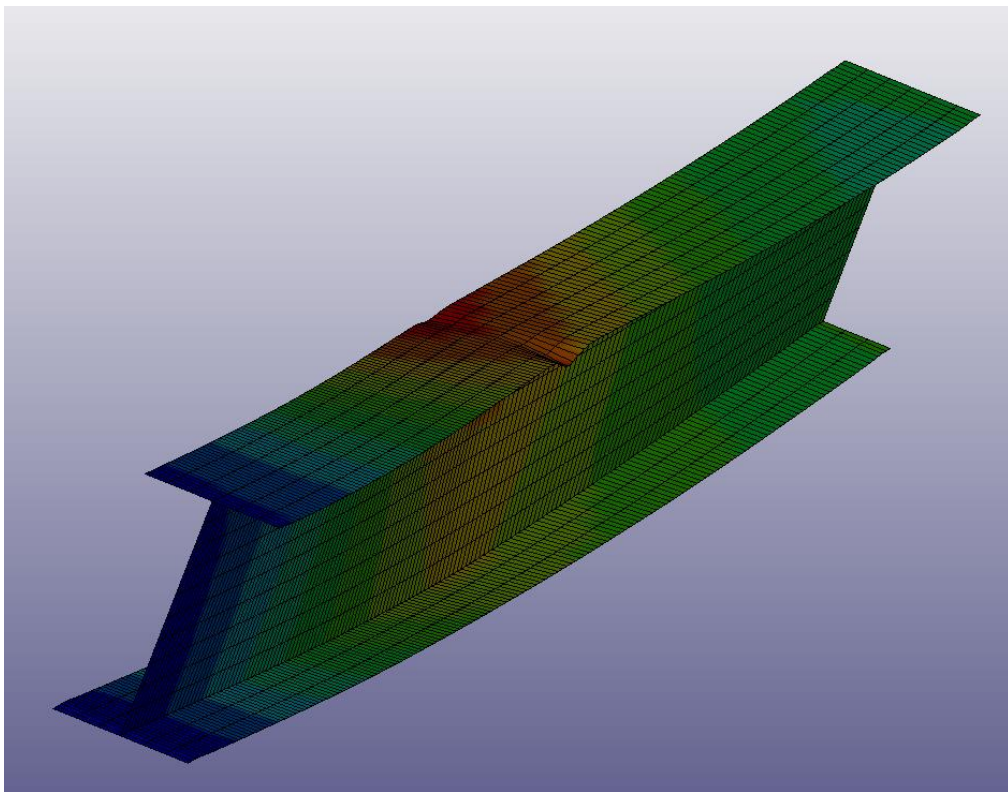


Figure 56. Lateral torsional buckling in mid-span loading of a simply supported beam under fire.

Figure 56 above shows the simulation result of simply supported beam heated from all four sides during structural fire analysis.

10 CONCLUSION AND FUTURE STEPS

This thesis investigated the nonlinear structural response of simply supported IPE beam subjected to mid-span load at both ambient and elevated temperatures. Five simulation tests and two fire tests, with a simply supported steel beam, were performed using LS-DYNA. Finite element model was modelled in LS-PrePost using the shell element using element formation 16. Static nonlinear implicit analysis and one explicit analysis were run in LS-DYNA during this thesis research. The structure fire analysis was carried out using an implicit solver due to less simulation running time, although an explicit solver is better for a large deformation and highly nonlinear material.

Lateral torsional buckling behaviour from the numerical simulation test is not an accidental consequence due to structure or material defects, but the real response mode of the structure. The consistency between the numerical simulation and experiment results also shows that FE code LS-DYNA effectively simulates LTB with material and geometrical nonlinearities. Based on the results in chapter 10, the following conclusions are drawn:

- (1) After observing the simulation, deformation modes and lateral displacement, it was noticed that under point load in the mid-span of a simply supported beam at both ambient and elevated temperatures leads to the lateral-torsional buckling. The maximum effect of displacement loading was in the mid-span of a beam by the local deformation in the upper flange of the IPE steel beam.
- (2) LS-DYNA was able to replicate the beam testing under mid-span loading on simply supported IPE beam as in the physical lab test, after comparing the result between simulation and experiment. There was a huge difference in load vs displacement curve between the LS-DYNA simulation and experimental results. The peak load and maximum displacement during the numerical simulation was 40 kN and 15 mm whereas the lab test it was 34.19 kN and 19 mm. The possible reason for this might be an error due to measurement, faulty equipment, external force, limitation of measuring devices during the experiment.
- (3) From mesh sensitivity analysis using implicit code results analysing the load vs displacement curve of four different finite element model of the simply supported beam with 2mm, 4mm, 6mm, 8mm, it was observed that the structure response was similar in all cases but there were huge changes in the peak load and the displacement. It was observed that there was some error in a mesh sensitivity analysis. Implicit static analysis was unsuccessful for the mesh sensitivity analysis. It was also found out that the smaller the mesh size the more simulation time was required in LS-DYNA.
- (4) From mesh sensitivity analysis using explicit code results analysing the load vs displacement curve of four different finite element model of the simply supported beam with 6mm, 8mm, 12mm and 14mm, it was observed that the structure response was similar in all cases but there were little changes in the peak load and displacement. Explicit static analysis was successful for

the mesh sensitivity analysis. By seeing the accuracy and the less solution time 8mm element size was sufficient.

- (5) From correlating the result from the implicit and explicit analysis it was found that compared to an explicit solver, implicit solver could achieve comparable results with drastically reducing computation time in LS-DYNA. The simulation time for the 6mm mesh sized finite element model took 58 seconds during implicit analysis while it took 2 hours 5 minutes during explicit analysis.
- (6) From the structural analysis of the simply supported beam subjected to the fire, it was found that the fire resistance time was less in higher loads. It was noticed fire resistance time was 7.15 minute during 5090 N loading and 3.30 minute during 12726 N loading.
- (7) In general, results illustrated previously in chapter 10 indicate that implicit and explicit static solver of LS-DYNA was able to capture the key phenomena of IPE steel beam under mid-span loading.

Recommendations for further development and use for the model introduced in this thesis are presented in the following:

The author suggests that finite element modelling can be modelled using beam element in LS- DYNA and results can be checked which is more accurate and less time consuming with the shell element result of this study.

Moreover, due to the more simulation consuming time for the structure fire analysis, implicit code was used for this thesis. The result can be seen using explicit code in LS-DYNA in the future, then fire residence time can be compared.

REFERENCES

- Askeland R.D. & Wright J.W. (2010). *Essentials of materials science and engineering*. Cengage Learning Inc.
- Akin J.E. (2006). *Finite Element Analysis with Error Estimators*. Burlington Butterworth-Heinemann.
- Baeker M. 2006. *Mechanical Behaviour of Engineering Materials*.
- Beer P. F. (2011). *Mechanics of Materials*.
- Bently Communities. (n.d). *Linear versus Nonlinear analysis*. Retrieved 04 December 2019 from <https://www.google.com/search?q=LINEAR+VS+NON+LINEAR+ANLYSIS&tbm=isch&ved=2>
- Benson D.J. (n.d.). *The History of LS-DYNA*. Retrieved 21 October 2019 from <https://www.d3view.com/wp-content/uploads/2007/06/benson.pdf>
- LS-DYNA support. (n.d.). *What is the difference between implicit explicit?* Retrieved 24 October from <https://www.dynasupport.com/faq/general/what-are-the-differences-between-implicit-and-explicit>
- LS-DYNA support. (n.d.). *Time step size*. <https://www.dynasupport.com/tutorial/ls-dyna-users-guide/time-step-size>
- LS_DYNA support. (n.d), *From engineering to true strain, true stress*. Retrieved on October 31 from <https://www.dynasupport.com/howtos/material/from-engineering-to-true-strain-true-stress>
- Engineering Notes. (n.d). *The behaviour of the material*. Retrieved on 10 December 2019 from <http://www.engineeringenotes.com/metallurgy/metal-deformation/deformation-of-metals-and-its-types-metallurgy/41673>
- Femto Engineering. (n.d.). *In FEA, what is linear and nonlinear analysis?* Retrieved 18 October 2019 from <https://www.femto.eu/stories/linear-non-linear-analysis-explained/>
- Jenkins M. (2019). *Structural Analysis Types*. Retrieved 23 October from <https://www.simscale.com/blog/2019/04/structural-analysis-dynamic-impact/>
- Krawinkler H. (2007). *Importance of good nonlinear analysis*. Retrieved on November 28 from Wiley online library.

Livermore Software Technology. (n.d), *LS-PrePost about*. Retrieved on 31 October from <https://www.lstc.com/products/ls-prepost>
 LS-DYNA Theory Manual. (2006). *Shell Formulations*. Retrieved on October 31 from <https://www.dynasupport.com/howtos/element/shell-formulations>

Livermore Software Technology. (n.d.). *LS-DYNA About*. Retrieved 22 October 2019 from <http://www.lstc.com/products/ls-dyna>

Iyenger S.R.K. and Jain R.K. (2009). *Numerical Methods*. Retrieved from <https://ebookcentral-proquest-com.ezproxy.hamk.fi/lib/hamk-ebooks/reader.action?docID=437713>

Ma Z., Havula J. & Heinisuo M. (2019). *Structural fire analysis of simple steel structures by using LS-DYNA*. Retrieved on December 10 from Journal of Structural Mechanics.

Murad J. (2019). Errors in FEA. Retrieved 22 October 2019 from <https://www.simscale.com/blog/2016/06/errors-in-fea-and-singularities/>

Rao S. Singiresu. (2004). *The Finite Element Method in Engineering*, Elsevier Science & Technology. ProQuest Ebook Central, <http://ebookcentral.proquest.com/lib/hamk-ebooks/detail.action?docID=286754>.

Radhakrishnan P., Subramanyan S. & Raju V. (2008) *CAD/CAM/CIM*, New Age International Ltd, 2008. ProQuest Ebook Central, <http://ebookcentral.proquest.com/lib/hamk-ebooks/detail.action?docID=437710>.
 Created from hamk-ebooks on 2019-10-23 10:45:09.

Rusu C. (2017). *What is Linear static analysis in FEA simulation?* Retrieved 23 October from <http://feaforall.com/linear-static-analysis-fea/>

sae.org, (n.d). *FEA Basic in thermal analysis*. Retrieved 23 October from <https://www.sae.org/learn/content/wb1726/>

Simscale blog (n.d). The CFL condition and How to choose Timestep size. <https://www.simscale.com/blog/2017/08/cfl-condition/>

Sormunen J. (2016). *Transient Load Simulation of Forwarder Rear Frame*. Retrieved 20 September 2019 from <https://trepo.tuni.fi/handle/123456789/24196>

Trivista Engineering Ltd. (2016). *FEA Dynamic Analysis*. Retrieved 23 October from <https://trivista.co.uk/design-and-analysis/fea-overview/dynamic-analysis/>

University of Ljubljana. (2019), *Background to Thermal Analysis*. Retrieved on 6 November from http://fgg-web.fgg.uni-lj.si/~pmoze/ESDEP/master/wg04b/l0200.htm#SEC_4_1

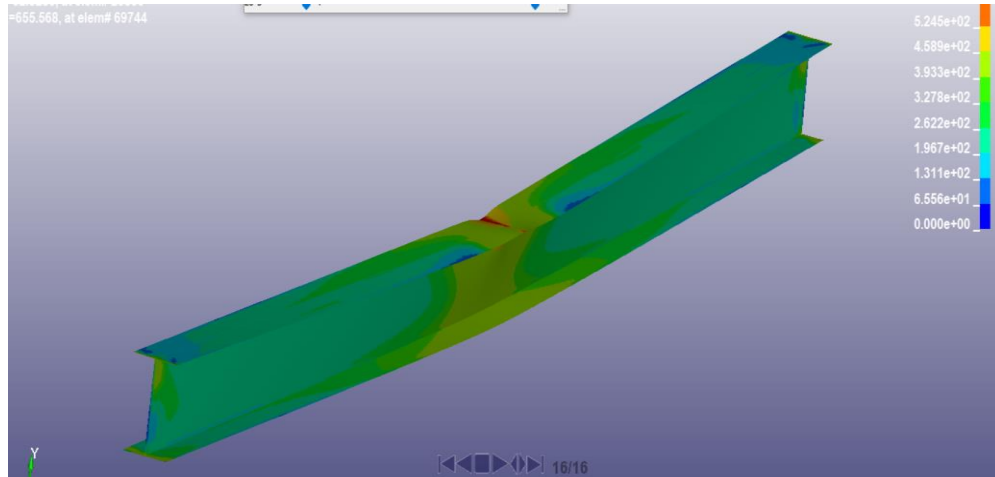
Wikipedia, (n.d). *Behaviour of metal*. Retrieved on 3 November from [https://en.wikipedia.org/wiki/Plasticity_\(physics\)](https://en.wikipedia.org/wiki/Plasticity_(physics))

Younis W. (2009). Up and running with Autodesk Inventor Simulation.

APPENDIX

Appendix 1

Von Mises Stress simulation



Appendix 2/1

Temperature Calculation from Excel sheet.

Temperature calculation of unprotected steel IPE beam with fire exposed from all side is explained in the following excel sheet.

Properties of steel									
Density of Steel(ρ)	7850	kg/m ³							IPE100
Coefficient of heat transfer(ac)	25	W/m ² k	From standard ISO Fire curve					Depth(H)	100 mm
Surface emmissivity(ϵ_m)	0,7		EN1991-1-1-2(carbon steel)					Width(B)	55 mm
Emmissivity of Fire(ϵ_f)	1		EN1991-1-1-2					Web thickness(t_w)	4,1 mm
Configuration factor(Φ)	1		EN1991-1-1-2					Flange thickness(t_f)	5,7 mm
								Root radius(r)	7 mm
								Area of IPE 100(A)	1030 mm ²
Unprotected Section(open section exposed)									
Section factor(A_m/V)	385,0485437								
Correction Factor(k_{sh})	0,724583964								
Surface area/(lA_m)	396,6		EN1993-1-2:2005						
Section factor(A_m/V)box	310								
		View factor(Φ)		1					
		Emissivity of fire(ϵ_f)		1	EN1991-1-2				
		Surface temperature(θ_m)		20					
		Surface emmissivity(ϵ_m)		1	EN1991-1-2				
		Specific heat of steel(C_a)		420					steel
		gas							
Time in second	Time in minute	Gas temperature(θ_g °C)	Design value of net heat flux (hnet,d)	hnet,c	hnet,r	$\Delta a, t(^{\circ}C)$	$\theta a, t(^{\circ}C)$		
0	0	20	0	0	0	0	0	0	20
5	0,0833333333	96,53781862	2361,072898	1913,445465	447,6274326	0,999	20,999		
10	0,1666666667	146,9519909	4086,765192	3148,824821	937,9403711	1,72916	22,7282		
15	0,25	184,6068329	5483,809939	4046,966893	1436,843046	2,32027	25,0484		
20	0,3333333333	214,6736435	6672,332121	4740,630525	1931,701597	2,82314	27,8716		
25	0,4166666667	239,7036237	7713,060217	5295,801448	2417,258769	3,26349	31,1351		
30	0,5	261,1446515	8641,504922	5750,23995	2891,264971	3,65632	34,7914		
35	0,5833333333	279,898045	9480,494334	6127,666695	3352,827639	4,01131	38,8027		
40	0,6666666667	296,5631595	10245,71353	6444,011802	3801,701732	4,33508	43,1378		
45	0,75	311,5588238	10948,48291	6710,526323	4237,956588	4,63243	47,7702		
50	0,8333333333	325,1892705	11597,28625	6935,476651	4661,8096	4,90695	52,6772		
55	0,9166666667	337,6824701	12198,67258	7125,132888	5073,539687	5,1614	57,8386		
60	1	349,2136658	12757,81887	7284,377685	5473,441187	5,39799	63,2365		
65	1,0833333333	359,9204764	13278,8975	7417,09832	5861,799179	5,61846	68,855		
70	1,1666666667	369,9129515	13765,32521	7526,448702	6238,876506	5,82427	74,6793		
75	1,25	379,2804764	14219,93738	7615,029995	6604,907387	6,01663	80,6959		
80	1,3333333333	388,0966424	14645,11328	7685,018521	6960,094762	6,19652	86,8924		
85	1,4166666667	396,4227619	15042,86825	7738,258459	7304,609789	6,36482	93,2572		

Appendix 2/2

90	1,5	404,3104565	15414,92298	7776,330402	7638,592574	6,52224	99,7795
95	1,583333333	411,8035977	15762,75658	7800,60299	7962,153595	6,66941	106,449
100	1,666666667	418,9397843	16087,64791	7812,2724	8275,375509	6,80688	113,256
105	1,75	425,7514844	16390,70817	7812,393012	8578,315158	6,9351	120,191
110	1,833333333	432,2669281	16672,90717	7801,901505	8871,005669	7,05451	127,245
115	1,916666667	438,5108147	16935,09461	7781,636027	9153,458582	7,16544	134,411
120	2	444,5048779	17178,01758	7752,351595	9425,665984	7,26822	141,679
125	2,083333333	450,2683421	17402,33522	7714,732602	9687,602622	7,36314	149,042
130	2,166666667	455,818295	17608,63103	7669,403037	9939,227994	7,45042	156,493
135	2,25	461,1699923	17797,42335	7616,934928	10180,48842	7,5303	164,023
140	2,333333333	466,3371111	17969,17445	7557,855349	10411,3191	7,60297	171,626
145	2,416666667	471,3319602	18124,29841	7492,652278	10631,64614	7,66861	179,294
150	2,5	476,1656567	18263,16806	7421,779523	10841,38854	7,72736	187,022
155	2,583333333	480,8482752	18386,12113	7345,660882	11040,46025	7,77939	194,801
160	2,666666667	485,3889741	18493,4658	7264,693679	11228,77212	7,82481	202,626
165	2,75	489,7961034	18585,48567	7179,251768	11406,23391	7,86374	210,49
170	2,833333333	494,0772974	18662,44429	7089,688105	11572,75619	7,8963	218,386
175	2,916666667	498,2395539	18724,58931	6996,33695	11728,25236	7,9226	226,309
180	3	502,289303	18772,15627	6899,515755	11872,64052	7,94272	234,251
185	3,083333333	506,2324673	18805,37215	6799,526785	12005,84536	7,95678	242,208
190	3,166666667	510,0745136	18824,45856	6696,658515	12127,80004	7,96485	250,173
195	3,25	513,8204986	18829,63478	6591,186821	12238,44796	7,96704	258,14
200	3,333333333	517,475109	18821,1205	6483,376007	12337,74449	7,96344	266,104
205	3,416666667	521,0426965	18799,13837	6373,479683	12425,65869	7,95414	274,058
210	3,5	524,5273093	18763,91637	6261,741515	12502,17485	7,93924	281,997
215	3,583333333	527,9327194	18715,68988	6148,395851	12567,29403	7,91883	289,916
220	3,666666667	531,2624475	18654,70365	6033,668266	12621,03538	7,89303	297,809
225	3,75	534,5197844	18581,2135	5917,776001	12663,4375	7,86193	305,671
230	3,833333333	537,7078109	18495,48782	5800,928343	12694,55948	7,82566	313,496
235	3,916666667	540,8294154	18397,80886	5683,326921	12714,48194	7,78433	321,281
240	4	543,8873093	18288,47379	5565,165961	12723,30783	7,73807	329,019
245	4,083333333	546,8840411	18167,79561	5446,632475	12721,16313	7,68701	336,706
250	4,166666667	549,8220096	18036,10371	5327,906417	12708,19729	7,63129	344,337
255	4,25	552,7034753	17893,74434	5209,160797	12684,58354	7,57106	351,908
260	4,333333333	555,5305704	17741,08077	5090,561762	12650,51901	7,50646	359,415
265	4,416666667	558,3053089	17578,49329	4972,268655	12606,22463	7,43767	366,852
270	4,5	561,0295948	17406,3789	4854,434051	12551,94485	7,36485	374,217
275	4,583333333	563,7052301	17225,15093	4737,203775	12487,94716	7,28817	381,505
280	4,666666667	566,333922	17035,23829	4620,716906	12414,52138	7,20781	388,713
285	4,75	568,9172894	16837,08464	4505,105781	12331,97886	7,12397	395,837
290	4,833333333	571,4568688	16631,14735	4390,495985	12240,65137	7,03684	402,874

720	12	705,4362483	3065,650239	451,7875359	2613,862703	1,29711	688,662
725	12,08333333	706,4624961	3028,960644	445,0159025	2583,944742	1,28159	689,943
730	12,16666667	707,4817626	2993,380684	438,4578309	2554,922853	1,26654	691,21
735	12,25	708,4941421	2958,86394	432,1039423	2526,759998	1,25193	692,462
740	12,33333333	709,4997271	2925,365938	425,9453012	2499,420637	1,23776	693,7
745	12,41666667	710,4986081	2892,844081	419,9733964	2472,870685	1,224	694,924
750	12,5	711,490874	2861,25759	414,1801224	2447,077468	1,21063	696,134
755	12,58333333	712,4766117	2830,567445	408,5577611	2422,009684	1,19765	697,332
760	12,66666667	713,4559067	2800,73632	403,0989646	2397,637355	1,18502	698,517
765	12,75	714,4288425	2771,728525	397,7967381	2373,931787	1,17275	699,69
770	12,83333333	715,3955013	2743,509948	392,644424	2350,865524	1,16081	700,851
775	12,91666667	716,3559636	2716,047991	387,6356859	2328,412305	1,14919	702
780	13	717,3103082	2689,311515	382,764494	2306,547021	1,13788	703,138
785	13,08333333	718,2586126	2663,270784	378,0251103	2285,245673	1,12686	704,264
790	13,16666667	719,2009528	2637,897406	373,4120746	2264,485331	1,11613	705,381
795	13,25	720,1374033	2613,164281	368,9201919	2244,244089	1,10566	706,486
800	13,33333333	721,0680373	2589,045548	364,5445186	2224,501029	1,09546	707,582
805	13,41666667	721,9929267	2565,516528	360,2803511	2205,236177	1,0855	708,667
810	13,5	722,9121418	2542,553682	356,1232138	2186,430468	1,07578	709,743
815	13,58333333	723,8257519	2520,134555	352,0688476	2168,065707	1,0663	710,809
820	13,66666667	724,733825	2498,237732	348,1131999	2150,124532	1,05703	711,866
825	13,75	725,6364277	2476,842792	344,2524135	2132,590378	1,04798	712,914
830	13,83333333	726,5336255	2455,930261	340,4828175	2115,447444	1,03913	713,953
835	13,91666667	727,4254829	2435,481575	336,8009176	2098,680657	1,03048	714,984
840	14	728,312063	2415,47903	333,2033874	2082,275643	1,02202	716,006
845	14,08333333	729,1934279	2395,905751	329,68706	2066,218691	1,01374	717,02
850	14,16666667	730,0696385	2376,745649	326,2489195	2050,49673	1,00563	718,025
855	14,25	730,9407549	2357,983385	322,8860938	2035,097291	0,99769	719,023
860	14,33333333	731,8068359	2339,604334	319,5958469	2020,008487	0,98991	720,013
865	14,41666667	732,6679394	2321,594554	316,3755723	2005,218981	0,98229	720,995
870	14,5	733,5241223	2303,940749	313,2227861	1990,717963	0,97482	721,97
875	14,58333333	734,3754405	2286,630242	310,1351207	1976,495121	0,9675	722,938
880	14,66666667	735,2219489	2269,650943	307,110319	1962,540624	0,96032	723,898
885	14,75	736,0637017	2252,991322	304,1462287	1948,845093	0,95327	724,851
890	14,83333333	736,9007519	2236,640378	301,2407966	1935,399582	0,94635	725,797
895	14,91666667	737,7331518	2220,587619	298,3920639	1922,195556	0,93956	726,737
900	15	738,5609528	2204,823032	295,5981612	1909,224871	0,93289	727,67
905	15,08333333	739,3842054	2189,337061	292,8573035	1896,479758	0,92633	728,596
910	15,16666667	740,2029593	2174,120585	290,1677866	1883,952798	0,9199	729,516
915	15,25	741,0172634	2159,164895	287,5279821	1871,636913	0,91357	730,43
920	15,33333333	741,8271659	2144,461675	284,9363343	1859,52534	0,90735	731,337

Appendix 2/4

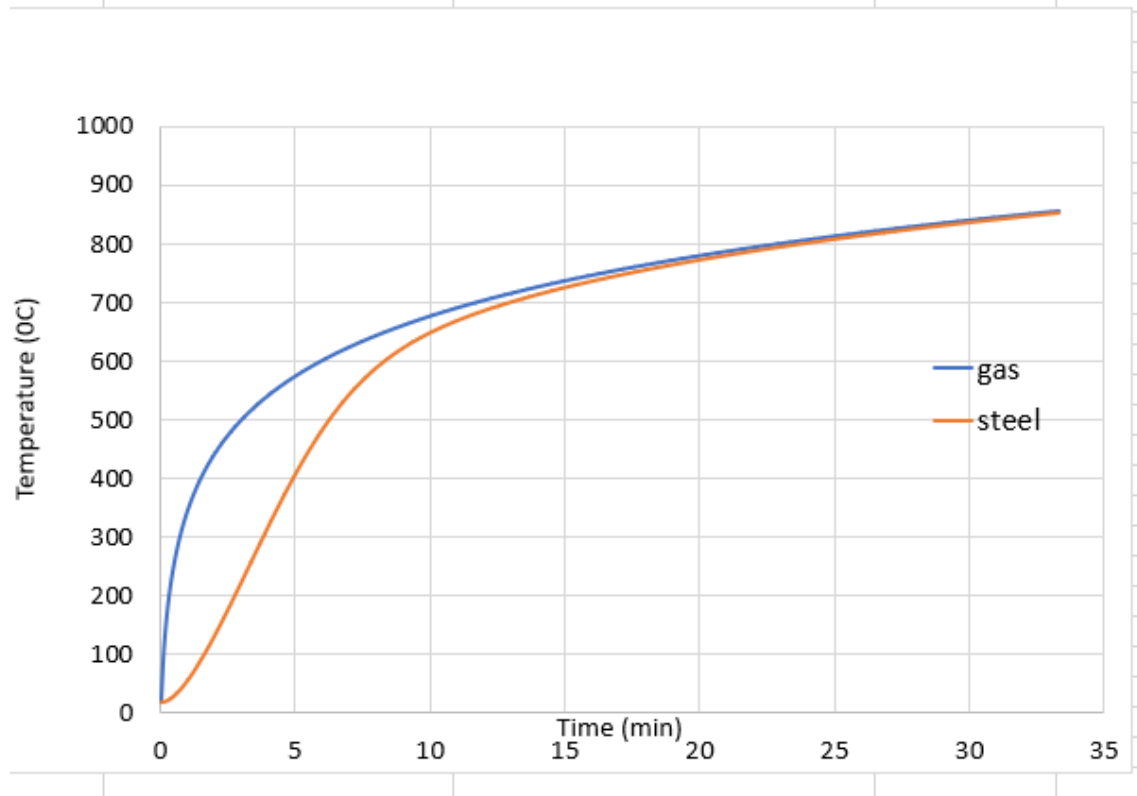
930	15,5	743,4339545	2115,781224	279,8916244	1835,8896	0,89521	733,134
935	15,58333333	744,2309329	2101,78915	277,4357794	1824,353371	0,88929	734,023
940	15,66666667	745,0236946	2088,019826	275,0225188	1812,997307	0,88347	734,906
945	15,75	745,8122837	2074,46662	272,650596	1801,816024	0,87773	735,784
950	15,83333333	746,5967441	2061,12319	270,3188175	1790,804373	0,87209	736,656
955	15,91666667	747,3771188	2047,983468	268,0260392	1779,957428	0,86653	737,523
960	16	748,1534501	2035,041643	265,7711651	1769,270478	0,86105	738,384
965	16,08333333	748,9257796	2022,292153	263,5531438	1758,73901	0,85566	739,239
970	16,16666667	749,6941484	2009,729671	261,370967	1748,358704	0,85034	740,09
975	16,25	750,458597	1997,349092	259,223667	1738,125425	0,8451	740,935
980	16,33333333	751,2191651	1985,14552	257,1103146	1728,035205	0,83994	741,775
985	16,41666667	751,975892	1973,114262	255,0300173	1718,084245	0,83485	742,61
990	16,5	752,7288161	1961,250817	252,9819177	1708,2689	0,82983	743,439
995	16,58333333	753,4779757	1949,550864	250,9651913	1698,585673	0,82488	744,264
1000	16,66666667	754,223408	1938,010253	248,9790452	1689,031208	0,82	745,084
1005	16,75	754,9651501	1926,624999	247,0227164	1679,602283	0,81518	745,899
1010	16,83333333	755,7032383	1915,391274	245,0954707	1670,295803	0,81042	746,71
1015	16,91666667	756,4377084	1904,305395	243,1966007	1661,108794	0,80573	747,516
1020	17	757,1685957	1893,363822	241,3254251	1652,038397	0,8011	748,317
1025	17,08333333	757,8959349	1882,563147	239,4812869	1643,08186	0,79653	749,113
1030	17,16666667	758,6197605	1871,900091	237,6635528	1634,236538	0,79202	749,905
1035	17,25	759,3401061	1861,371496	235,8716118	1625,499884	0,78757	750,693
1040	17,33333333	760,057005	1850,974317	234,104874	1616,869443	0,78317	751,476
1045	17,41666667	760,7704902	1840,705622	232,3627701	1608,342852	0,77882	752,255
1050	17,5	761,4805939	1830,562581	230,6447499	1599,917831	0,77453	753,029
1055	17,58333333	762,187348	1820,542465	228,9502817	1591,592184	0,77029	753,8
1060	17,66666667	762,890784	1810,642639	227,2788517	1583,363787	0,7661	754,566
1065	17,75	763,5909329	1800,860559	225,6299626	1575,230596	0,76197	755,328
1070	17,83333333	764,2878253	1791,193766	224,0031334	1567,190632	0,75788	756,086
1075	17,91666667	764,9814914	1781,639884	222,3978985	1559,241986	0,75383	756,839
1080	18	765,6719608	1772,196617	220,8138069	1551,38281	0,74984	757,589
1085	18,08333333	766,3592629	1762,861741	219,2504217	1543,611319	0,74589	758,335
1090	18,16666667	767,0434266	1753,633105	217,7073195	1535,925786	0,74198	759,077
1095	18,25	767,7244805	1744,508627	216,1840899	1528,324537	0,73812	759,815
1100	18,33333333	768,4024527	1735,486288	214,6803345	1520,805954	0,7343	760,55
1105	18,41666667	769,0773709	1726,564134	213,1956672	1513,368467	0,73053	761,28
1110	18,5	769,7492626	1717,740268	211,7297128	1506,010556	0,7268	762,007
1115	18,58333333	770,4181548	1709,012853	210,2821074	1498,730746	0,7231	762,73
1120	18,66666667	771,0840741	1700,380103	208,8524972	1491,527606	0,71945	763,449
1125	18,75	771,7470468	1691,840288	207,4405386	1484,39975	0,71584	764,165
1130	18,83333333	772,407099	1683,391726	206,0458976	1477,345828	0,71226	764,878

Appendix 2/5

1140		19	773,7185436	1666,761871	203,3072781	1463,454593	0,70523	766,291
1145	19,08333333		774,3699864	1658,577447	201,9626765	1456,614771	0,70176	766,993
1150	19,16666667		775,018609	1650,47801	200,6341453	1449,843865	0,69834	767,692
1155	19,25		775,6644359	1642,4621	199,3213935	1443,140707	0,69495	768,387
1160	19,33333333		776,3074909	1634,528295	198,0241374	1436,504158	0,69159	769,078
1165	19,41666667		776,9477979	1626,675212	196,7421008	1429,933111	0,68827	769,766
1170	19,5		777,5853801	1618,901502	195,4750146	1423,426488	0,68498	770,451
1175	19,58333333		778,2202607	1611,205854	194,2226164	1416,983237	0,68172	771,133
1180	19,66666667		778,8524624	1603,586987	192,9846505	1410,602336	0,6785	771,812
1185	19,75		779,4820079	1596,043653	191,7608675	1404,282786	0,67531	772,487
1190	19,83333333		780,1089192	1588,574638	190,5510241	1398,023614	0,67214	773,159
1195	19,91666667		780,7332185	1581,178754	189,354883	1391,823871	0,66902	773,828
1200	20		781,3549272	1573,854843	188,1722125	1385,68263	0,66592	774,494
1205	20,08333333		781,9740669	1566,601775	187,0027866	1379,598989	0,66285	775,157
1210	20,16666667		782,5966667	1559,418448	185,8463845	1373,572063	0,65981	775,817
1215	20,25		783,2047235	1552,303784	184,7027907	1367,600993	0,6568	776,473
1220	20,33333333		783,8162819	1545,25673	183,5717944	1361,684936	0,65382	777,127
1225	20,41666667		784,4253543	1538,276259	182,4531901	1355,823069	0,65086	777,778
1230	20,5		785,0319608	1531,361366	181,3467766	1350,014589	0,64794	778,426
1235	20,58333333		785,6361212	1524,511068	180,2523574	1344,25871	0,64504	779,071
1240	20,66666667		786,2378554	1517,724404	179,1697405	1338,554664	0,64217	779,713
1245	20,75		786,8371825	1511,000436	178,0987379	1332,901698	0,63932	780,353
1250	20,83333333		787,434122	1504,338245	177,039166	1327,299079	0,6365	780,989
1255	20,91666667		788,0286926	1497,736931	175,9908451	1321,746085	0,63371	781,623
1260	21		788,6209131	1491,195614	174,9535994	1316,242014	0,63094	782,254
1265	21,08333333		789,210802	1484,713433	173,9272568	1310,786176	0,6282	782,882
1270	21,16666667		789,7983777	1478,289544	172,911649	1305,377895	0,62548	783,507
1275	21,25		790,3836581	1471,923123	171,9066113	1300,016512	0,62279	784,13
1280	21,33333333		790,9666611	1465,613359	170,9119822	1294,701377	0,62012	784,75
1285	21,41666667		791,5474045	1459,359461	169,9276039	1289,431857	0,61747	785,368
1290	21,5		792,1259056	1453,160653	168,9533215	1284,207331	0,61485	785,983
1295	21,58333333		792,7021817	1447,016172	167,9889837	1279,027189	0,61225	786,595
1300	21,66666667		793,2762498	1440,925275	167,034442	1273,890833	0,60967	787,205
1305	21,75		793,8481268	1434,887228	166,0895509	1268,797678	0,60712	787,812
1310	21,83333333		794,4178294	1428,901317	165,1541679	1263,747149	0,60459	788,416
1315	21,91666667		794,985374	1422,966838	164,2281536	1258,738684	0,60207	789,018
1320	22		795,5507769	1417,083101	163,3113708	1253,77173	0,59958	789,618
1325	22,08333333		796,1140542	1411,24943	162,4036856	1248,845744	0,59712	790,215
1330	22,16666667		796,6752219	1405,465162	161,5049662	1243,960196	0,59467	790,81
1335	22,25		797,2342957	1399,729646	160,6150839	1239,114562	0,59224	791,402
1340	22,33333333		797,7912911	1394,042243	159,733912	1234,308331	0,58984	791,992

Appendix 2/8

	Formula source eurocode	
$\Delta\theta_{a,t}(\Delta a,t)$	$(ksh \cdot A_m/v) \cdot h_{net,d} \cdot \Delta t / Ca \cdot \rho$	EN1993-1-2:2005
ksh	$(0,9 \cdot (A_m/V))^{box} / (A_m/V)$	EN1993-1-2:2005
A_m/V open section exposed to fire	Perimeter/cross-section area	EN1993-1-2:2005
$h_{net,r}$	$\Phi \cdot \epsilon_f \cdot \epsilon_m [5,67 \cdot 10^{-8}] \cdot (\theta_r + 273)^4 - (\theta_m + 273)^4$	EN1993-1-2:2005
$h_{net,c}$	$\alpha_c(\theta_g - \theta_m)$	EN1993-1-2:2006
$h_{net,d}$	$(h_{net,c}) + (h_{net,r})$	EN1993-1-2:2007



Appendix 3/1

General Controls, LS-DYNA implicit code input

For the implicit static analysis in LS-DYNA following keywords were used for this research work.

```

1  $# LS-DYNA Keyword file created by LS-PrePost(R) V4.7.0 - 06Nov2019
2  $# Created on Nov-18-2019 (15:02:14)
3  *KEYWORD
4  *TITLE
5  $#
6  LS-DYNA keyword deck by LS-PrePost
7  *CONTROL_ACCURACY
8  $#      osu      inn      pidosu      iacc
9  .....      1      4      0      1
10 *CONTROL_HOURLASS
11 $#      ihq      qh
12 .....      1      0.1
13 *CONTROL_IMPLICIT_AUTO
14 $#      iaauto      iteopt      itewin      dtmin      dtmax      dtexp      kfail      kcycle
15 .....      1      11      5      0.0      0.0      0.0      0      0
16 *CONTROL_IMPLICIT_DYNAMICS
17 $#      imass      gamma      beta      tdybir      tdydth      tdybur      irate      alpha
18 .....      0      0.6      0.38      0.01.00000E281.00000E28      0      0.0
19 *CONTROL_IMPLICIT_GENERAL
20 $#      imflag      dt0      imform      nsbs      igs      cnstn      form      zero_v
21 .....      1      0.01      2      1      1      0      0      0
22 *CONTROL_IMPLICIT_SOLUTION
23 $#      nsolvr      ilimit      maxref      dctl      ectol      rctl      lstol      abstol
24 .....      12      1      15      0.001      0.01      0.91.0000E-10
25 $#      dnorm      diverg      istif      nlprint      nlnorm      d3itctl      cpchk
26 .....      1      1      1      2      4      1      0
27 $#      arcctl      arcdir      arclen      arcmt      arcdmp      arcpsi      arcalf      arctim
28 .....      0      0      0.0      1      2      0      0      0
29 $#      lsmtd      lsdire      irad      srad      awgt      sred
30 .....      5      2      0.0      0.0      0.0      0.0
31 *CONTROL_IMPLICIT_SOLVER
32 $#      lsolvr      lprint      negev      order      drcm      drcprm      autospc      autotol
33 .....      2      1      2      0      4      0.0      1      0.0
34 *CONTROL_OUTPUT
35 $#      npopt      neecho      nrefup      iaccop      opifs      ipnint      ikedit      iflush
36 .....      0      0      0      0      0.0      0      100      5000
37 $#      iprtf      ierode      tetl0s8      msgmax      ipcurv      gmdt      ipldbl      eocs
38 .....      0      0      2      50      0      0.0      0      0
39 $#      tolev      newleg      frfreq      minfo      solsig      msgflg      cdetol
40 .....      2      0      1      0      0      0      10.0
41 $#      phschng      demden      icrfile      spc2bnd      -      shlsig      hisnout
42 .....      0      0      0      0      0      0      0
43 *CONTROL_SHELL
44 $#      wrpang      esort      irnxx      istupd      theory      bwc      miter      proj
45 .....      20.0      0      -1      0      2      2      2      0
46 $#      rotasc1      intgrd      lamsht      cstyp6      thshel
47 .....      1.0      0      0      1      0
48 $#      psstupd      sidt4tu      cntco      itsflg      irquad      w-mode      stretch      icrq
49 .....      0      0      0      0      2      0.0      0.0      0
50 $#      nfail1      nfail4      psnfail      keepcs      delfr      drcpsid      drcprm      intperr
51 .....      0      0      0      0      0      0      1.0      0
52 *CONTROL_TERMINATION
53 $#      endtim      endcyc      dtmin      endeng      endmas      nosol
54 .....      1.0      0      0.001      0.01.000000E8      0

```


Appendix 3/2

```

55 *DATABASE_ABSTAT
56 $#      dt      binary      lcur      ioopt
57      0.001      3          0          1
58 *DATABASE_BNDOUT
59 $#      dt      binary      lcur      ioopt
60      0.001      3          0          1
61 *DATABASE_DEFORC
62 $#      dt      binary      lcur      ioopt
63      0.001      3          0          1
64 *DATABASE_ELOUT
65 $#      dt      binary      lcur      ioopt      option1      option2      option3      option4
66      0.001      3          0          1          0          0          0          0
67 *DATABASE_GLSTAT
68 $#      dt      binary      lcur      ioopt
69      0.001      3          0          1
70 *DATABASE_JNTFORC
71 $#      dt      binary      lcur      ioopt
72      0.001      3          0          1
73 *DATABASE_MATSUM
74 $#      dt      binary      lcur      ioopt
75      0.001      3          0          1
76 *DATABASE_NODFOR
77 $#      dt      binary      lcur      ioopt
78      0.001      3          0          1
79 *DATABASE_NODOUT
80 $#      dt      binary      lcur      ioopt      option1      option2
81      0.001      3          0          1          0.0          0
82 *DATABASE_RCFORC
83 $#      dt      binary      lcur      ioopt
84      0.001      3          0          1
85 *DATABASE_BINARY_D3PLOT
86 $#      dt      lcdt      beam      npltc      psetid
87      0.01      0          0          0          0
88 $#      ioopt      rate      cutoff      window      type      pset
89      0          0.0          0.0          0.0          0          0
90 *DATABASE_EXTENT_BINARY
91 $#      neiph      neips      maxint      strflg      sigflg      epsflg      rltflg      engflg
92      0          0          3          0          1          1          1          1
93 $#      cmpflg      ieverp      beamip      dcomp      shge      stssz      n3thdt      ialemat
94      0          0          0          1          1          1          2          1
95 $#      nintsld      pkp_sen      sclp      hydro      msscl      therm      intout      nodout
96      0          0          1.0          0          0          0          0
97 $#      dtdt      resplt      neipb      quadr      cubic
98      0          1          0          0          0
99 *BOUNDARY_PRESCRIBED_MOTION_SET_ID
100 $#      id
101      lDisplacementLoading
102 $#      nsid      dof      vad      lcid      sf      vid      death      birth
103      5          2          2          1          -20.0          01.000000E28          0.0
104 *BOUNDARY_SPC_SET_ID
105 $#      id
106      lFixedSupport
107 $#      nsid      cid      dofz      dofz      dofz      dofrx      dofry      dofrz
108      1          0          1          1          1          0          0          0

```

Appendix 3/3

109	*SET_NODE_LIST_TITLE								
110	Fixedsupport								
111	\$#	sid	da1	da2	da3	da4	solver		
112		1	0.0	0.0	0.0	0.0	0.0MECH		
113	\$#	nid1	nid2	nid3	nid4	nid5	nid6	nid7	nid8
114		10831	5986	9121	9122	9123	9124	8836	10832
115		10833	10834	10546	8553	10842	10846	10845	10841
116		10548	9132	9136	9135	9131	8838	5989	10851
117		11410	11412	10849	10549	9141	9700	9702	9139
118		8839	0	0	0	0	0	0	0
119	*BOUNDARY_SPC_SET_ID								
120	\$#	id							heading
121		2	RollerSupport						
122	\$#	nsid	cid	dofx	dofy	dofz	dofrx	dofry	dofrz
123		2	0	1	1	0	0	0	0
124	*SET_NODE_LIST_TITLE								
125	RollerSupport								
126	\$#	sid	da1	da2	da3	da4	solver		
127		2	0.0	0.0	0.0	0.0	0.0MECH		
128	\$#	nid1	nid2	nid3	nid4	nid5	nid6	nid7	nid8
129		10836	10837	10838	10547	10835	10262	9125	9126
130		9127	9128	8837	10843	10844	10840	10830	10839
131		8835	9129	9133	9134	9130	9120	11409	11411
132		10848	10829	10847	8834	9137	9699	9701	9138
133		9119	0	0	0	0	0	0	0
134	*BOUNDARY_SPC_SET_ID								
135	\$#	id							heading
136		3	FixedXdirection						
137	\$#	nsid	cid	dofx	dofy	dofz	dofrx	dofry	dofrz
138		3	0	1	0	0	0	0	0
139	*SET_NODE_LIST_TITLE								
140	Fixedxdirection								
141	\$#	sid	da1	da2	da3	da4	solver		
142		3	0.0	0.0	0.0	0.0	0.0MECH		
143	\$#	nid1	nid2	nid3	nid4	nid5	nid6	nid7	nid8
144		571	1711	2281	2282	2283	2284	1996	572
145		573	574	286	3	582	586	585	581
146		288	2292	2296	2295	2291	1998	3424	591
147		1150	1152	589	289	2301	2860	2862	2299
148		1999	3991	3992	3993	3994	3995	3996	3997
149		3706	6562	6561	6560	6559	6558	6557	6556
150		5986	4018	4017	4016	4015	4010	4009	4006
151		6273	6571	6574	6575	6580	6581	6582	6583
152		8553	4503	4588	4587	4585	4582	4581	4020
153		3709	6585	7146	7147	7150	7152	7153	7068
154		5989	0	0	0	0	0	0	0
155	*BOUNDARY_SPC_SET_ID								
156	\$#	id							heading
157		4	RollerXdirection						
158	\$#	nsid	cid	dofx	dofy	dofz	dofrx	dofry	dofrz
159		4	0	1	0	0	0	0	0
160	*SET_NODE_LIST_TITLE								
161	Rollerxdirection								
162	\$#	sid	da1	da2	da3	da4	solver		
163		4	0.0	0.0	0.0	0.0	0.0MECH		

Appendix 3/4

```

160 *SET_NODE_LIST_TITLE
161 Rollerxdirection
162 $#      sid      dal      da2      da3      da4      solver
163      4      0.0      0.0      0.0      0.0MECH
164 $#      nid1      nid2      nid3      nid4      nid5      nid6      nid7      nid8
165      6565      6564      6563      10262      6566      6567      6568      6569
166      6272      4004      4003      4002      4001      4000      3999      3998
167      2      6576      6577      6578      6579      8835      6573      6572
168      6570      6555      4005      4007      4008      4011      4012      4013
169      4014      285      7151      7154      7155      7145      8834      7149
170      7148      6584      3989      4019      4583      4584      4586      4589
171      4590      4580      284      2286      2285      575      576      577
172      578      287      2287      2288      1997      2293      2289      579
173      583      584      580      570      2294      2290      2280      2859
174      2297      587      1149      1151      588      569      2861      2298
175      2279      0      0      0      0      0      0      0
176 *PART
177 $#                                          title
178 Upperflange
179 $#      pid      secid      mid      eosid      hgid      grav      adpopt      tmid
180      1      1      1      0      0      0      0      0
181 *SECTION_SHELL_TITLE
182 UpperFlange
183 $#      secid      elform      shrf      nip      propt      qr/irid      icip      setyp
184      1      16      1.0      7      1.0      0      0      1
185 $#      t1      t2      t3      t4      nloc      marea      idof      edgset
186      5.7      5.7      5.7      5.7      0.0      0.0      0.0      0
187 *MAT_PIECEWISE_LINEAR_PLASTICITY_TITLE
188 Steel
189 $#      mid      ro      e      pr      sigy      etan      fail      tdel
190      17.85000E-9      210000.0      0.3      355.0      0.01.00000E21      0.0
191 $#      c      p      lcss      lcsr      vp
192      0.0      0.0      0      0      0.0
193 $#      eps1      eps2      eps3      eps4      eps5      eps6      eps7      eps8
194      0.0      0.0035844      0.0245015      0.0332803      0.060702      0.0773121      0.1123726      0.1294901
195 $#      es1      es2      es3      es4      es5      es6      es7      es8
196      403.0937      432.2084      465.8787      499.7923      572.912      601.4433      642.5938      657.3689
197 *PART
198 $#                                          title
199 Web
200 $#      pid      secid      mid      eosid      hgid      grav      adpopt      tmid
201      2      2      1      0      0      0      0      0
202 *SECTION_SHELL_TITLE
203 Websection
204 $#      secid      elform      shrf      nip      propt      qr/irid      icip      setyp
205      2      16      1.0      7      1.0      0      0      1
206 $#      t1      t2      t3      t4      nloc      marea      idof      edgset
207      4.1      4.1      4.1      4.1      0.0      0.0      0.0      0
208 *PART
209 $#                                          title
210 Lowerflange
211 $#      pid      secid      mid      eosid      hgid      grav      adpopt      tmid
212      3      3      1      0      0      0      0      0

```

Appendix 4/1

General Controls, LS-DYNA implicit code input for structure analysis in fire

For the thermal problems in LS-PrePost are solved using implicit time integration. For implicit analysis following keywords were used for this thesis:

```

1  ## LS-DYNA Keyword file created by LS-PrePost(R) V4.7.0 - 06Nov2019
2  ## Created on Dec-13-2019 (17:29:01)
3  *KEYWORD
4  *TITLE
5  ##
6  LS-DYNA keyword deck by LS-PrePost
7  *CONTROL_ACCURACY
8  ##      osu      inn      pidosu      iacc
9  ##      1        4        0        1
10 *CONTROL_IMPLICIT_AUTO
11 ##      iauto      iteopt      itewin      dtmin      dtmax      dtemp      kfail      kcycle
12 ##      0          11        5        0.0      0.0      0.0      0        0
13 *CONTROL_IMPLICIT_DYNAMICS
14 ##      imass      gamma      beta      tdybir      tdydth      tdybur      irate      alpha
15 ##      0          0.5      0.25      0.01.00000E281.00000E28      0        0.0
16 *CONTROL_IMPLICIT_GENERAL
17 ##      imflag      dt0      imform      nsbs      igs      cnstn      form      zero_v
18 ##      1          0.001      2        1        2        0        0        0
19 *CONTROL_IMPLICIT_SOLUTION
20 ##      nsolvr      ilimit      maxref      dtol      ectol      rctol      lstol      abstol
21 ##      12          15        20      0.001      0.01      0.01      0.91.00000E-10
22 ##      dnorm      diverg      istif      nlprint      nlnorm      d3itctl      cpchk
23 ##      2          1        1        0        2        0        0
24 ##      arcoct1      arcdir      arclen      arcmtth      arcdmp      arcpst1      arcalf      arctim
25 ##      0          0        0.0      1        2        0        0
26 ##      lsmttd      lmdir      irad      srad      awgt      sred
27 ##      5          2        0.0      0.0      0.0      0.0
28 *CONTROL_IMPLICIT_SOLVER
29 ##      lsolvr      lprint      negev      order      drcm      drcprm      autospc      autotol
30 ##      2          2        2        0        4        0.0      1        0.0
31 *CONTROL_SHELL
32 ##      wrpang      esort      irnxx      istupd      theory      bwc      miter      proj
33 ##      20.0        1        -1      0        2        2        2        0
34 ##      rotasc1      intgrd      lamsht      cstyp6      thshel
35 ##      1.0        0        0        1        0
36 ##      psstupd      sidt4tu      cntco      itsflg      irqvad      w-mode      stretch      icrq
37 ##      0          0        0        0        2        0.0      0.0      0
38 ##      nfail1      nfail4      psnfail      keepcs      delfr      drcpsid      drcprm      intperr
39 ##      0          0        0        0        0        0        1.0      0
40 *CONTROL_SOLUTION
41 ##      soln      nlq      isnan      lcint      lcacc      nodcf
42 ##      0          0        0        100      0        1
43 *CONTROL_START
44 ##      begtim
45 ##      0.0
46 *CONTROL_TERMINATION
47 ##      endtim      endcyc      dtmin      endeng      endmas      nosol
48 ##      20.0        0        0.001      0.01.000000E8      0
49 *CONTROL_THERMAL_NONLINEAR
50 ##      refmax      tol      dcp      lumpbc      thlst1      nlthpr      phchpn
51 ##      10          0.0      0.5      0        0.0      1        0.0
52 *CONTROL_THERMAL_SOLVER
53 ##      atype      ptype      solver      cgtol      gpt      eqheat      fwork      sbc
54 ##      1          1        31.00000E-4      8        1.0      1.0      0.0

```

Appendix 4/2

```

55 $# msglvl      maxitr      abstol      reltol      omega      unused      unused      tsf
56           0          5001.0000E-101.00000E-4      1.0          1.0
57 $# mxdmp      dtvf      varden
58           0          0.0          0
59 *CONTROL_THERMAL_TIMESTEP
60 $#      ts      tip      its      tmin      tmax      dtemp      tscp      lcts
61           0          1.0          0.1          0.0          0.0          1.0          0.5          0
62 *CONTROL_TIMESTEP
63 $# dtinit      tssfacc      isdo      tslimit      dt2ms      lctm      erode      mslst
64           0.0          0.9          0          0.0          0.0          0          0          0
65 $# dt2msf      dt2mslc      imslc      unused      unused      rmscl      unused      ihdo
66           0.0          0          0          0          0          0.0          0          0
67 *DATABASE_BNDOUT
68 $#      dt      binary      lcur      ioopt
69           0.001          3          0          1
70 *DATABASE_GLSTAT
71 $#      dt      binary      lcur      ioopt
72           0.001          3          0          1
73 *DATABASE_NODOUT
74 $#      dt      binary      lcur      ioopt      option1      option2
75           0.001          3          0          1          0.0          0
76 *DATABASE_RCFORC
77 $#      dt      binary      lcur      ioopt
78           0.001          3          0          1
79 *DATABASE_IPRINT
80 $#      dt      binary      lcur      ioopt
81           0.001          3          0          1
82 *DATABASE_BINARY_D3PLOT
83 $#      dt      lcdt      beam      npltc      psetid
84           0.01          0          0          0          0
85 $# ioopt      rate      cutoff      window      type      pset
86           0          0.0          0.0          0.0          0          0
87 *DATABASE_EXTENT_BINARY
88 $# neiph      neips      maxint      strflg      sigflg      epsflg      rtlflg      engflg
89           0          11          3          1          1          1          1          1
90 $# cmpflg      ieverp      beamip      dcomp      shge      stssz      n3thdt      ialemat
91           0          0          0          1          1          1          2          1
92 $# nintsld      pkp_sen      sclp      hydro      msscl      therm      intout      nodout
93           0          0          1.0          0          0          0
94 $# dttdt      resplt      neipb      quadr      cubic
95           0          0          0          0          0
96 *BOUNDARY_SPC_SET_ID
97 $#      id
98           1FixedSupport
99 $#      nsid      cid      dofz      dofz      dofz      dofz      dofz      dofz
100          1          0          1          1          1          0          0          0
101 *SET_NODE_LIST_TITLE
102 Fixedsupport
103 $#      sid      da1      da2      da3      da4      solver
104           1          0.0          0.0          0.0          0.0MECH
105 $#      nid1      nid2      nid3      nid4      nid5      nid6      nid7      nid8
106           2737      3764      3763      3421      3079      3080      2908      3594
107           3086      3084      2910      3770      3768      3423      1885      3090
108           3088      2911      3774      3772      3424          0          0          0

```

Appendix 4/3

```

109 *BOUNDARY_SPC_SET_ID
110 $#      id                                     heading
111      2Roller_Support
112 $#      nsid      cid      dofz      dofz      dofz      dofz      dofz      dofz
113      2          0          1          1          0          0          0          0
114 *SET_NODE_LIST
115 $#      sid      dal      da2      da3      da4      solver
116      2          0.0      0.0      0.0      0.0MECH
117 $#      nid1      nid2      nid3      nid4      nid5      nid6      nid7      nid8
118      3593      3081      3082      2909      3766      3765      3422      2907
119      3085      3083      3078      3769      3767      3591      3761      3089
120      3087      3077      3773      3771      3590          0          0          0
121 *BOUNDARY_SPC_SET_ID
122 $#      id                                     heading
123      3FixedXdirection
124 $#      nsid      cid      dofz      dofz      dofz      dofz      dofz      dofz
125      3          0          1          0          0          0          0          0
126 *SET_NODE_LIST_TITLE
127 Fixedxdirection
128 $#      sid      dal      da2      da3      da4      solver
129      3          0.0      0.0      0.0      0.0MECH
130 $#      nid1      nid2      nid3      nid4      nid5      nid6      nid7      nid8
131      856      1030      1029      1028      1027      685      2053      2054
132      2055      2056      2737      1037      1713      2064      2068      2067
133      2063      3594      1041      1042      1038          3      1045      859
134      2072      2405      2403      2071      1885      1377      1379      1046
135      688      343      4448      4447      4105      344      172      350
136      348      174      4454      4452      4107      354      352      175
137      4458      4456      4108          0          0          0          0          0
138 *BOUNDARY_SPC_SET_ID
139 $#      id                                     heading
140      4Rollerxdirection
141 $#      nsid      cid      dofz      dofz      dofz      dofz      dofz      dofz
142      4          0          1          0          0          0          0          0
143 *SET_NODE_LIST_TITLE
144 Rollerxdirection
145 $#      sid      dal      da2      da3      da4      solver
146      4          0.0      0.0      0.0      0.0MECH
147 $#      nid1      nid2      nid3      nid4      nid5      nid6      nid7      nid8
148      4450      345      346      173      4449      4106      4453      855
149      349      347      342      4451      4275      4457      170      353
150      351      341      4455      4274      2057      2058      2059      2060
151      3593      1712      1034      1033      1032      1031          2      2061
152      2065      2066      2062      2907      1881      1036      1040      1039
153      1035      1025      2069      2404      2406      2070      3761      1044
154      1378      1380      1043          0          0          0          0          0

```

Appendix 4/4

```

155 *DEFINE_TABLE_TITLE
156 S355_Plastic_Temp
157 $#      tbid      sfa      offa
158          19
159 $#          value      lcid
160          20.0      7
161          100.0      8
162          200.0      9
163          300.0      10
164          400.0      11
165          500.0      12
166          600.0      13
167          700.0      14
168          800.0      15
169          900.0      16
170          1000.0      17
171 *DEFINE_CURVE_TITLE
172 S355_Plastic_T20
173 $#      lcid      sidr      sfa      sfo      offa      offo      dattyp      lcint
174          7      0      1.0      1.0      0.0      0.0      0      0
175 $#          al      ol
176          0.0      304.8
177          1.9706999592e-04      323.1
178          6.3610001234e-04      338.3
179          0.001561      357.0
180          0.002507      370.1
181          0.003465      380.7
182          0.0054      389.9
183          0.006375      396.7
184          0.007352      408.6
185          0.008333      413.4
186          0.010301      421.2
187          0.013269      429.2
188          0.016253      433.3
189          0.01825      434.0
190          0.14825      492.0
191 *DEFINE_CURVE_TITLE
192 S355_Plastic_T100
193 $#      lcid      sidr      sfa      sfo      offa      offo      dattyp      lcint
194          8      0      1.0      1.0      0.0      0.0      0      0
195 $#          al      ol
196          0.0      304.1
197          1.9706999592e-04      323.1
198          6.3610001234e-04      338.3
199          0.001561      357.0
200          0.002507      370.1
201          0.003465      380.7
202          0.0054      396.7
203          0.006375      403.1
204          0.007352      408.6
205          0.008333      413.4
206          0.010301      421.2
207          0.013269      429.1
208          0.016253      433.3
209          0.01825      434.0

```

Appendix 4/5

210			0.14825						492.0
211	*DEFINE_CURVE_TITLE								
212	S355_Plastic_T200								
213	\$#	lcid	sidr	sfa	sfo	offa	offo	dattyp	lcint
214		9	0	1.0	1.0	0.0	0.0	0	0
215	\$#		al		ol				
216			0.0		245.1				
217			5.2999999753e-05		256.1				
218			2.8800001019e-04		270.6				
219			7.22999997555e-04		285.1				
220			0.001636		304.3				
221			0.002574		318.3				
222			0.003524		329.5				
223			0.005447		346.6				
224			0.006416		353.4				
225			0.00739		359.4				
226			0.008367		364.6				
227			0.010329		373.0				
228			0.013291		381.6				
229			0.016271		385.9				
230			0.018267		386.8				
231			0.148267		444.82				
232	*DEFINE_CURVE_TITLE								
233	S355_Plastic_T300								
234	\$#	lcid	sidr	sfa	sfo	offa	offo	dattyp	lcint
235		10	0	1.0	1.0	0.0	0.0	0	0
236	\$#		al		ol				
237			0.0		186.2				
238			1.5799999528e-04		206.8				
239			3.9800000377e-04		218.6				
240			8.2800001837e-04		232.6				
241			0.001729		252.2				
242			0.002655		266.7				
243			0.003596		278.5				
244			0.005504		296.7				
245			0.006467		304.0				
246			0.007435		310.4				
247			0.008408		316.0				
248			0.010362		325.0				
249			0.013316		334.2				
250			0.016292		338.9				
251			0.018288		339.8				
252			0.148288		390.7				
253	*DEFINE_CURVE_TITLE								
254	S355_Plastic_T400								
255	\$#	lcid	sidr	sfa	sfo	offa	offo	dattyp	lcint
256		11	0	1.0	1.0	0.0	0.0	0	0
257	\$#		al		ol				
258			0.0		115.2				
259			1.9999999495e-05		122.3				
260			1.4800000645e-04		133.6				
261			9.6999999369e-04		161.4				
262			0.001863		178.2				
263			0.002782		191.1				
264			0.003715		201.5				

Appendix 4/6

264		0.003715							201.5
265		0.005611							217.8
266		0.006569							224.5
267		0.007532							230.2
268		0.0085							235.2
269		0.010448							243.3
270		0.013395							251.7
271		0.016368							255.9
272		0.018363							256.7
273		0.148363							295.2
274	*DEFINE_CURVE_TITLE								
275	S355_Plastic_T500								
276	\$#	lcid	sidr	sfa	sfo	offa	offo	dattyp	lcint
277		12	0	1.0	1.0	0.0	0.0	0	0
278	\$#		al		ol				
279			0.0		93.5				
280		8.4999999672e-05			103.7				
281		1.5599999460e-04			107.3				
282		9.9500000942e-04			127.8				
283		0.001897			140.2				
284		0.002823			149.7				
285		0.003763			157.4				
286		0.005668			169.4				
287		0.00663			174.3				
288		0.007597			178.5				
289		0.008568			182.2				
290		0.010521			188.2				
291		0.013473			194.3				
292		0.016448			197.5				
293		0.018443			198.0				
294		0.148443			227.7				
295	*DEFINE_CURVE_TITLE								
296	S355_Plastic_T600								
297	\$#	lcid	sidr	sfa	sfo	offa	offo	dattyp	lcint
298		13	0	1.0	1.0	0.0	0.0	0	0
299	\$#		al		ol				
300			0.0		44.1				
301		8.8000000687e-05			50.4				
302		1.5500000154e-04			52.4				
303		9.6299999859e-04			64.3				
304		0.001845			71.6				
305		0.002755			77.2				
306		0.003682			81.7				
307		0.005567			88.9				
308		0.00652			91.7				
309		0.00748			94.3				
310		0.008444			96.4				
311		0.010387			100.0				
312		0.013328			103.6				
313		0.016298			105.5				
314		0.018292			105.9				
315		0.148292			121.8				

Appendix 4/7

316	*DEFINE_CURVE_TITLE								
317	S355_Plastic_T700								
318	\$#	lcid	sidr	sfa	sfo	offa	offo	dattyp	lcint
319		14	0	1.0	1.0	0.0	0.0	0	0
320	\$#		al		ol				
321			0.0		18.4				
322			8.6000000010e-05		21.2				
323			1.5199999325e-04		22.1				
324			9.4900000840e-04		27.3				
325			0.001824		30.6				
326			0.002728		33.1				
327			0.00365		35.1				
328			0.005527		38.3				
329			0.006478		39.6				
330			0.007435		40.7				
331			0.008397		41.7				
332			0.010336		43.3				
333			0.013274		44.9				
334			0.016241		45.7				
335			0.018235		45.9				
336			0.148235		52.8				
337	*DEFINE_CURVE_TITLE								
338	S355_Plastic_T800								
339	\$#	lcid	sidr	sfa	sfo	offa	offo	dattyp	lcint
340		15	0	1.0	1.0	0.0	0.0	0	0
341	\$#		al		ol				
342			0.0		12.3				
343			1.3600000239e-04		13.8				
344			2.1399999969e-04		14.1				
345			0.001085		16.5				
346			0.002005		17.9				
347			0.002944		19.0				
348			0.003894		19.9				
349			0.005815		21.3				
350			0.006784		21.9				
351			0.007756		22.4				
352			0.008732		22.8				
353			0.010693		23.5				
354			0.013653		24.2				
355			0.016633		24.6				
356			0.018629		24.7				
357			0.148629		28.4				
358	*DEFINE_CURVE_TITLE								
359	S355_Plastic_T900								
360	\$#	lcid	sidr	sfa	sfo	offa	offo	dattyp	lcint
361		16	0	1.0	1.0	0.0	0.0	0	0
362	\$#		al		ol				
363			0.0		9.2				
364			6.6000000515e-05		9.9				
365			2.2200000240e-04		10.5				
366			0.001105		12.1				
367			0.002033		13.1				
368			0.002978		13.8				
369			0.003933		14.4				
370			0.005862		15.4				

Appendix 4/8

```

371      0.006834      15.7
372      0.007809      16.1
373      0.008788      16.4
374      0.010752      16.8
375      0.013716      17.3
376      0.016698      17.6
377      0.018694      17.6
378      0.148694      20.24
379 *DEFINE_CURVE_TITLE
380 S355_Plastic_T1000
381 $#      lcid      sidr      sfa      sfo      offa      offo      dattyp      lcint
382      17      0      1.0      1.0      0.0      0.0      0      0
383 $#      al      ol
384      0.0      6.1
385      7.4000003224e-05      6.5
386      2.39999999394e-04      6.8
387      0.001148      7.7
388      0.002092      8.2
389      0.003048      8.6
390      0.004013      8.9
391      0.005958      9.4
392      0.006936      9.6
393      0.007916      9.8
394      0.008899      9.9
395      0.010871      10.2
396      0.013843      10.4
397      0.016829      10.5
398      0.018826      10.6
399      0.148826      12.2
400 *DEFINE_CURVE_TITLE
401 Load_curve
402 $#      lcid      sidr      sfa      sfo      offa      offo      dattyp      lcint
403      1      0      0.01      1.0      0.0      0.0      0      0
404 $#      al      ol
405      0.0      0.0
406      200.0      1.0
407      2000.0      1.0
408 *DEFINE_CURVE_TITLE
409 Youngsmodulus_Temperature
410 $#      lcid      sidr      sfa      sfo      offa      offo      dattyp      lcint
411      2      0      1.0      1.0      0.0      0.0      0      0
412 $#      al      ol
413      20.0      210000.0
414      100.0      210000.0
415      200.0      189000.0
416      300.0      168000.0
417      400.0      147000.0
418      500.0      126000.0
419      600.0      65100.0
420      700.0      27300.0
421      800.0      18900.0
422      900.0      14175.0
423      1000.0      9450.0
424      1100.0      4725.0
425      1200.0      0.0

```

Appendix 4/9

```

426 *DEFINE_CURVE_TITLE
427 Thermalexpansion_Temperature
428 $#      lcid      sidr      sfa      sfo      offa      offo      dattyp      lcint
429      .      4      0      1.0      1.0      0.0      0.0      0      0
430 $#      .      .      al      .      ol
431      .      .      .      20.0      1.2000000424e-05
432      .      .      .      100.0      1.2479999896e-05
433      .      .      .      200.0      1.2880000213e-05
434      .      .      .      300.0      1.3279999621e-05
435      .      .      .      400.0      1.3679999938e-05
436      .      .      .      500.0      1.4080000255e-05
437      .      .      .      600.0      1.4479999663e-05
438      .      .      .      700.0      1.4879999981e-05
439      .      .      .      750.0      1.5079999685e-05
440      .      .      .      800.0      1.4102999558e-05
441      .      .      .      860.0      1.3095000213e-05
442      .      .      .      900.0      1.3408999621e-05
443      .      .      .      1000.0      1.4082000234e-05
444      .      .      .      1100.0      1.4629999896e-05
445 *DEFINE_CURVE_TITLE
446 PR_CURVE
447 $#      lcid      sidr      sfa      sfo      offa      offo      dattyp      lcint
448      .      5      0      1.0      1.0      0.0      0.0      0      0
449 $#      .      .      al      .      ol
450      .      .      .      20.0      0.3
451      .      .      .      100.0      0.3
452      .      .      .      200.0      0.3
453      .      .      .      300.0      0.3
454      .      .      .      400.0      0.3
455      .      .      .      500.0      0.3
456      .      .      .      600.0      0.3
457      .      .      .      700.0      0.3
458      .      .      .      800.0      0.3
459      .      .      .      900.0      0.3
460      .      .      .      1000.0      0.3
461      .      .      .      1100.0      0.3
462      .      .      .      1200.0      0.3
463 *DEFINE_CURVE_TITLE
464 Temperature_time_curve
465 $#      lcid      sidr      sfa      sfo      offa      offo      dattyp      lcint
466      .      18      0      0.01      1.0      0.0      0.0      0      0
467 $#      .      .      al      .      ol
468      .      .      .      0.0      20.0
469      .      .      .      5.0      20.999
470      .      .      .      10.0      22.72816
471      .      .      .      15.0      25.04842
472      .      .      .      20.0      27.87156
473      .      .      .      25.0      31.0
474      .      .      .      30.0      34.0
475      .      .      .      35.0      38.0
476      .      .      .      40.0      43.0
477      .      .      .      45.0      47.0
478      .      .      .      50.0      52.0
479      .      .      .      55.0      57.0
480      .      .      .      60.0      63.0

```

Appendix 4/10

481		65.0	68.0
482		70.0	74.0
483		75.0	80.0
484		80.0	86.0
485		85.0	93.0
486		90.0	99.0
487		95.0	106.0
488		100.0	113.0
489		105.0	120.0
490		110.0	127.0
491		115.0	134.0
492		120.0	141.0
493		125.0	149.0
494		130.0	156.0
495		135.0	164.0
496		140.0	171.0
497		145.0	179.0
498		150.0	187.0
499		155.0	194.0
500		160.0	202.0
501		165.0	210.0
502		170.0	218.0
503		175.0	226.0
504		180.0	234.0
505		185.0	242.0
506		190.0	250.0
507		195.0	258.0
508		200.0	266.0
509		205.0	274.0
510		210.0	281.0
511		215.0	289.0
512		220.0	297.0
513		225.0	305.0
514		230.0	313.0
515		235.0	321.0
516		240.0	329.0
517		245.0	336.0
518		250.0	344.0
519		255.0	351.0
520		260.0	359.0
521		265.0	366.0
522		270.0	374.0
523		275.0	381.0
524		280.0	388.0
525		285.0	395.0
526		290.0	402.0
527		295.0	409.0
528		300.0	416.0
529		305.0	423.0
530		310.0	430.0
531		315.0	436.0
532		320.0	443.0
533		325.0	449.0
534		330.0	455.0
535		335.0	461.0

Appendix 4/11

857			1945.0		850.0						
858			1950.0		850.0						
859			1955.0		850.0						
860			1960.0		851.0						
861			1965.0		851.0						
862			1970.0		851.9828						
863			1975.0		852.0						
864			1980.0		852.0						
865			1985.0		853.0						
866			1990.0		853.0						
867			1995.0		853.0						
868			2000.0		854.0						
869	*INITIAL_TEMPERATURE_SET										
870	\$#	nsid	temp	loc							
871		6	20.0	0							
872		6	20.0	-1							
873		6	20.0	1							
874	*SECTION_SHELL_TITLE										
875	Upper_Flange										
876	\$#	secid	elform	shrf	nip	propt	qr/irid	icomp	setyp		
877		1	16	1.0	7	1.0	0	0	1		
878	\$#	t1	t2	t3	t4	nloc	marea	idof	edgset		
879		5.7	5.7	5.7	5.7	0.0	0.0	0.0	0		
880	*SECTION_SHELL_TITLE										
881	Web_section										
882	\$#	secid	elform	shrf	nip	propt	qr/irid	icomp	setyp		
883		2	16	1.0	7	1.0	0	0	1		
884	\$#	t1	t2	t3	t4	nloc	marea	idof	edgset		
885		4.1	4.1	4.1	4.1	0.0	0.0	0.0	0		
886	*SECTION_SHELL_TITLE										
887	Lowerflange										
888	\$#	secid	elform	shrf	nip	propt	qr/irid	icomp	setyp		
889		3	16	1.0	7	1.0	0	0	1		
890	\$#	t1	t2	t3	t4	nloc	marea	idof	edgset		
891		5.7	5.7	5.7	5.7	0.0	0.0	0.0	0		
892	*ELEMENT_SHELL										
893	\$#	eid	pid	n1	n2	n3	n4	n5	n6	n7	n8
894		1	1	346	173	342	347	0	0	0	0
895		2	1	172	344	348	174	0	0	0	0
896		3	1	2	345	349	855	0	0	0	0
897		4	1	345	346	347	349	0	0	0	0
898		5	1	343	685	3	350	0	0	0	0
899		6	1	344	343	350	348	0	0	0	0
900		7	1	342	341	351	347	0	0	0	0
901		8	1	175	174	348	352	0	0	0	0
902		9	1	170	855	349	353	0	0	0	0
903		10	1	3	688	354	350	0	0	0	0
904		11	1	341	340	355	351	0	0	0	0
905		12	1	176	175	352	356	0	0	0	0
906		13	1	853	170	353	357	0	0	0	0
907		14	1	688	689	358	354	0	0	0	0
908		15	1	340	339	359	355	0	0	0	0
909		16	1	177	176	356	360	0	0	0	0
910		17	1	4443	853	357	361	0	0	0	0
911		18	1	689	690	362	358	0	0	0	0

Appendix 5

Material properties calculation sheet for MAT_255 according to Eurocode.

Mechanical properties of Carbon Steel			Ipe 100beam	
Modulus of Elasticity(E)	210000 N/mm ²		h	100 mm
Shear modulus	81000 N/mm ²		b	55 mm
Density	7850 kg/m ³		tw	4,1 mm
Yield strength at 20degree(fy)	355 N/mm ²		tf	5,7 mm
Ultimate tensile strength(fu)	510 N/mm ²		r	7 mm
Poisson ratio	0.30		c(flange)	18,45 mm
coefficient of linear thermal expansion	12*10 ⁻⁶		c(web)	74,6 mm
Modulus of Elasticity(Ea,θ)	210000 mpa		ε	0,691574036

Steel Temperature	Reduction factor(ky,θ)for effective yield strength	Effective yield strength(fy,θ)	For Proportional limit(Kp,θ)	Linear elastic range(Ke,θ)	Proportional limit(fp,θ)
20	1	355	1	1	355
100	1	355	1	1	355
200	1	355	0,807	0,9	319,5
300	1	355	0,613	0,8	284
400	1	355	0,42	0,7	248,5
500	0,78	276,9	0,36	0,6	213
600	0,47	166,85	0,18	0,31	110,05
700	0,23	81,65	0,075	0,13	46,15
800	0,11	39,05	0,05	0,09	31,95
900	0,06	21,3	0,0375	0,0675	23,9625
1000	0,04	14,2	0,025	0,045	15,975
1100	0,02	7,1	0,0125	0,0225	7,9875
1200	0	0	0	0	0

Appendix 6

Thermal expansion versus temperature curve plotted from LS-PrePost

